Master's Thesis

DEVELOPMENT OF A RESEARCH TOOL FOR PHOSPHOHISTIDINE

Ohyeon Kwon

Department of Chemistry

Graduate School of UNIST

2017

DEVELOPMENT OF A RESEARCH TOOL FOR PHOSPHOHISTIDINE

Ohyeon Kwon

Department of Chemistry

Graduate School of UNIST

DEVELOPMENT OF A RESEARCH TOOL FOR PHOSPHOHISTIDINE

A thesis/dissertation
submitted to the Graduate School of UNIST
in partial fulfillment of the
requirements for the degree of
Master of Science

Ohyeon Kwon

06. 13. 2017 of submission

Approved by

Advisor
Jung-Min Kee

DEVELOPMENT OF A RESEARCH TOOL FOR PHOSPHOHISTIDINE

Ohyeon Kwon

This certifies that the thesis/dissertation of Ohyeon Kwon is approved.

06. 13. 2017 of submission

signature

Advisor: Jung-Min Kee

signature

Hyun-Woo Rhee: Thesis Committee Member #1

signature

Young S. Park: Thesis Committee Member #2

Abstract

Post-translational modification of protein is an important phenomenon in biology. Protein phosphorylation is one of post-translational modification and is responsible for signal transduction system and many kinds of cellular metabolisms. Especially, our research focused on histidine phosphorylation.

Chapter 1 introduces the characteristics of histidine phosphorylation and the related research so far. Histidine phosphorylation is N-phosphorylation, which is the phosphorylation on N atom of imidazole to form P-N bond and has acid labile property. Histidine phosphorylation was observed in many biological events. The most famous histidine phosphorylation is two-component system (TCS), which is the fundamental signal transduction system in bacteria. Also, it was found in eukaryotes such as nucleoside diphosphate kinase (NDPK), protein phosphohistidine phosphatase 1 (PHPT1), histone H4 and so on. However, because of its acid-labile chemical instability, there were insufficient tools for studying histidine phosphorylation and histidine phosphorylation was rarely explored. Currently available tools for phosphohistidine are radiolabeling analysis and antibody detection, which are not suitable for continuous enzyme assays. So we try to develop new tool for phosphohistidine, continuous and available for kinetic assay.

Chapter 2 describes our main research subject and progress. We devised Sox-based fluorescence sensor for phosphohistidine, which was basically a short peptide having kinase recognition domain, phosphorylation site (histidine) and Sox fluorophore. When histidine was phosphorylated, histidine phosphate group and Sox fluorophore chelated with magnesium cation and increased fluorescence by chelation-enhanced fluorescence (CHEF) effect, while no fluorescence when histidine was not phosphorylated. We designed simple peptide sensors, and then they were chemically phosphorylated and evaluated for their feasibility as phosphohistidine sensors.

In chapter 3, we briefly describe the protein labeling strategy using isotope-labeled desthiobiotin tags by APEX system. Especially, we synthesized a series of isotope-labeled desthiobiotinyl tyramine tags through enzymatic decarboxylation and acid coupling reaction.

Contents

List of Figures

List of Schemes

List of Tables

List of Abbreviations

ADP	Adenosine 3-diphosphate
AFU	Arbitrary fluorescence unit
APEX	Ascorbate peroxidase
Arg	Arginine
Asp	Aspartate
ATP	Adenosine 3-triphosphate
Boc	tert-butoxycarbonyl
CHEF	Chelation-enhanced fluorescence effect
CID	Collision-induced dissociation
CSox	Cystein-Sox
Cys	Cysteine
DBT	d-Desthiobiotinyl tyramide
DCC	N,N'-dicyclohexylcarbodiimide
DCM	Dichloromethane
DCU	N,N'-dicyclohexylurea
DIPEA	N,N-diisopropylethylamine
DMF	N,N-dimethylformamide
DNA	Deoxyribonucleic acid
E. coli	*Escherichia coli*
EDC	1-Ethyl-3-(3-dimethylaminopropyl)carbodiimide
ELISA	Enzyme-linked immunosorbent assay
ESI	Electrospray ionization
Fmoc	Fluorenylmethyloxycarbonyl
GFP	Green fluorescent protein
Gly	Glycine
HBTU	2-(1H-benzotriazol-1-yl)-1,1,3,3-tetramethyluronium hexafluorophosphate
HCl	Hydrochloric acid
His	Histidine
HK	Histidine kinase
HPLC	High performance liquid chromatography
KOH	Potassium hydroxide
Lys	Lysine

MALDI	Matrix-assisted laser desorption ionization
MPA	3-mercaptopropionic acid
mRNA	Messenger ribonucleic acid
MS	Mass spectrometry
NBS	N-bromosuccinimide
NDP	Nucleoside diphosphate
NDPK	Nucleoside diphosphate kinase
NHS	N-hydroxysuccinimide
NMR	Nuclear magnetic Resonance
NTP	Nucleoside triphosphate
pArg	Phosphoarginine
pHis	Phosphohistidine
PI(3)P	phosphatidylinositol 3 phosphate
pLys	Phospholysine
POI	Protein of interest
PPA	Potassium phosphoramidate
pSer	Phosphoserine
pThr	Phosphothreonine
PTM	Post-translational modification
pTyr	Phosphotyrosine
RR	Response Regulator
Ser	Serine
SILAC	Stable isotope labeling by amino acids in cell culture
SixA	Signal inhibitory factor-X
SPPS	Solid phase peptide synthesis
TBDPS	tert-butyldipnhnylsilyl
TCS	Two-component system
TEA	Triethylamine
TES	Triethylsilane
TFA	Trifluoroacetic acid
Thr	Threonine
TLC	Thin-layer chromatography
TMG	1,1,3,3-tetramethylguanidine
Trt	Triphenylmethyl, trityl
Tyr	Tyrosine

UV	Ultraviolet

Chapter 1. Introduction – Chemical Tools for Histidine Phosphorylation

1.1 Protein Phosphorylation

Proteins have important roles in living organisms. *In vivo*, they are synthesized from DNAs through several steps; DNAs (Deoxyribonucleic acids) are first transcribed into complementary mRNAs (messenger Ribonucleic acids), and proteins are synthesized from the mRNAs via translation. After proteins are synthesized, they can be covalently modified, and such phenomenon is called ***post-translational modification (PTM)***.

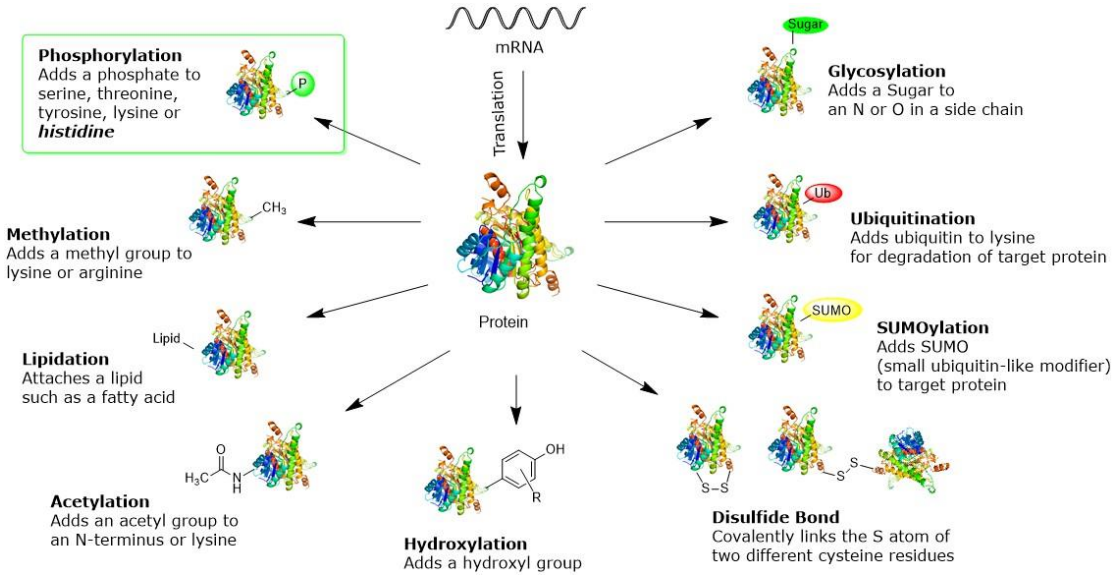

Figure 1-1. Post-translational modification

Protein phosphorylation[1,2] is an important PTM in biology; proteins are phosphorylated by protein kinases using ATP as a phosphate donor; the ATP is converted into ADP and one phosphate group is attached on the protein. The phosphorylation events can lead to the modulation of enzymatic activities or the association with other proteins on the phosphorylated residues in a sequence-specific manner. Also, the phosphate group on the phosphorylated proteins can be transferred to another proteins and signal is transduced. Hence, study of protein phosphorylation will be helpful for understanding of cellular functions and metabolisms.

1.2 Protein Histidine Phosphorylation

Among 20 kinds of amino acids, protein phosphorylation on serine, threonine and tyrosine residues are best known. However, histidine, lysine or arginine phosphorylation has been long known but they have been much less explored because of their chemical instability.[3,4)]

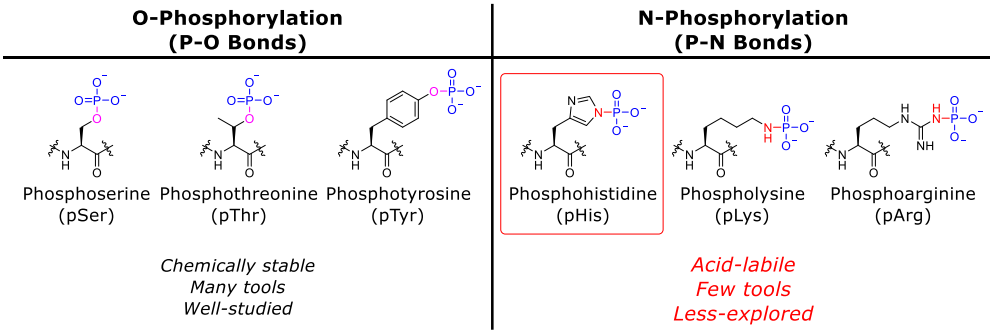

Figure 1-2. Protein phosphorylation on residues

Compared with phosphoserine (pSer), phosphothreonine (pThr) and phosphotyrosine (pTyr), phosphohistidine (pHis) has low stability since N-P bond has higher energy than O-P bond. ΔG of hydrolysis of pHis is -12 to 13 kcal/mol whereas hydroxyamino acids have -6.5 to -9.5 kcal/mol. pHis has acidic-labile characteristics; nitrogen in phosphohistidine can be easily protonated than oxygen in pSer, pTyr and pThr phosphoester, and the imidazole group can be a good leaving group for the hydrolysis of the N-P bond

1.3 Biological Function of Protein Histidine Phosphorylation

1.3.1 Two-component System (TCS)[5)]

Phosphorylation of histidine residues is well known in so-called two-component signal transduction systems (TCSs), which are important signaling systems in prokaryotes, as well as in plants and fungi. TCSs consist of histidine kinases (HKs) and response regulators (RRs). Basically, histidine kinases are receptor-like proteins on bacterial cellular membrane and bear sensor domains on the extracellular side. When sensor domains are stimulated, histidine kinases undergo conformational changes and its catalytic kinase domain (CA domain) gets activated, which then autophosphorylates a histidine residue of the dimerization domain (DHp domain). One example of histidine kinase is **CheA** involved in bacterial chemotaxis. **CheA** exists in intracellular cytoplasm not in cellular membrane. It does not bear a sensor domain, but interacts with the cytoplasmic domains of many chemoreceptors.

The phosphoryl group on the pHis of the HK then gets transferred to an Asp residue of a receiver domain in RR protein, and signaling process is continued. The phosphorylated of RR induces a conformational change of effector domain, to bind into DNA and control transcription process or to activate its own enzymatic activity for downstream signaling transduction.

1.3.2 Phosphohistidine Phosphatase in TCSs[6)]

Along with the studies of His kinases, studies of phosphohistidine phosphatases have been carried out. An *E. coli* phosphohistidine phosphatase that specifically catalyzes the dephosphorylation of $pHis^{717}$ in HPt domain of ArcB, which is a histidine kinase of TCS, was investigated and designated as signal inhibitory factor-X (SixA). SixA is a 17.2 kDa protein which has two histidine residues, His^{8} and His^{108}, and His^{8}, included in arginine-histidine-glycine (RHG) motif, is crucial for enzymatic ability demonstrated by the loss of function from the mutant protein lacking His^{8}. When His^{717} in HPt is phosphorylated, phosphohistidine becomes a phosphate donor for the OmpR response regulator, which is a transcriptional regulator in the osmoregulation of porin composition of the E. coli outer membrane. Hence, SixA works as a modulator in phosphorelay system of prokaryotes.

1.3.3 Nucleoside Diphosphate Kinase (NDPK) in Eukaryotes

There have been a number of studies focusing on protein histidine phosphorylation in mammalian cells. So far, the best known protein histidine kinases are two isoforms of NDPK (Nucleoside Diphosphate Kinase); NDPK-A (Nm23H1)[7)] and NDPK-B (NM23H2)[8,9)]. NDPK-A has been reported to phosphorylate annexin 1 on a histidine residue[10,11)] and NDPK-B is responsible for the His phosphorylation in KCa3.1 potassium channel and its activation.[9,12)] Also, NDPK-B phosphorylates His^{266} in the β-subunit (G_β) of trimeric G-proteins and helps the activation of G_s by transferring the phosphoryl group to GDP and forming GTP which binds to alpha-subunit of G_s and activates it.[8,13)]

With maintaining NDP/NTP levels, NDPK transfers phosphoryl groups from NTP to NDP through autophosphorylation of a His residue in its active site (His^{118} in human NDPK).[14)] Yet, it is unclear how it can phosphorylate histidine residues in other proteins.

1.3.4 Ca^{2+}-activated K^+ Channel KCa3.1

The Ca^{2+}-activated K^+ Channel KCa3.1, which is composed of 370 amino acids, is responsible for the influx of Ca^{2+}, which leads to the activation of T cells and B cells.[9,15)] KCa3.1 was found in blood cells, epithelia, and smooth muscle cells, and its function is the replacement of cytosolic Ca^{2+} into K^+ and thereby it controls the membrane potential to balance with K^+

equilibrium potential.[16-19] This change of membrane potential can affect various physiological responses in many types of cells, such as mitogen activation of T-lymphocytes, and regulation of cell volume in erythrocytes, Cl^- secretion in exocrine epithelial cells and proliferation of T and B cells, vascular smooth muscle cells and keratinocytes.[20-27] Pharmacological targeting of KCa3.1 channel is expected to have effects in proliferative diseases and autoimmune diseases, such as restenosis, transplant rejection, secretory diarrheas, sickle cell anemia, cystic fibrosis, etc.[17,18,25,28] Comparing with its homologues, KCa3.1 has a unique sequence of 14 amino acids on C-terminus and this sequence has a binding affinity to NDPK-B. In fact, NDPK-B phosphorylates KCa3.1 at His^{358} with regulation by phosphatidylinositol 3 phosphate (PI(3)P) and the phosphorylation event activates KCa3.1.

1.3.5 Histone H4

Histones are DNA-binding proteins in the nucleus. Compared with other proteins, they have lots of arginine, lysine and histidine amino acids, which are positively charged in physiological conditions around pH 7. As DNA is negatively charged, histones with positive charges electrostatically bind to DNA. In regenerating rat liver cells, it was found that two kinases catalyzed phosphorylation to form acid-labile and alkali-stable protein phosphates on histone H1 and H4, and it was subsequently confirmed as pHis in histone H4 whereas phospholysine in histone H1.[29,30] Histone H4 contains two histidine residue sites, His^{18} and His^{75}. Yet, it is unclear which position is phosphorylated by histone histidine kinases, and the specific histone histidine kinases are still remained elusive. The biological effect of histidine phosphorylation on histone is not fully demonstrated, but it is expected to regulate gene activation, DNA replication or mitosis

1.3.6 Summary of Known Phosphohistidine Proteins in Biology

Roles	Proteins
Intermediate of enzymes in phosphotransfer to other components	Nucleoside diphosphate kinase (NDPK)[31,32], ATP-citrate lyase[33], Glucose-6-phosphate[34], 6-Phosphofructo-2-kinase[35], Phosphoglycerate mutase[36,37], Phospholipase D[38], Prostatic acid phosphatase[39], Succinyl-CoA synthetase[40]
Substrates of histidine kinases	Annexin I[10], ATP-citrate lyase[41], Heterotrimeric G protein[8,42,43,44], Histone H4[30,45,46], KCa3.1 potassium channel[9,15], Thymidylate synthase[47]

Histidine Kinases	Two-component signaling pathways[48,49,50,51] , NDPK[8,9,41], Histone H4 histidine kinase[29,52,53,54,55]
Phosphohistidine Phosphatases	PHPT1[56,57,58], Protein phosphatase 1A, 2A, and 2C[59,60]

1.4 Methods for Studying Phosphohistidine

1.4.1 Preparation of Phosphohistidine[61]

Phosphohistidine can be prepared chemically using potassium phosphoramidate (PPA) at pH 7. Phosphohistidine-containing polypeptides can be prepared by PPA-mediated chemical phosphorylation. Potassium phosphoramidate does not phosphorylate any other amino acid residues at neutral pH. For protein autophosphorylation, bacterial histidine kinases and ATP can be utilized.

1.4.2 Detection - Isotope-labeling ^{32}P and Amino Acid Analysis[62,63]

Conventional method for protein quantity was an amino acid analysis. Generally, protein of interest was hydrolyzed by strong acid at high temperature (such as, 6M HCl, 110 ^{O}C, 24 hours). The POI was hydrolyzed into single amino acids and these were analyzed quantitatively by HPLC or electrophoresis. In case of phosphohistidine proteins, however, acid hydrolysis was not suitable since phosphohistidine is acid-labile and base-stable. Thus, base hydrolysis was adopted, of which condition was under 3M KOH at 105 ^{O}C for 3 hours.

[γ-^{32}P]ATP was generally used to make isotope-labeled phosphoproteins and useful for protein kinase assay. POI was incubated with [γ-^{32}P]ATP and its kinase with appropriate physiological condition. Phosphoimage in electrophoresis or radioactivity test easily defined isotope-labeled phosphoproteins.

On the other hand, phosphorylation could occur on histidine as well as on serine, threonine and tyrosine residues. While pTyr is are stable both in acid and base, pSer and pThr are unstable under basic conditions. Since pHis is stable in base but labile in acid, it can be indirectly distinguished from pSer, pThr, or pTyr by acid/base treatment.

1.4.3 Detection - Mass Spectrometry[64]

Mass spectrometry (MS) analysis is fundamental in many of chemistry research. There have been few reports of using MS analysis for detection of pHis proteins because of its acid-lability. Synthetic pHis-peptide was analyzed by matrix-associated laser desorption ionization

(MALDI)-high-energy collision-induced dissociation (CID) MS and electrospray ionization (ESI) MS. For example, histone H4 was phosphorylated chemically using potassium phosphoramidate, and two histidine residues were phosphorylated. Then, it was digested by trypsin or endoproteinase Asp-N and two different pHis-containing fragments were detected.

1.4.4 Detection - Antibodies and Western Blots[65,66]

Antibodies have specific and strong interactions with their respective antigens and are utilized in specific detection and quantification method such as ELISA and western blots. Generally, an immunogen gets injected into animals such as rabbits and mice and the antibodies against the immunogen are generated. Then, serum from the animals is affinity-purified to provide the desired antibodies. In case of small antigens, they are conjugated with carrier proteins which are immunogenic, called haptens, and the conjugated materials are injected. However, the generation of pHis-specific antibodies was extremely challenging because pHis was not stable immunization *in vivo*. To address this challenge, stable synthetic pHis analogues were designed and prepared by Kee *et. al.* and it was successfully employed to generate anti-pHis antibodies.

These antibodies marked an important milestone in pHis research, since they enabled specific detection and quantification of pHis proteins. Using these antibodies, novel pHis proteins from *E. coli* have been discovered and enzymatic phosphorylation assays were successfully carried out.

1.5 Conclusion and Future perspectives

Protein phosphorylation is one of important event above post-translational modification. Histidine phosphorylation was first observed over 50 years ago, but its research lagged behind compared with serine/threonine/tyrosine phosphorylation because of the acid-lability and lack of detection tools of phosphohistidine. There have been many attempts to devise detection method for phosphohistidine, but simple and real time methods for measuring pHis levels are required. In Chapter 2, we will describe our progress on the development of fluorescence-based chemical probes for real-time measurement of histidine kinases and pHis phosphatase enzyme activities.

1.6 Reference

1) Tarrant, M. K.; and Cole, P. A. The Chemical Biology of Protein Phosphorylation. *Ann. Rev. Biochem.* **2009**, 78, 797–825
2) Hunter, T. Why Nature Chose Phosphate to Modify Proteins. *Phil. Trans. Royal So. B: Biol. Sci.* **2012**, *367* (1602), 2513–2516
3) Kee, J.-M.; and Muir, T. W. Chasing Phosphohistidine, an Elusive Sibling in the Phosphoamino Acid Family. *ACS Chem. Biol.* **2012**, *7* (1), 44–51
4) Attwood, P. V.; Piggott, M. J.; Zu, X. L.; and Besant, P. G. Focus on Phosphohistidine. *Amino Acids* **2007**, *32* (1), 145–156
5) Attwood, P. V. Histidine Kinases from Bacteria to Humans. *Biochem. Soc. Trans.* **2013**, *41* (4), 1023–1028
6) Attwood, P. V. P-N Bond Protein Phosphatases. *Biochim. Biophys. Acta.* **2013**, *1834* (1), 470–478
7) Wagner, P. D.; Steeg, P. S.; and Vu, N. D. Two-component kinase-like activity of nm23 correlates with its motility-suppressing activity. *Proc. Natl. Acad. Sci. U.S.A.* **1997**, *94*, 9000-9005
8) Cuello, F.; Schulze, R. A.; Heemeyer, F.; Meyer, H. E.; Lutz, S.; Jakobs, F.; Niroomand, K. H.; and Wieland, T. Activation of heterotrimeric G proteins by a high energy phosphate transfer via nucleoside diphosphate kinase (NDPK) B and G_{β} subunits: complex formation of NDPK B with $G_{\beta\gamma}$ dimers and phosphorylation of His-266 in G_{β}. *J. Biol. Chem*. **2003**, *278*, 7220-7226
9) Srivastava, S.; Li, Z.; Ko, K.; Choudhury, P.; Albaqumi, M.; Johnson, A. K.; Yan, Y.; Backer, J. M.; Unutmaz, D.; Coetzee, W. A.; and Skolnik, E. Y. Histidine phosphorylation of the potassium channel KCa3.1 by nucleoside diphosphate kinase B is required for activation of KCa3.1 and CD4 T cells. *Mol. Cell* **2006**, *24*, 665-675
10) Muimo, R.; Hornickova, Z.; Riemen, C. E.; Gerke, V.; Matthews, H. R.; and Mehta, A. Histidine phosphorylation of annexin I in airway epithelia. *J. Biol. Chem.* **2000**, *275*, 36632–36636
11) Treharne, K. J.; Riemen, C. E.; Marshall, L. J.; Muimo, R.; and Mehta, A. Nucleoside diphosphate kinase-A component of the $[Na^+]$- and $[Cl^-]$-sensitive phosphorylation cascade in human and murine airway epithelium. *Pflügers Arch* **2001**. *443*, (Suppl. 1), S97–S102
12) Di, L.; Srivastava, S.; Zhdanova, O.; Sun, Y.; Li, Z.; and Skolnik, E. Y. Nucleoside diphosphate kinase B knock-out mice have impaired activation of the K^+ channel KCa3.1, resulting in defective T cell activation. *J. Biol. Chem.* **2010**, *285*, 38765–38771
13) Hippe, H. J.; Lutz, S.; Cuello, F.; Knorr, K.; Vogt, A.; Jakobs, K. H.; Wieland, T.; and Niroomand, K. H. Activation of heterotrimeric G proteins by a high energy phosphate transfer

via nucleoside diphosphate kinase (NDPK) B and G_β subunits: specific activation of $G_s\alpha$ by an NDPK B–$G_{\beta\gamma}$ complex in H10 cells. *J. Biol. Chem.* **2003***, 278*, 7227–7233

14) Giraud, M-F.; Georgescauld, F.; Lascu, I.; and Dautant, A. Crystal structures of S120G mutant and wild type of human nucleoside diphosphate kinase A in complex with ADP. *J. Bioeng. Biomembr*. **2006**, *38*, 261–264

15) Srivastava, S.; Choudhury, P.; Li, Z.; Liu, G.; Nadkarni, V.; Ko, K.; Coetzee, W. A.; and Skolnik, E. Y. Phosphatidylinositol 3-phosphate indirectly activates KCa3.1 via 14 amino acids in the carboxy terminus of KCa3.1. *Mol. Biol. Cell* **2006**, *17*, 146−154.

16) Bond, C. T.; Maylie, J.; and Adelman, J. P. Small-conductance calcium-activated potassium channels. *Ann. N.Y. Acad. Sci.* **1999**, *868*, 370–378.

17) Jensen, B. S.; Strobaek, D.; Olesen, S. P.; and Christophersen, P. The Ca^{2+}-activated K^+ channel of intermediate conductance: a molecular target for novel treatments? *Curr. Drug Targets* **2001**, *2*, 401–422

18) Wulff, H.; Beeton, C.; and Chandy, K. G. Potassium channels as therapeutic targets for autoimmune disorders. *Curr. Opin. Drug Discov. Devel.* **2003**, *6*, 640–647.

19) Stocker, M. Ca^{2+}-activated K^+ channels: molecular determinants and function of the SK family. *Nat. Rev. Neurosci.* **2004**, *5*, 758–770.

20) Fanger, C. M.; Rauer, H.; Neben, A. L.; Miller, M. J.; Wulff, H.; Rosa, J. C.; Ganellin, C. R.; Chandy, K. G.; and Cahalan, M. D. Calcium-activated potassium channels sustain calcium signaling in T lymphocytes. Selective blockers and manipulated channel expression levels. *J. Biol. Chem.* **2001**, *276*, 12249–12256.

21) Ghanshani, S.; Wulff, H.; Miller, M. J.; Rohm, H.; Neben, A.; Gutman, G. A.; Cahalan, M. D.; and Chandy, K. G. Up-regulation of the IKCa1 potassium channel during T-cell activation. Molecular mechanism and functional consequences. *J. Biol. Chem.* **2000**, *275*, 37137–37149

22) Khanna, R.; Chang, M. C.; Joiner, W. J.; Kaczmarek, L. K.; and Schlichter, L. C. hSK4/hIK1, a calmodulin-binding KCa channel in human T lymphocytes. Roles in proliferation and volume regulation. *J. Biol. Chem.* **1999**, *274*, 14838–14849

23) Koegel, H.; and Alzheimer, C. Expression and biological significance of Ca^{2+}-activated ion channels in human keratinocytes. *FASEB J.* **2001**, *15*, 145–154.

24) Köhler, R.; Wulff, H.; Eichler, I.; Kneifel, M.; Neumann, D.; Knorr, A.; Grgic, I.; Kämpfe, D.; Si, H.; Wibawa, J.; Real, R.; Borner, K.; Brakemeier, S.; Orzechowski, H. D.; Reusch, H. P.; Paul, M.; Chandy, K. G.; and Hoyer, J. Blockade of the intermediate-conductance calcium activated potassium channel as a new therapeutic strategy for restenosis. *Circulation* **2003**, *108*, 1119–1125.

25) Maher, A. D.; and Kuchel, P. W. The Gardos channel: a review of the Ca^{2+}-activated K^+ channel in human erythrocytes. *Int. J. Biochem. Cell Biol.* **2003**, *35*, 1182–1197.

26) Ouadid-Ahidouch, H.; Roudbaraki, M.; Delcourt, P.; Ahidouch, A.; Joury, N.; and Prevarskaya, N. Functional and molecular identification of intermediate-conductance Ca(2+)-activated K(+) channels in breast cancer cells: association with cell cycle progression. *Am. J. Physiol.* **2004**, *287*, C125–C134.

27) Wulff, H.; Knaus, H. G.; Pennington, M.; and Chandy, K. G. K^+ channel expression during B cell differentiation: implications for immunomodulation and autoimmunity. *J. Immunol.* **2004**, *173*, 776–786.

28) Rufo, P. A.; Merlin, D.; Riegler, M.; Ferguson-Maltzman, M. H.; Dickinson, B. L.; Brugnara, C.; Alper, S. L.; and Lencer, W. I. The antifungal antibiotic, clotrimazole, inhibits chloride secretion by human intestinal T84 cells via blockade of distinct basolateral K? conductances. Demonstration of efficacy in intact rabbit colon and in an in vivo mouse model of cholera. *J. Clin. Investig.* **1997**, 100, 3111–3120

29) Smith, D. L.; Chen, C. C.; Bruegger, B. B.; Holtz, S. L.; Hal-pern, R. M.; and Smith, R. A. Characterization of Protein Kinases Forming Acid-Labile Histone Phosphates in Walker-256 Carcinosarcoma Cell Nuclei, *Biochemistry* **1974**, *13*, 3780.

30) Chen, C. C.; Smith, D. L.; Bruegger, B. B.; Halpern, R. M.; and Smith, R. A. Occurrence and distribution of acid-labile histone phosphates in regenerating rat liver. *Biochemistry* **1974**, *13*(18), 3785–3789

31) Kimura, N.; Shimada, N.; Ishijima, Y.; Fukuda, M.; Takagi, Y.; and Ishikawa, N. Nucleoside diphosphate kinases in mammalian signal transduction systems: recent development and perspective. *J. Bioenerg. Biomembr.* **2003**, *35*,41−47.

32) Walinder, O. Identification of a phosphate-incorporating protein from bovine liver as nucleoside diphosphate kinase and isolation of 1-^{32}P-phosphohistidine 3-^{32}P-phosphohistidine and N- ε-^{32}P-phospholysine from erythrocytic nucleoside diphosphate kinase incubated with adenosine triphosphate-^{32}P. *J. Biol. Chem.* **1968**, *243*, 3947− 3952.

33) Williams, S.; Sykes, B.; and Bridger, W. Phosphorus-31 nuclear magnetic-resonance study of the active-site phosphohistidine and regulatory phosphoserine residues of rat-liver ATP-citrate lyase. *Biochemistry* **1985**, *24*, 5527−5531.

34) Ghosh, A.; Shieh, J.-J.; Pan, C.-J.; and Chou, J. Y. Histidine 167 is the phosphate acceptor in glucose-6-phosphatase-*β* forming a phosphohistidine enzyme intermediate during catalysis. *J. Biol. Chem.* **2004**, *279*, 12479−12483.

35) Pilkis, S. J.; Regen, D. M.; Stewart, H. B.; Pilkis, J.; Pate, T. M.; and El-Maghrabi, M. R. Evidence for two catalytic sites on 6- phosphofructo-2-kinase/fructose 2,6-bisphosphatase.

Dynamics of substrate exchange and phosphoryl enzyme formation. *J. Biol. Chem.* **1984**, *259*, 949−958.

36) Rose, Z. B. Evidence for a phosphohistidine protein intermediate in the phosphoglycerate mutase reaction. Arch. *Biochem. Biophys.* **1970**, *140*, 508−513.

37) Vander Heiden, M. G.; Locasale, J. W.; Swanson, K. D.; Sharfi, H.; Heffron, G. J.; Amador-Noguez, D.; Christofk, H. R.; Wagner, G.; Rabinowitz, J. D.; Asara, J. M.; and Cantley, L. C. Evidence for an alternative glycolytic pathway in rapidly proliferating cells. *Science* **2010**, *329*, 1492−1499.

38) Gottlin, E. B.; Rudolph, A. E.; Zhao, Y.; Matthews, H. R.; and Dixon, J. E. Catalytic mechanism of the phospholipase D superfamily proceeds via a covalent phosphohistidine intermediate. *Proc. Natl. Acad. Sci. U.S.A.* **1998**. *95*, 9202−9207.

39) Ostrowski, W. Isolation of τ-phosphohistidine from a phosphoryl-enzyme intermediate of human prostatic acid-phosphatase. *Biochim. Biophys. Acta* **1978**, *526*, 147−153.

40) Boyer, P. D.; Peter, J. B.; Ebner, K. E.; Deluca, M.; and Hultquist, D. Identification of phosphohistidine in digests from a probable intermediate of oxidative phosphorylation. *J. Biol. Chem.* **1962**, *237*, 3306−3308.

41) Wagner, P. D.; and Vu, N. D. Phosphorylation of ATP- citrate lyase by nucleoside diphosphate kinase. *J. Biol. Chem.* **1995**, *270*, 21758−21764

42) Wieland, T.; Nürnberg, B.; Ulibarri, I.; Kaldenberg-Stasch, S.; Schultz, G.; and Jakobs, K. H. Guanine nucleotide-specific phosphate transfer by guanine nucleotide-binding regulatory protein *β*-subunits. Characterization of the phosphorylated amino acid. *J. Biol. Chem.* **1993**, *268*, 18111−18118.

43) Hippe, H.-J.; Wolf, N. M.; Abu-Taha, I.; Mehringer, R.; Just, S.; Lutz, S.; Niroomand, F.; Postel, E. H.; Katus, H. A.; Rottbauer, W.; and Wieland, T. The interaction of nucleoside diphosphate kinase B with Gβγ dimers controls heterotrimeric G protein function. *Proc. Natl. Acad. Sci. U.S.A.* **2009**, *106*, 16269−16274

44) Kowluru, A. Identification and characterization of a novel protein histidine kinase in the islet beta cell: evidence for its regulation by mastoparan, an activator of G-proteins and insulin secretion. *Biochem. Pharmacol.* **2002**, *63*, 2091−2100.

45) Chen, C. C.; Bruegger, B. B.; Kern, C. W.; Lin, Y. C.; Halpern, R. M.; and Smith, R. A. Phosphorylation of nuclear proteins in rat regenerating liver. *Biochemistry* **1977**, *16*, 4852−4855.

46) Fujitaki, J. M.; Fung, G.; Oh, E. Y.; and Smith, R. A. Characterization of chemical and enzymatic acid-labile phosphorylation of histone H4 using phosphorus-31 nuclear magnetic resonance. *Biochemistry* **1981**, *20*, 3658−3664.

47) Fraczyk, T.; Ruman, T.; Rut, D.; Dabrowska-Mas, E.; Ciesla, J.; Zielinski, Z.; Sieczka, K.; Debski, J.; Golos, B.; Winska, P.; Walajtys-Rode, E.; Shugar, D.; and Rode, W. Histidine phosphorylation, or tyrosine nitration, affect thymidylate synthase properties. *Pteridines* **2009**, *20*, 137−142.

48) Khorchid, A.; and Ikura, M. Bacterial histidine kinase as signal sensor and transducer. *Int. J. Biochem. Cell Biol.* **2006**, *38*, 307−312.

49) Stock, A. M.; Robinson, V. L.; and Goudreau, P. N. Two-component signal transduction. *Annu. Rev. Biochem.* **2000**, *69*, 183−215.

50) Kruppa, M.; and Calderone, R. Two-component signal transduction in human fungal pathogens. *FEMS Yeast Res.* **2006**, *6*, 149−159.

51) Grefen, C.; and Harter, K. Plant two-component systems: principles, functions, complexity and cross talk. *Planta* **2004**, *219*, 733−742.

52) Smith, D. L.; Bruegger, B. B.; Halpern, R. M.; and Smith, R. A. New histone kinases in nuclei of rat tissues. *Nature* **1973**, *246*, 103− 104.

53) Huang, J. M.; Wei, Y. F.; Kim, Y. H.; Osterberg, L.; and Matthews, H. R. Purification of a protein histidine kinase from the yeast Saccharomyces cerevisiae. The first member of this class of protein kinases. *J. Biol. Chem.* **1991**, *266*, 9023−9029.

54) Besant, P.; and Attwood, P. Detection of a mammalian histone H4 kinase that has yeast histidine kinase-like enzymic activity. *Int. J. Biochem. Cell Biol.* **2000**, *32*, 243−253.

55) Tan, E.; Besant, P. G.; Zu, X. L.; Turck, C. W.; Bogoyevitch, M. A.; Lim, S. G.; Attwood, P. V.; and Yeoh, G. C. Histone H4 histidine kinase displays the expression pattern of a liver oncodevelopmental marker. *Carcinogenesis* **2004**, *25*, 2083−2088.

56) Ek, P.; Pettersson, G.; Ek, B.; Gong, F.; Li, J. P.; and Zetterqvist, O. Identification and characterization of a mammalian 14-kDa phosphohistidine phosphatase. *Eur. J. Biochem.* **2002**, *269*, 5016−5023.

57) Maurer, A.; Wieland, T.; Meissl, F.; Niroomand, F.; Mehringer, R.; Krieglstein, J.; and Klumpp, S. The β-subunit of G proteins is a substrate of protein histidine phosphatase. *Biochem. Biophys. Res. Commun.* **2005**, *334*, 1115−1120.

58) Klumpp, S.; Bechmann, G.; Mäurer, A.; Selke, D.; and Krieglstein, J. ATP-citrate lyase as a substrate of protein histidine phosphatase in vertebrates. *Biochem. Biophys. Res. Commun.* **2003**, *306*, 110−115.

59) Kim, Y.; Huang, J.; Cohen, P.; and Matthews, H. R. Protein phosphatases 1, 2A, and 2C are protein histidine phosphatases. *J. Biol. Chem.* **1993**, *268*, 18513−18518.

60) Matthews, H. R.; and MacKintosh, C. Protein histidine phosphatase activity in rat liver and spinach leaves. *FEBS Lett.* **1995**, *364*, 51−54.

61) Scharf, B. E. Summary of Useful Methods for Two-Component System Research. *Current Opinion in Microbiology* **2010**, *13*, 246–252.

62) Besant, P. G.; and Attwood, P. V. Detection and Analysis of Protein Histidine Phosphorylation. *Mol. Cell Biochem.* **2009**, *329*, 93–106.

63) Tan, E.; Zu, X. L.; Yeoh, G. C.; Besant, P. G.; and Attwood, P. V. Detection of Histidine Kinases via a Filter-Based Assay and Reverse-Phase Thin-Layer Chromatographic Phosphoamino Acid Analysis. *Anal Biochem* **2003**, *323*, 122–126.

64) Zu, X. L.; Besant, P. G.; Imhof, A.; and Attwood, P. V. Mass Spectrometric Analysis of Protein Histidine Phosphorylation. *Amino Acids* **2007**, *32*, 347–357.

65) Kee, J.-M.; Oslund, R. C.; Couvillon, A. D.; and Muir, T. W. A Second-Generation Phosphohistidine Analog for Production of Phosphohistidine Antibodies. *Org Lett* **2015**, *17*, 187–189.

66) Kee, J.-M.; Villani, B.; Carpenter, L. R.; and Muir, T. W. Development of Stable Phosphohistidine Analogues. *J. Am. Chem. Soc.* **2010**, *132* (41), 14327–14329.

67) Oslund, R. C.; Kee, J.-M.; Couvillon, A. D.; Bhatia, V. N.; Perlman, D. H.; and Muir, T. W. A Phosphohistidine Proteomics Strategy Based on Elucidation of a Unique Gas-Phase Phosphopeptide Fragmentation Mechanism. *J. Am. Chem. Soc.* **2014**, *136* (37), 12899–12911.

68) Kee, J.-M.; Oslund, R. C.; Perlman, D. H.; and Muir, T. W. A Pan-Specific Antibody for Direct Detection of Protein Histidine Phosphorylation. *Nature Chem. Biol.* **2013**, *9* (7), 416–421.

69) Fuhs, S. R.; Meisenhelder, J.; Aslanian, A.; Ma, L.; Zagorska, A.; Stankova, M.; Binnie, A.; Al-Obeidi, F.; Mauger, J.; Lemke, G.; Yates, J. R.; and Hunter, T. Monoclonal 1- and 3-Phosphohistidine Antibodies: New Tools to Study Histidine Phosphorylation. *Cell* **2015**, *162*, 198–210.

Chapter 2. Sox-Based Fluorescence Sensor for Phosphohistidine

2.1 Introduction

2.1.1 Need for Fluorescence-based Protein Phosphorylation Sensors

Intracellular phosphorylation is accomplished by enzymatic function of protein kinase against extracellular stimuli.[1-4] Phosphorylation has an important role in cellular metabolism as well as intercellular communication in eukaryotes.[5] Protein kinase superfamily accounts for approximately 2 % of the human genome and includes 500 kinases.[2] Protein kinases catalyze transferring of the γ-phosphoryl group from adenosine-5-triphosphate (ATP) to free a hydroxyl, amino, or imidazole group in the target peptide or protein[10,11]. For the operation of kinases, divalent metal ions[6-9], most commonly Mg^{2+}, are necessary as they activate the ATP and there are other many factors controlling the activity of kinases such as its phosphorylation state, subcellular localization or binding interactions within protein complexes.[24,25] Since protein kinase has a critical role and its malfunction results in severe diseases[12-16], protein kinase regulation has been of high interest and become a major therapeutic targets over past decades[17]. Indeed, many pharmaceutical and biotechnology companies have focused on the development of protein kinase inhibitors. Hence, specific and sensitive tools to measure the target kinase activities are essential in study of drug discoveries as well as signaling mechanisms[18-23].

A commonly used assay for protein kinase activity is a radioactivity-based assay in which phosphoryl group transfer from [γ-^{32}P]ATP to a peptide or protein substrate is quantified by scintillation counting. This method is discontinuous and requires the enzymatic reaction of kinase to be stopped for the subsequent processing steps. Thus, it does not provide direct kinetic information, requires special handling and generates radioactive waste. In addition, [γ-^{32}P]ATP is used for all kinases, so it is not applicable to simultaneous measurement of multiple kinases. Another phosphorylation detection method is using specific antibodies directly against phosphorylated residues, but it also needs post-reaction processing steps such as ELISA and Western blots after cell lysis.

Recently, fluorescence spectroscopy has been rising as a beneficial tool and become a major research tool in biological research because of its high sensitivity (up to a 1000-fold higher than absorption spectrometry), selectivity, experimental simplicity, short detection time and compatibility with standard instrumentation. Compared with traditional assays, fluorescence spectroscopy is applicable to continuous assays and gives an excellent spatial and temporal resolution *in cellulo* as well as observation of kinase activity in real time measurement.

2.1.2 Design and Strategy for CHEF-based Phosphorylation Sensors

To accomplish facile continuous and real-time histidine kinase activity, we chose Sox-based fluorescence chemosensors, which are peptide-based kinase substrates comprising non-natural Sox fluorophore[26,27]. As most kinases have their specific substrates, the peptide sequence is mimicked from the known substrate of the kinase of interest (KOI). By changing the kinase substrate sequence, various kinase sensors specific for each KOI can be prepared. Sox is the fluorophore 8-hydroxy-5-(*N,N*-dimethylsulfamoyl)-2-methylquinoline, which exhibits chelation-enhanced fluorescence (CHEF) by divalent metal ions. Sox was firstly devised for sensing divalent metal ions, especially for Zn^{2+} ion because of high chelation binding between Zn^{2+} ion and Sox molecule. Mg^{2+} ion shows weaker chelation binding than Zn^{2+} ion, but this mild binding makes it possible to apply Sox fluorophore in protein kinase sensor. When the peptide sensor is phosphorylated, the phosphoryl group assists Mg^{2+} ion to chelate Sox molecule. Sox molecule then shows increased fluorescence by CHEF effect. Accordingly, the fluorescence of the Sox molecule can tell us whether the peptide sensor is phosphorylated or not under same Mg^{2+} ion concentration and it is highly suitable as kinase chemosensor.

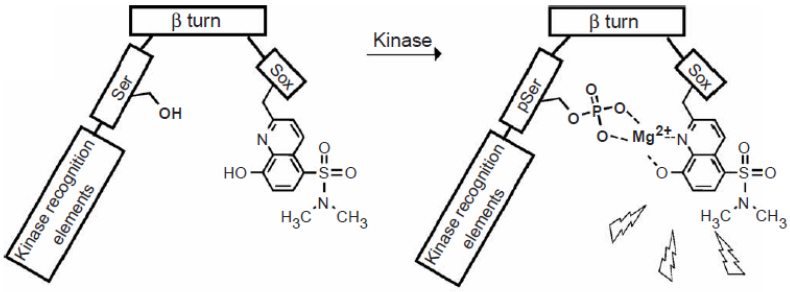

Figure 2-1. Kinase sensor for serine phosphorylation. *(*Shults *et. al., Nat. Meth.* **2005**)[33]

Shults *et. al.*[30] reported Sox-based peptide chemosensor of the kinase for hydroxyl group (serine/threonine/tyrosine) phosphorylation. However, Sox-based peptide chemosensor has not been applied into histidine phosphorylation. Since there was no real time assay for histidine phosphorylation, we designed Sox-based peptide chemosensor for histidine phosphorylation.

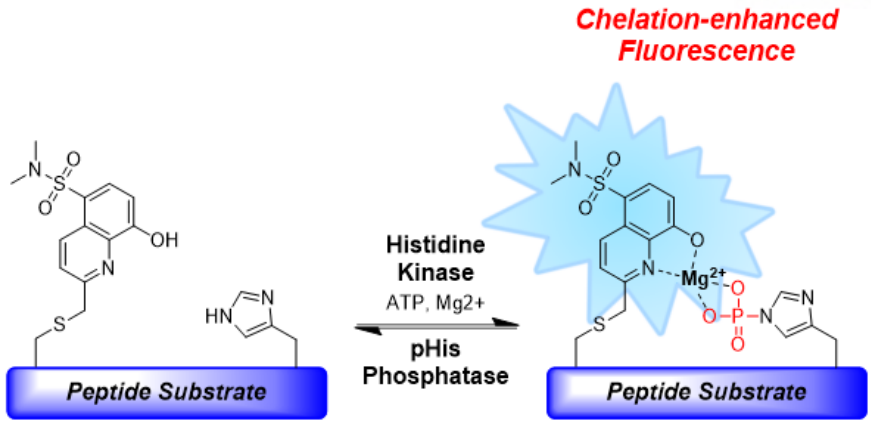

Figure 2-2. Design and Strategy for the kinase sensor for phosphohistidine

Previously, the peptide substrate was prepared using non-natural amino acid Fmoc-Sox-OH[29,30] via Solid Phase Peptide Synthesis (SPPS). Instead of non-natural amino acid, we used cysteine and it was reacted with Sox-halide to accomplish cysteine derivative of Sox fluorophore termed as CSox[27,31,32].

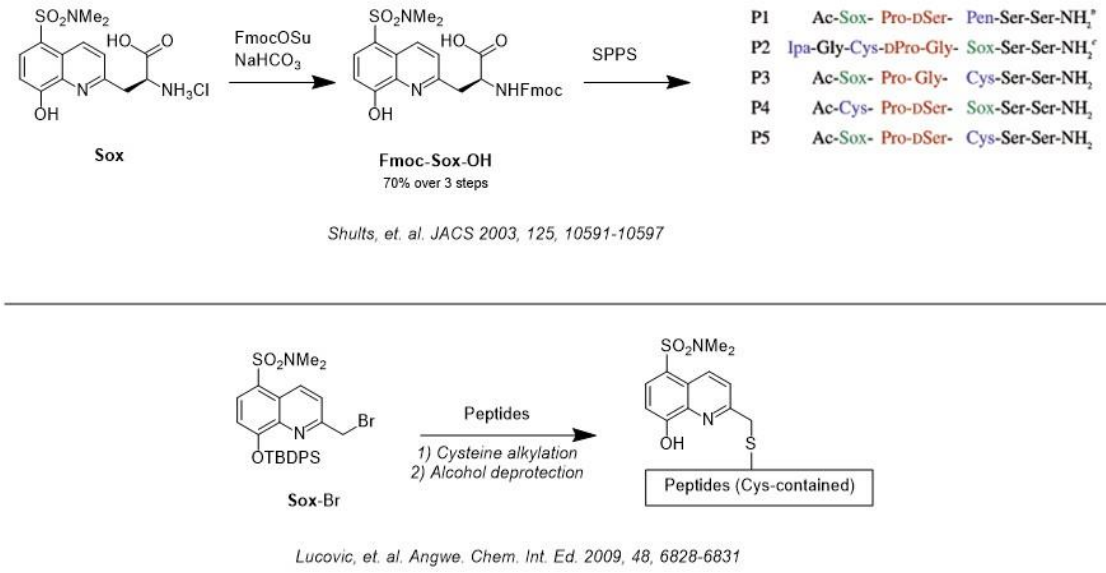

Figure 2-3. Two different approaches for Sox-contained kinase sensor;

1) Non-natural amino acid, Fmoc-Sox-OH and SPPS (up) and
2) Sox-Br and alkylation on Cysteine (down)

2.2 Result and Discussion

2.2.1 Preparation of Sox-Br

For cysteine modification, Sox bromide (Sox-Br, **7**) was synthesized following the methods by Imperiali's group with some improvements. In particular, Imperiali's group made Sox-Br (**7**) from compound **4** (3 steps) without chromatographic purification. However, we tried purification in each step; compound **5** was unable because of the high reactivity of aldehyde group, but compound **6** was isolated clean. In the step of Sox-Br (**7**) synthesis, N-bromosuccinimide (NBS) and triphenylphosphine were pre-mixed in dichloromethane and added dropwise into the perfectly dried compound **6**. To increase the reaction rate, we used the amount of NBS and triphenylphosphine as 5 molar equivalents against compound (**6**), and reaction time was decreased but the yield was moderate.

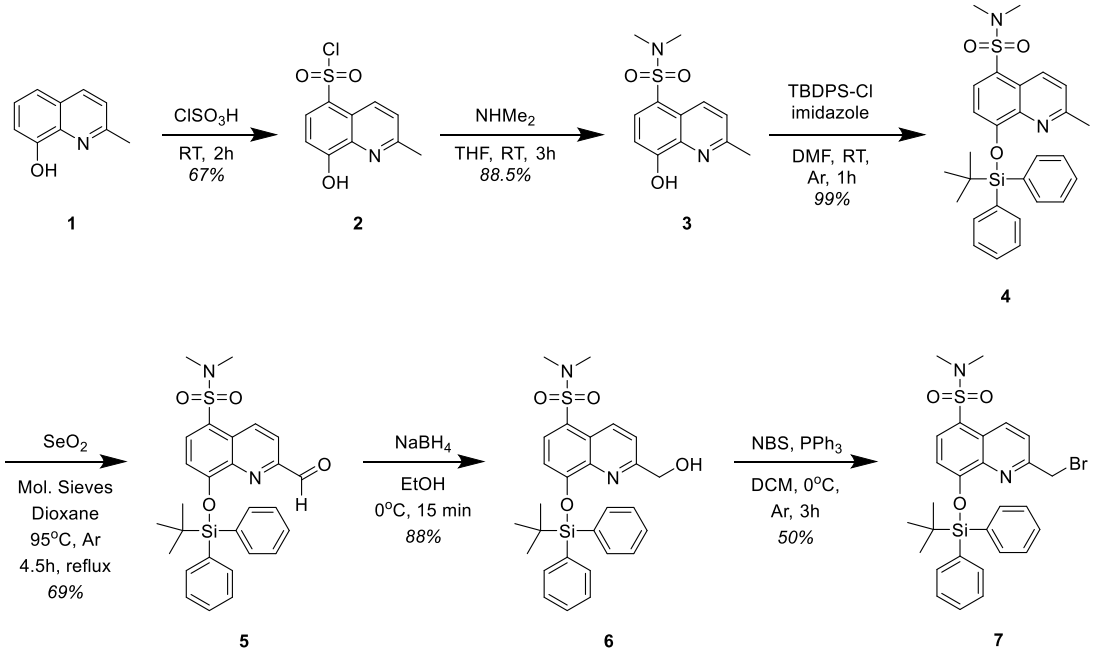

Scheme 2-1. *Synthesis of Sox-Br*

2.2.2 Design of Model substrate

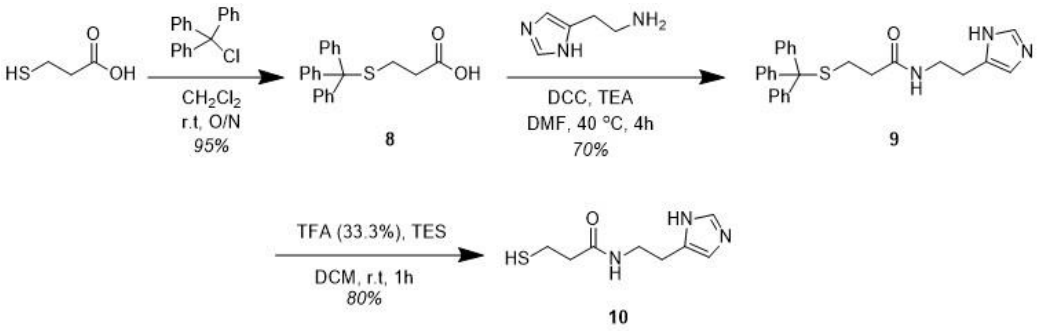

Scheme 2-2. *Synthesis of Model Substrate*

A model substrate (**10**), mimicking cysteine-histidine dipeptide, was synthesized to confirm whether 1) cysteine modification to construct CSox and phosphorylation of histidine-mimic imidazole were possible and 2) fluorescence was different after phosphorylation.

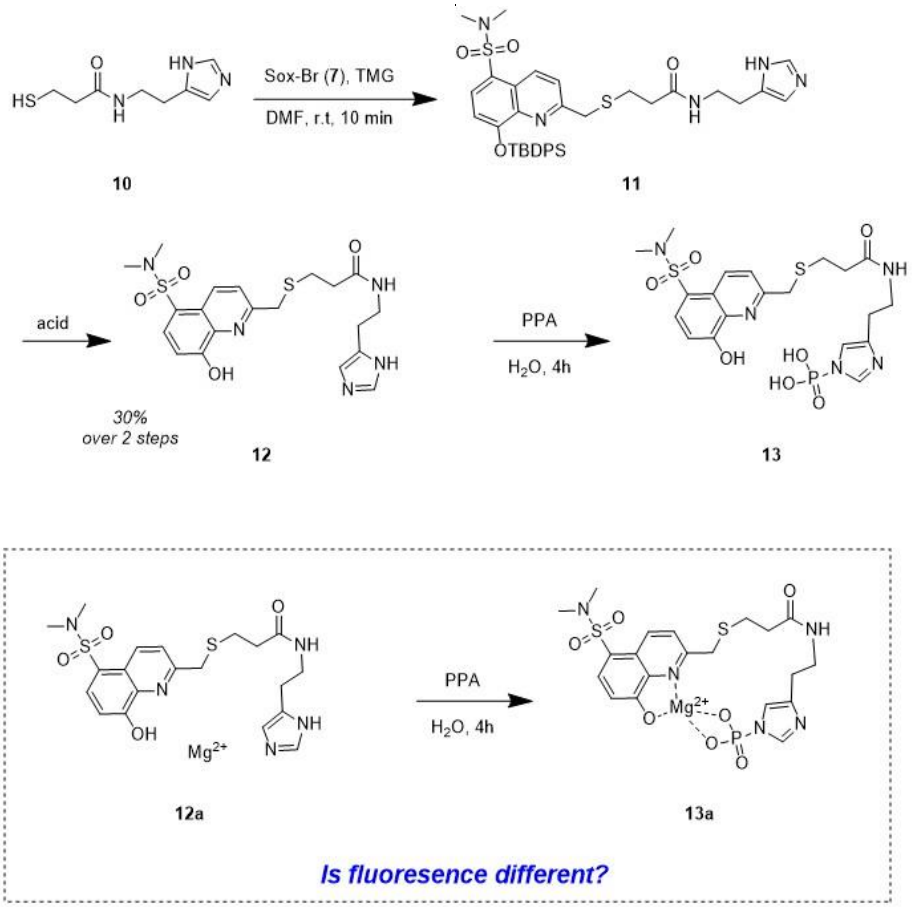

Scheme 2-3. *Synthesis of Model kinase sensor (**12**) and Phosphorylation (**13**)*

The model substrate (**10**) was alkylated with Sox-Br on the thiol to afford the model kinase sensor (**12**). It was then phosphorylated with PPA under Mg^{2+} and the fluorescence change was observed.

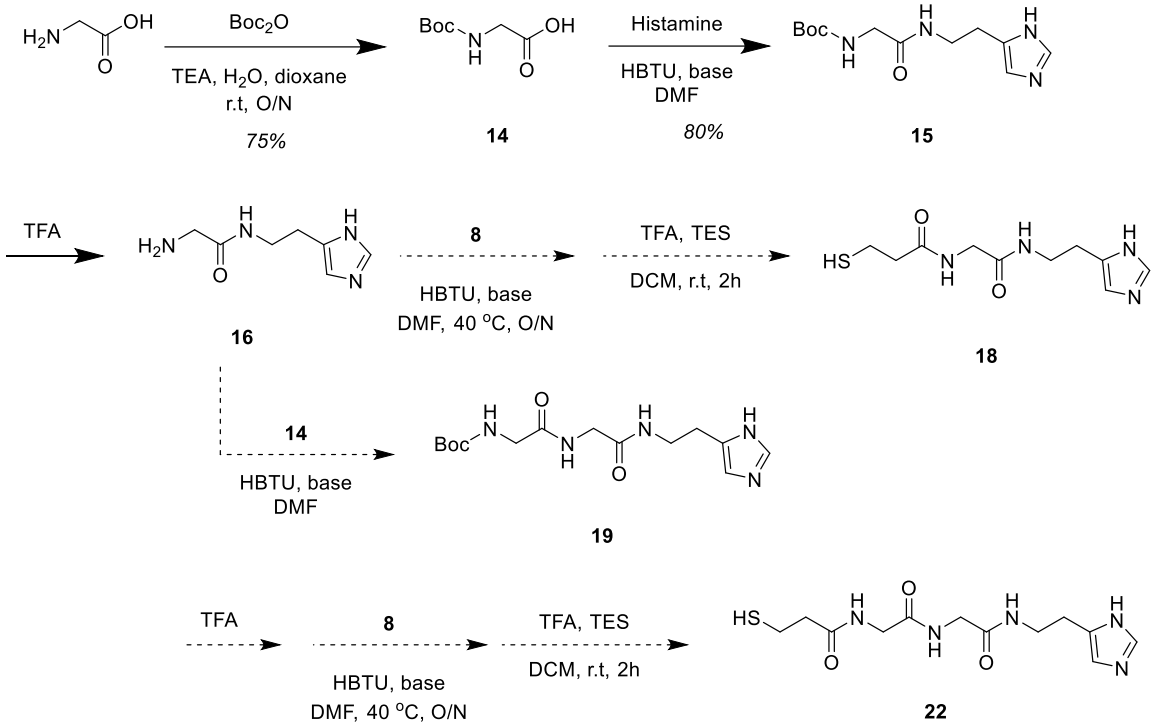

Scheme 2-4. *Other Two Model Substrates for Linker Optimization*

Also, two kinds of model substrates (**18** and **22**) were prepared to identify the length effect between CSox and Phosphorylimidazole in three-dimensional structure. To extend the length, we used a glycine linker.

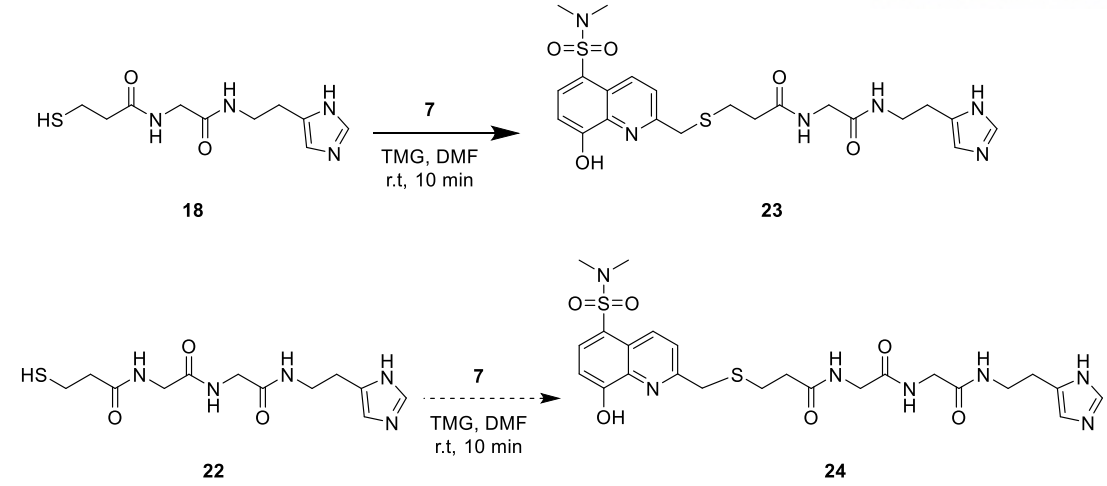

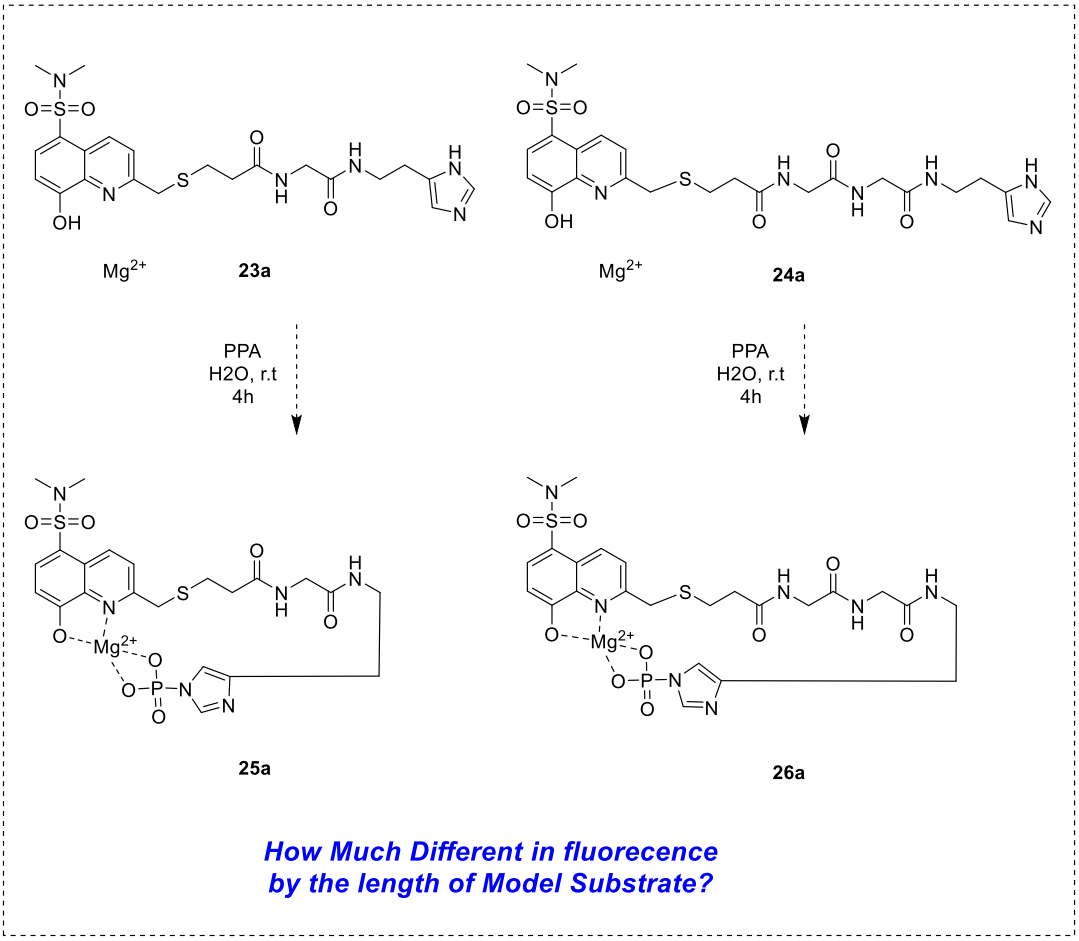

Scheme 2-5. *Linker-Dependent Fluorescence Difference*

Before designing the substrate sensors specific for KOI, simple model substrates were designed, synthesized and tested whether Sox and phosphorylation on histidine successfully emitted increased fluorescence.

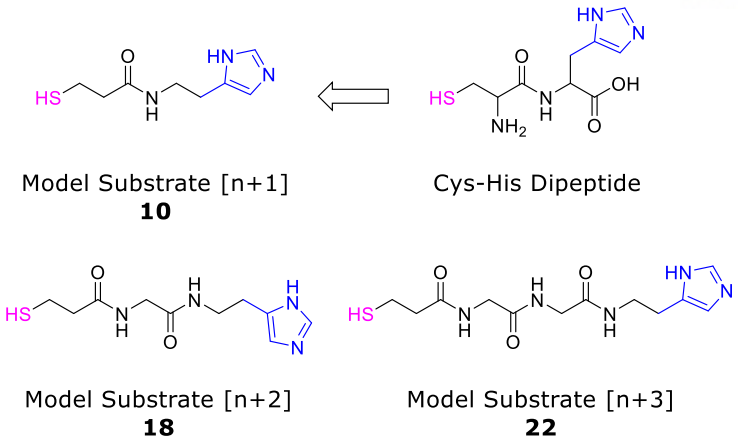

Figure 2-4. Design of the model substrates

Model substrates were targeted to short peptides which were parts of the substrate sensors of KOI. They should contain a cysteine to reacts with Sox-Br to form CSox and a histidine for pHis formation. Simplest model substrate was cysteine-histidine dipeptide. Generally, reactions with amino acids were hard to apply in solution phase reaction. Rather, they usually adopted Solid Phase Peptide Synthesis (SPPS). We tried to make model substrates in solution phase, and chose Cys-His dipeptide mimicked model substrate, which was the ligation of mercaptopropionic acid (MPA) and histamine [n+1]. This model substrate contained necessary residue groups, which were the thiol from cysteine and imidazole from histidine and discarded unnecessary parts.

On the other hand, three-dimensional distance was considered, and a glycine or a couple of glycine was inserted between MPA and histamine [n+2 and n+3].

2.2.3 Preparation of Model Substrates

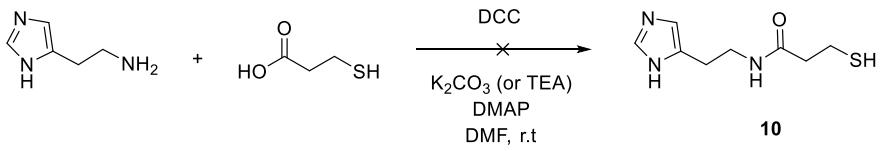

Scheme 2-6. *Coupling of histamine and 3-mercaptopropionic acid (failed)*

We began with the carboxylic acid coupling reaction between histamine and 3-mercaptoproponic acid (MPA). There are many kinds of commercially available coupling reagents activating carboxylic acids such as N,N'-dicyclohexylcarbodiimide (DCC), 1-Ethyl-3-(3-dimethylaminopropyl)carbodiimide (EDC) and HBTU (2-(1H-benzotriazol-1-yl)-1,1,3,3-tetramethyluronium hexafluorophosphate). We tried to use DCC, but the byproduct N,N'-dicyclohexylurea (DCU) from DCC was hard to remove after the reaction.

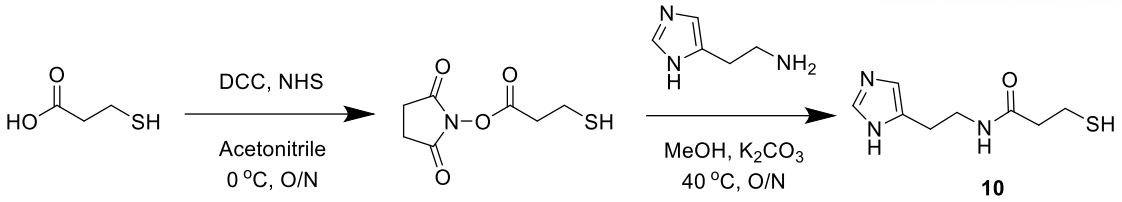

Scheme 2-7. *Coupling of histamine and 3-mercaptopropionic acid using DCC/NHS chemistry*

As DCC had relatively slow reactivity, we adapted DCC/NHS chemistry and divided the reaction into two steps. Interestingly, DCU is slightly soluble in hexane, dichloromethane, ethyl acetate or N,N-dimethylformamide and well-soluble in alcohols, but rarely soluble in acetonitrile. Using acetonitrile solvent, DCU was easily removed and the product was obtained quite pure. However, the final product was not obtained. According to the previous trials, controlling thiol group was much important than other factors, and we decided to protect free thiol group at first using trityl (triphenylmethyl) chloride.

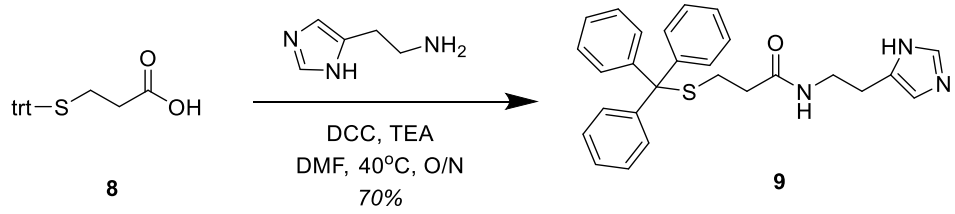

Scheme 2-8. *Coupling of histamine and trt-protected 3-mercaptopropionic acid*

Trityl protection was easily applied in 3-mercaptopropionic acid, and 3-tritylthiopropionic acid (**8**) was reacted with histamine. The product (**9**) was purified and confirmed by NMR. Using a base potassium carbonate, yield was lower than 20% and the reason was that histamine commercial source was di-hydrochloride salt form (histamine-2HCl) and the water formation between hydrochloric acid and potassium carbonate, which is an obstacle to DCC reactivity. Changing the base to triethylamine, yield was improved up to 70% with good purity.

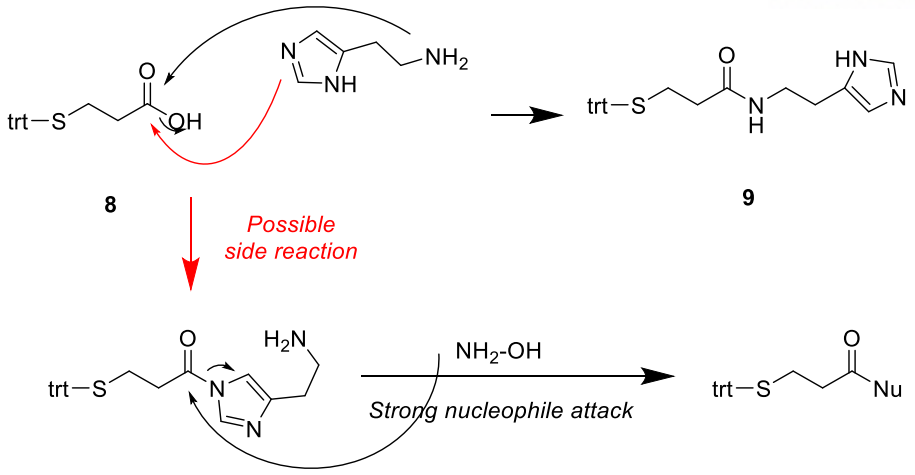

Figure 2-5. Possible side reaction and HA breakage test

Histamine has a primary amine as well as secondary amines, which are less reactive, but also possible to react with DCC-activated ester to form acyl imidazole. It was confirmed that strong nucleophile such as hydroxylamine was added and it may break acyl imidazole since imidazole is a good leaving group, whereas stable amide is unaffected.

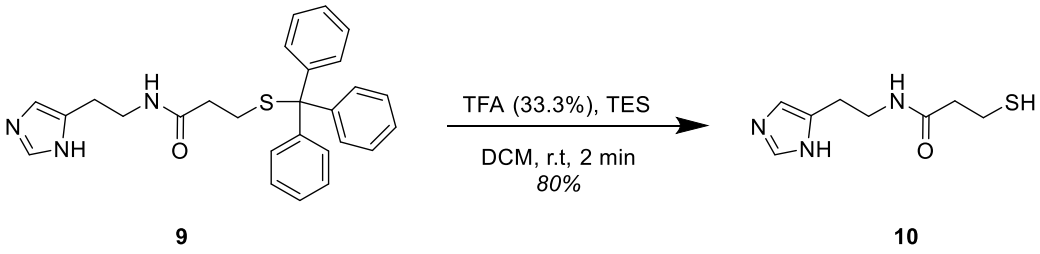

Scheme 2-9. *Trityl deprotection*

Trityl deprotection was successfully achieved by treating trifluoroacetic acid (TFA). Reaction was very fast and ended up within a couple of minutes. Then the reaction solvent (DCM) and TFA were removed by rotary evaporator. The remained residue which was the mixture of white solid and oil-like liquid was washed by hexane. The white solid, triphenylmethane, was dissolved in hexane and removed and the liquid, desired product, was not mixed with hexane and made a layer beneath hexane layer. The hexane was removed by pipet suction carefully and hexane wash was repeated several times.

2.2.4 **Preparation of Model Kinase Sensor**

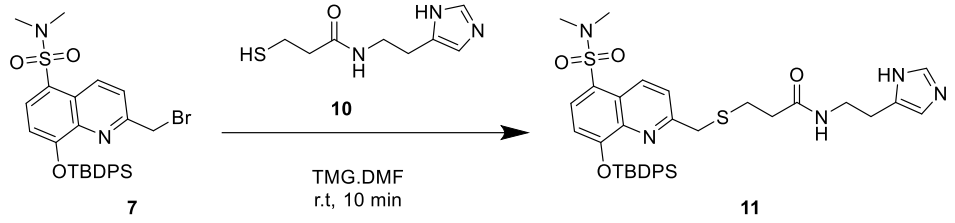

Scheme 2-10. *Sox-alkylation*

Now that the model substrate (**10**) and Sox-Br (**7**) were prepared, thiol alkylation was executed and model kinase sensor [n+1] (**11**) was prepared. But it was hard to get pure product using column chromatography, as the product trailed on TLC. Eventually, we purified the product by High-Performance Liquide Chromatography (HPLC, 100% solvent A (clean H_2O) to 30% solvent A (H_2O) and 70% solvent B (9:1 of MeCN and H_2O) in 15 minutes, T_R=13.1 min.), and obtained the pure product. Theoretically, however, the product should be compound **11**, but obtained product was compound **12**.

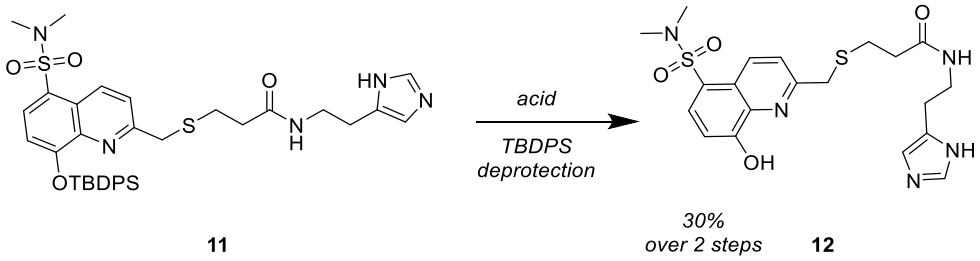

Scheme 2-11. *Preparation of Model kinase sensor*

Actually, we saved one step for the final product, but still do not fully understand why TBDPS protecting group was removed during Sox-alkylation. Yield of compound **12** was 30% over 2 steps. Later, my colleague tested the stability of Sox-Br in various base species; Sox-Br was degraded fast on TMG, but moderately stable in DIPEA; Sox-Br was degraded in 1 hour by TMG, but it was durable in 18 hours in DIPEA. I followed the method of Imperiali's group and insisted to use TMG for fast reaction, but DIPEA would be more proper base.

2.2.5 Linker Optimization of Model Kinase Sensors

A glycine linker was used to control the distance between Sox fluorophore and target histidine residue. We designed cysteine-glycine-histidine (Cys-Gly-His) and cysteine-glycine-glycine-histidine (Cys-Gly-Gly-His) mimics, that is, MPA-Gly-Histamine and MPA-Gly-Gly-Histamine.

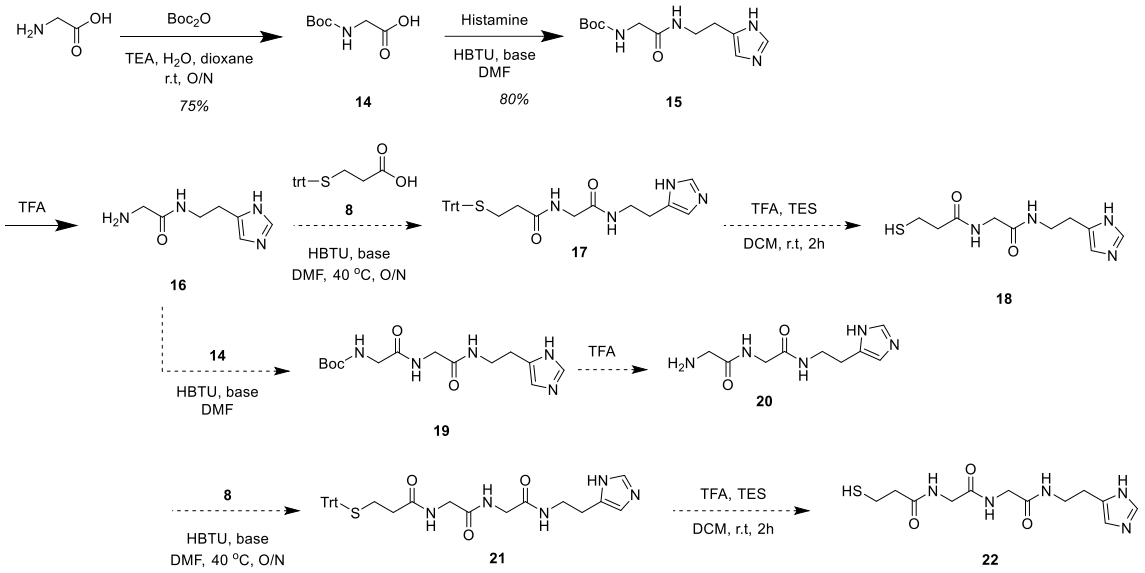

***Scheme 2-12**. Preparation of linker dependent substrates*

Our initial synthesis was C-terminus to N-terminus synthesis; which means that Boc-glycine was ligated with histamine, Boc group was deprotected and the free amine of N-terminus on glycine was ligated with 3-tritylthiopropionic acid. This reaction scheme is similar with that of SPPS method. Also coupling reagent was changed from DCC to HBTU. Actually, however, it was failed to obtain compound **17** (trt-MPA-gly-histamine) because compound **16** (gly-histamine) and **17** had similar chemical properties such as polarity and mobility and it was impossible to separate them using chromatographic tools.

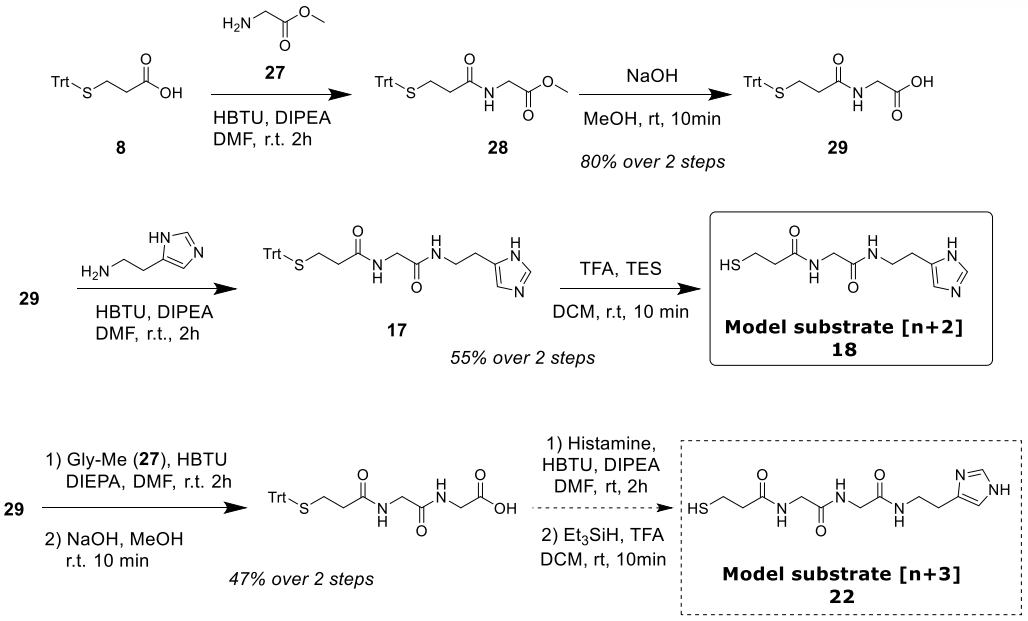

***Scheme 2-13**. Another approach to prepare linker dependent substrates*

So, we detoured synthetic design; instead of protecting N-terminus, C-terminus carboxylic acid was protected, and synthetic direction was N-terminus to C-terminus. As a result, we succeeded to obtain model substrate [n+2] (**16**), whereas model substrate [n+3] (**22**) was failed. It was kind of limitation of amino acid synthesis *in solution* method. Accordingly, we decided to apply SPPS methods and the tetrapeptides model kinase sensor [n+3] was synthesized

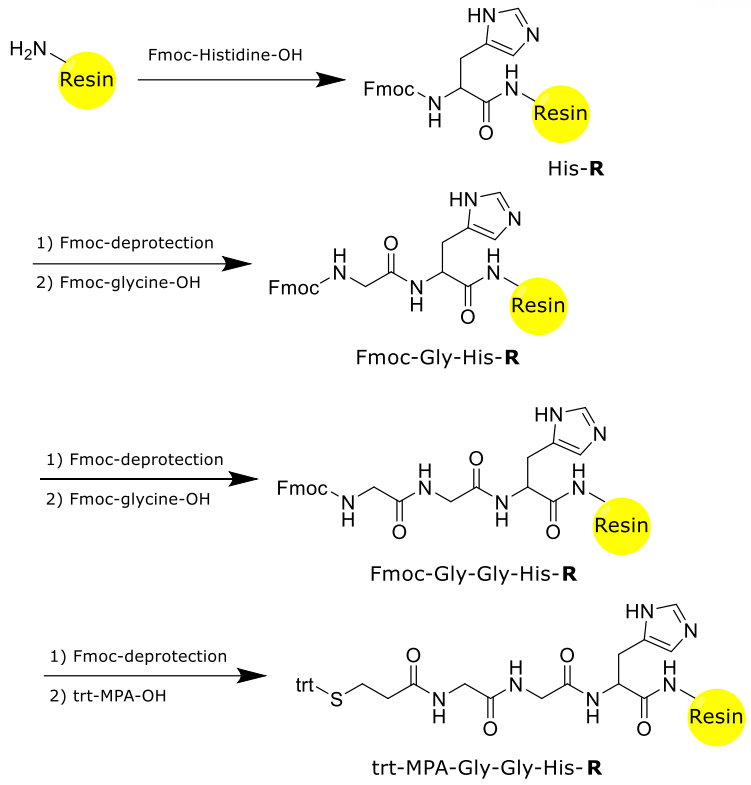

Scheme 2-14. *SPPS method for preparation of model substrates*

SPPS method is an easy way to synthesize peptides, but it requires and consumes large amount of reagents and yield was low. Rather, *in solution* synthesis uses less amount of reagents than SPPS method, but the reactions using amino acid were hard to apply in solution synthesis.

For fast progress, all model kinase sensors [n+1, n+2 and n+3] were prepared by SPPS methods.

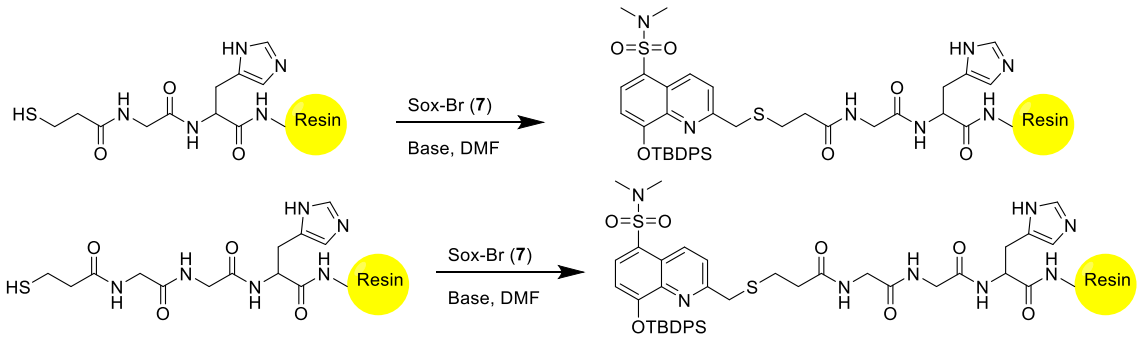

Scheme 2-15. *Sox alkylation on resin strategies*

When the model substrates were synthesized by SPPS method, they were not cleaved from the resin and Sox-alkylation on thiol group was executed. This on-resin alkylation was advantageous

for the product isolation since the reagents and unnecessary chemicals were easily removed and flushed away and the product was stably cleaved from the resin. Peptide cleavage from the resin requires 95% TFA, while trityl group deprotection needs to 5% TFA. Thus, Trityl group was selectively removed without affecting to resin and free thiol was selectively alkylated with Sox fluorophore.

2.2.6 Fluorescence Assay and Phosphorylation Test of Model Kinase Sensors

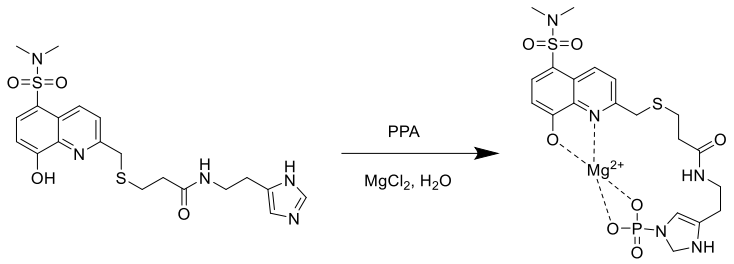

Scheme 2-16. *Phosphorylation of model kinase sensor [n+1]*

Since the model kinase sensor [n+1] was ready, chemical phosphorylation was carried out using potassium phosphoramidate (PPA). In our strategy, imidazole group should be phosphorylated and if magnesium ion existed, fluorescence intensity would be increased. To verify it, fluorescence assays were measured by Tecan (the fluorescence spectrometer). In 96-well corning black plate, sensor molecule stock solution (dissolved in methanol), magnesium stock solution (dissolved in water) and PPA stock solution (dissolved in water) were diluted in distilled water (in 200 μL of total volume). Fluorescence was measured at 360 nm excitation and 485 nm emission.

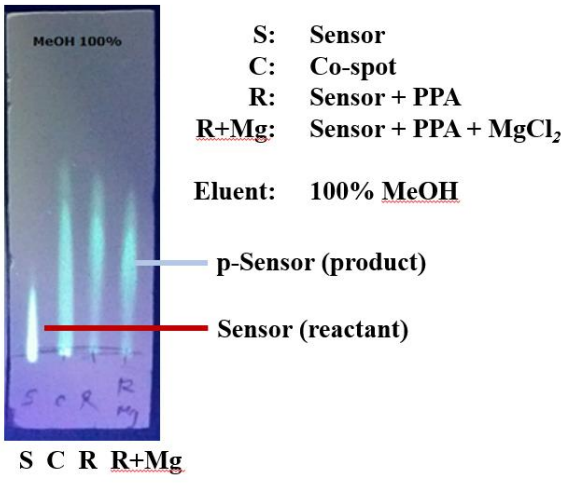

Figure 2-6. TLC monitoring of model kinase sensor phosphorylation (306 nm UV exposure)

At first, we checked TLC whether it could distinguish the reactant and product. Reactant, the unphosphorylated model sensor, showed very low R_f value (about 0.2) and streaked from the base point, whereas the reacted product (expected to the phosphorylated product) resulted in higher R_f value (about 0.4) when reacted for 6 hours in distilled water.

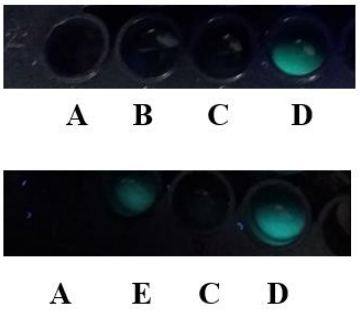

A: DI water (control)
B: 1 mM sensor
C: 1 mM sensor + 100 mM PPA
D: 1 mM sensor + 100 mM PPA +10 mM $MgCl_2$
E: 1 mM sensor + 10 mM $MgCl_2$

Figure 2-7. UV exposure on 96-well black plate and observation of fluorescence by naked eye.

This assay also can be visualized in naked eye by direct UV exposure (304 nm) on the 96-well plate in dark room. The sensor molecule itself did not show the fluorescence regardless of phosphorylation in the absence of Mg^{2+}. Fortunately, the phosphorylated sensor molecule (the sensor molecule + PPA) released strong intensity of fluorescence when incubated with 10 mM Mg^{2+}.

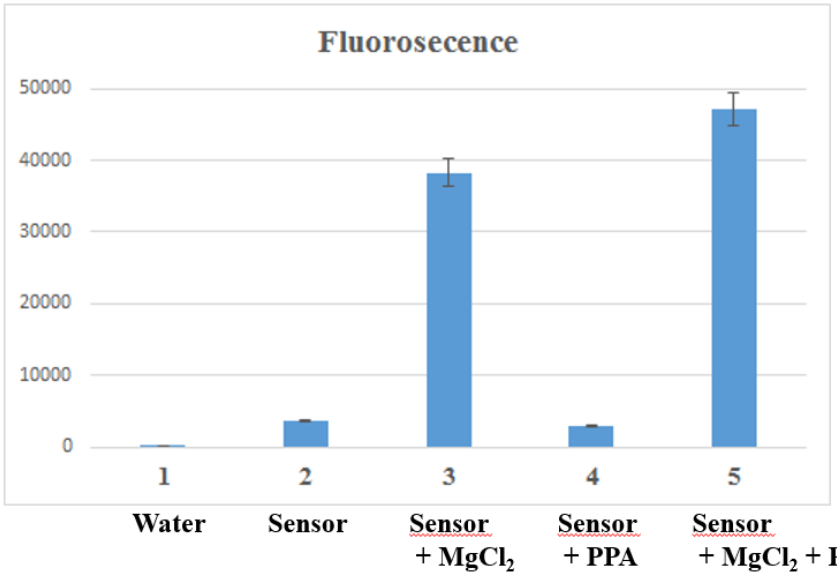

Figure 2-8. Fluorescence assay of model kinase sensor; 1) distilled water (control); 2) 1 mM sensor molecule; 3) 1mM sensor molecule and 10 mM $MgCl_2$; 4) 1mM sensor molecule and 100 mM PPA; 5) 1mM sensor molecule, 100 mM PPA and 10mM $MgCl_2$.

The fluorescence of sensor molecule itself was weak no matter whether it was phosphorylated or not, and CHEF by magnesium ion showed increased fluorescence for both phosphorylated and unphosphorylated sensors. However, the phosphorylated sensor with Mg^{2+} ion exhibited a little stronger fluorescence than the unphosphorylated sensor, although the difference was not significant. However, it was expected that optimization of the reaction condition such as changing the ratio and concentration of the sensor molecule and magnesium ion may improve the application of histidine phosphorylation sensor.

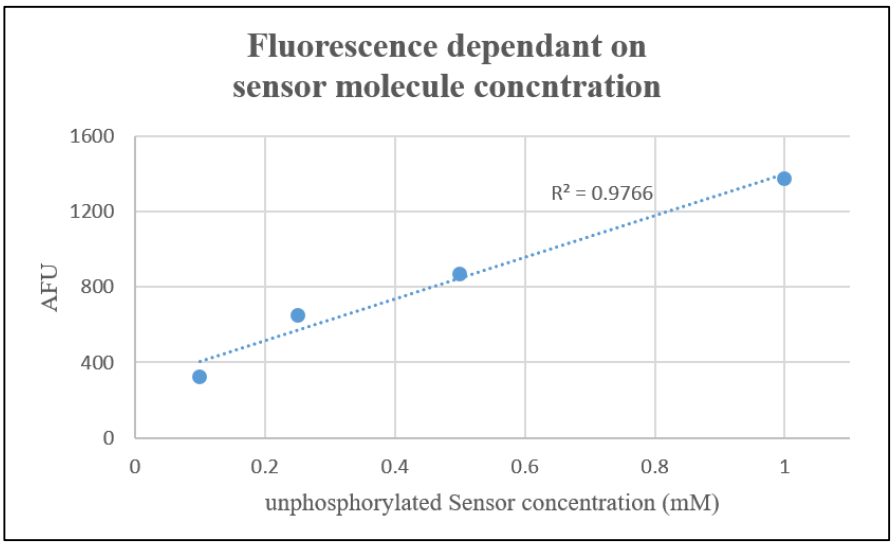

Figure 2-9. Fluorescence change by sensor molecule concentration

First, the sensor molecule was tested the linear relationship between the concentration and fluorescence. Also, magnesium ion concentration was changed and fluorescence was measured to find K_d for Mg^{2+} and the maximum fluorescence for the unphosphoryated sensor. $MgCl_2$ concentration was increased up to 1500 mM, but fluorescence was over the measurable range of equipment from the 1000 mM $MgCl_2$.

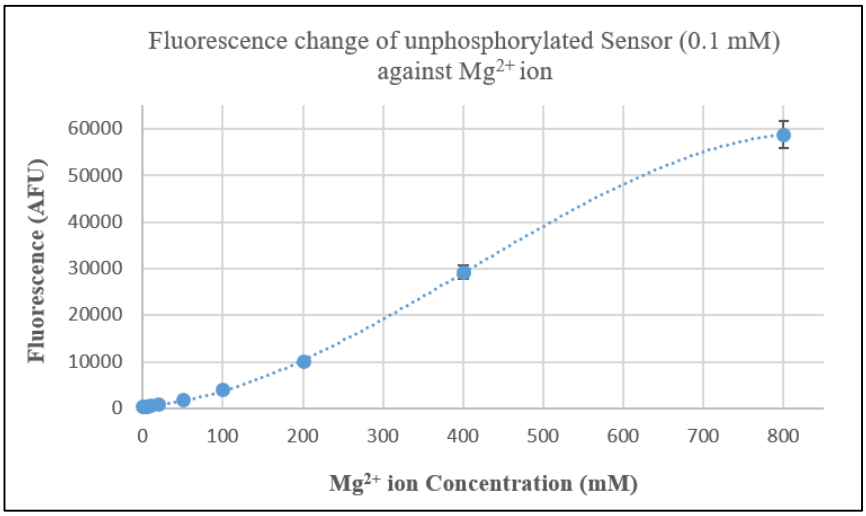

Figure 2-10. The fluorescence change in dependence of magnesium ion. X-axis: the concentration of magnesium ion (mM) in 1mM unphosphorylated sensor molecule [n+1] molecule.

Next, the sensor molecule was tested at 100 μM and the Mg^{2+} concentration was 10 mM and phosphorylation reaction was for 30 minutes with 10 mM PPA under pH 7.5 phosphate buffer. The result was consistent with previous data and the difference of fluorescence between phosphorylated sensor and non-phosphorylated sensor was definitely distinguished.

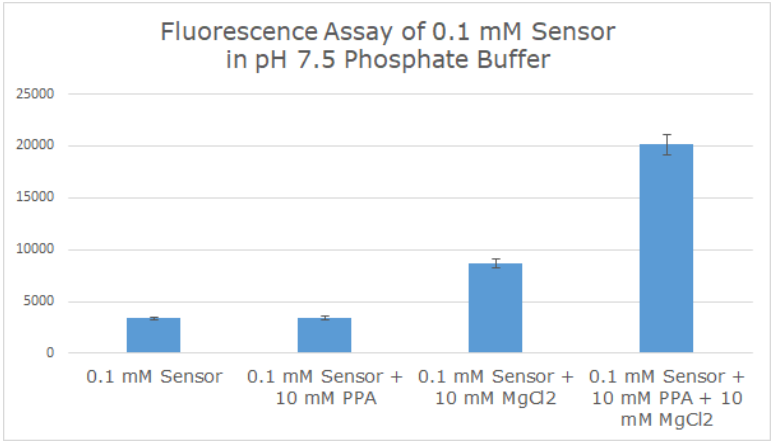

Figure 2-11. Phosphorylation and fluorescence of the 100 μM sensor molecule with 10 mM $MgCl_2$. pH 7.5 100 mM phosphate buffer

To verify that the increase of fluorescence was due to the phosphorylation and CHEF effect and phosphorylation was successful, we tried to analyze the product using NMR, but it was unsuccessful due to small scale, insufficient amount for NMR detection. Instead, we carried out

indirect tests; it is well-known that phosphohistidine is quite stable under mild basic condition but unstable under acidic condition. We added concentrated HCl into the phosphorylated sensor molecule and fluorescence was quenched. Actually, at low pH, the nitrogen on quinoline of Sox fluorophore became protonated and the fluorescence was totally quenched. When the pH was adjusted back to pH 7.5, the fluorescence intensity remained much lower than the original phosphorylate sensor, indicating the pHis decomposition under acid led to fluorescence decrease.

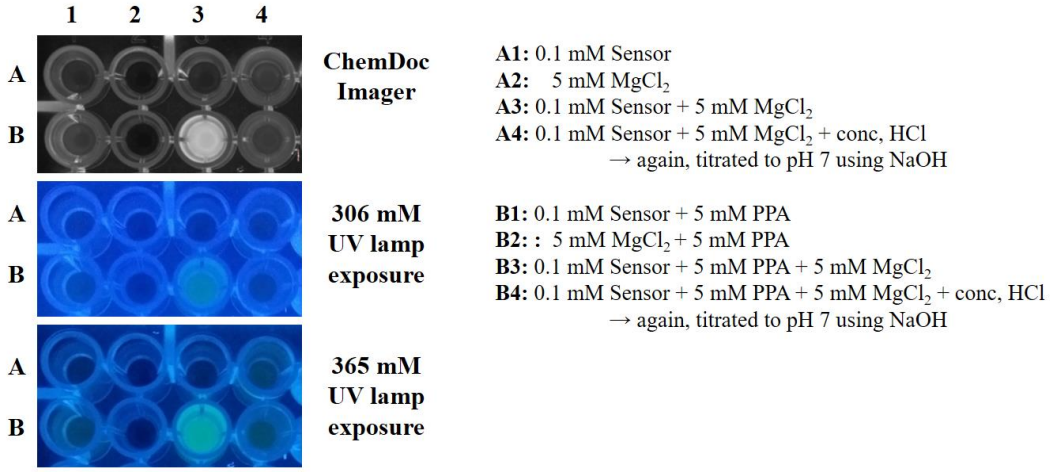

Figure 2-12. Dephosphorylation test by acid treatment.

2.2.7 Future Direction: Preparation of the Substrates for Histidine kinases

Since we tested the possibilities of the increase of fluorescence by Sox fluorophore via chelation of magnesium cation with phosphorylated imidazole of histidine or histidine mimics, we decided to synthesize the substrate for histidine kinase. We chose histone H4 protein and its kinase for our study. It is known that histone H4 has two positions for histidine phosphorylation (His^{18} and His^{75}) and we chose one position, His^{18}. The sequence around His^{18} is GGAKR**H**RKVL. Generally, the enzyme-specific recognition sites for kinase substrates are a few amino acids, So, we set the 10 amino acid sequences as a base for sensor peptides. As we do not know the optimal position of Sox in the substrate for kinase reaction, we planned six sensor peptides for the test.

Gly-Gly-Ala-Lys-Arg-His-Arg-Lys-Val-Leu
GGAKRHRKVL

fragment of Histone H4 (wt)
fH4(wt)

GGAKCHRKVL	GGAKRHCKVL
fH4(n+1)	fH4(n-1)
GGACRHRKVL	GGAKRHRCVL
fH4(n+2)	fH4(n-2)
GGCKRHRKVL	GGAKRHRKCL
fH4(n+3)	fH4(n-3)

Scheme 2-17. *Design of histone H4-mutated fragments*

Six kinds of sensor peptides will verify which position is most suitable for the control of distance between the phosphate group in phosphohistidine and Sox fluorophore, formed by cysteine alkylation with Sox halide. Then, comparing the phosphorylation between [n+α] and [n-α] positions' sensor peptides, we will determine which residue should be mutated into cysteine; if the enzyme-recognition site is changed into cysteine with Sox alkylated, it might not function as the enzyme-recognition site and the enzyme-mediated phosphorylation can be difficult.

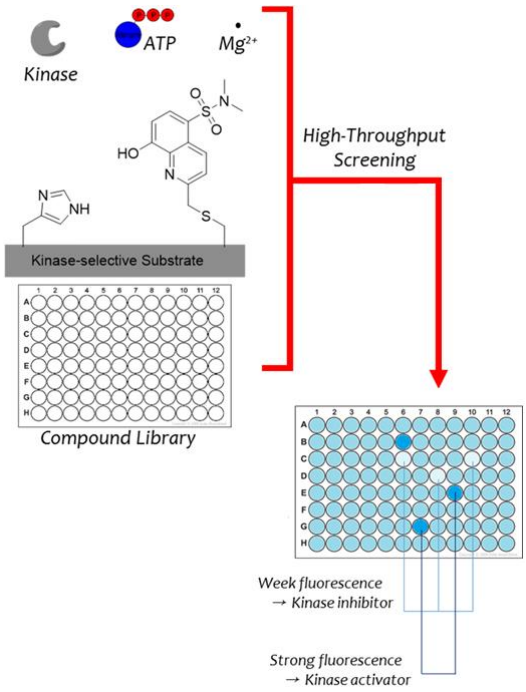

Figure 2-13. Application of Sox-based kinase sensor; inhibitor screening

2.3 Conclusion

Histidine phosphorylation has been already known, even earlier than tyrosine, but it was not explored well because of the lack of tools for studying phosphohistidine. Sox fluorophore had been applied in serine, tyrosine, or threonine (O-phosphorylation)-containing proteins and measured their kinase activity, but it had not been applied in histidine or arginine (N-phosphorylation). Therefore, we introduced Sox fluorophore into histidine-containing model substrates and demonstrated the feasibility to evaluate histidine kinase activity using fluorescence measurement. Sox-based histidine kinase sensor will offer a new method for quick and real-time assays of histidine phosphorylation and dephosphorylation, and it will be a significant growth for the phosphohistidine research.

2.4 Methods

8-hydroxy-2-methylquinoline-5-sulfonyl chloride (2)

8-hydroxy-2-methylquinole (**1**, 0.5 g, 3.14 mmol, purchased from Alfa Aesar) was dissolved in chlorosulfonic acid (2.5 ml, 37.6 mmol, purchased from Sigma Aldrich) and stirred at 25 ^{O}C for 2 hours. The reaction mixture was added to a separatory funnel containing a slurry of ice in brine (125 mL) and dichloromethane (125 mL). The separatory funnel was shaken briefly and the dichloromethane layer was run into a flask with potassium carbonate. The resulting solution was filtered and evaporated and the resulting yellow product was obtained. (0.541 g, 2.11 mmol, 67 %) The obtained product was used in next reaction without further purification.

TLC R_f = 0.63 (silica, $CHCl_3$/MeOH, 4:1) R_f = 0.39 (silica, ethyl acetate)

^{1}H NMR (400 MHz, Chloroform-d) δ 8.97 (d, *J* = 8.8 Hz, 1H), 8.30 (d, *J* = 8.5 Hz, 1H), 7.63 (d, *J* = 8.8 Hz, 1H), 7.19 (d, *J* = 8.5 Hz, 1H), 2.81 (s, 3H).

5-(N,N-dimethyl)sulfamoyl-8-hydroxy-2-methylquinoline (3)

2M Dimethylamine in tetrahydrofuran (3.5 mL, 7 mmol, purchased from Alfa Aesar) was added under nitrogen to tetrahydrofuran (150 mL). 8-Hydroxy-2-methylquinoline-5-sulfonyl chloride (**2**, 322 mg, 1.25 mmol) was added in small portions over 3 hours (about 10 mg per addition in every 4 minutes) at room temperature. The solution was incubated for an additional 10 minutes, and it was concentrated with a rotary evaporator. To remove remained excess dimethylamine, the residue was re-dissolved in dichloromethane and re-evaporated in three times. The obtained slightly pink-orange solid was purified by column chromatography (silica gel, 1:2 of ethyl acetate/hexane). The product was obtained as a white solid (294 mg, 1.11 mmol, 88.5 %)

TLC R_f = 0.38 (silica, 2:1, hexane/ethyl acetate)

^{1}H NMR (400 MHz, Chloroform-d) δ 8.97 (d, *J* = 8.7 Hz, 1H), 8.09 (d, *J* = 8.3 Hz, 1H), 7.47 (d, *J* = 8.7 Hz, 1H), 7.18 (d, *J* = 8.2 Hz, 1H), 2.76 (s, NC**CH$_3$**, 3H), 2.75 (s, N**(CH$_3$)$_2$**, 6H)

8-tert-butyldiphenylsilyloxy-5-(N,N-dimethyl)sulfamoyl-2-methylquinoline (4)

5-(N,N-dimethyl)sulfamoyl-8-hydroxy-2methylquinoline (**3**, 540 mg, 2.03 mmol) and imidazole (150 mg, 2.2mmol) were dissolved in dry DMF (3 mL). Tert-butyldiphenylsilyl chloride (TBDPSiCl, purchased from Alfa Aesar, 567 μL, 2.2 mmol) was added under nitrogen and stirred for 2 hours at room temperature. The solution was diluted with ethyl acetate (250 mL), washed with saturated ammonium chloride solution (50 mL) and brine (50mL x2), dried over $MgSO_4$ and evaporated under low pressure. The crude solid was purified by silica gel column chromatography (1:9 of ethyl acetate / hexane). (1.01g, 99%)

TLC R_f = 0.10 (silica, 9:1, hexane/ethyl acetate), R_f = 0.32 (silica, 4:1, hexane/ethyl acetate)

^{1}H NMR (400 MHz, $CDCl_3$) δ 8.79 (d, *J* = 8.9Hz, 1H), 7.96 (d, *J* = 8.3 Hz. 1H), 7.74 (d, *J* = 6.6 Hz, 4H), 7.34 (t, *J* = 7.2 Hz, 2H), 7.30 – 7.25 (m, 4H), 7.17 (d, *J* = 8.9 Hz, 1H), 7.14 (d, *J* = 8.3 Hz, 1H) 2.71 (s, 6H), 2.18 (s, 3H), 1.16 (s, 9H)

8-tert-butyldiphenylsilyloxy-5-(N,N-dimethyl)sulfamoyl-2-formylquinoline (5)

8-tert-butyldiphenylsilyloxy-5-(N,N-dimethyl)sulfamoyl-2-methylquinoline (**4**, 162.63 mg, 0.322 mmol) was added to a dray flask with dry 1,4-dioxane and molecular sieves under nitrogen. Selenium dioxide was added and the reaction was stirred at 95 ^{O}C for 17 hours. After the reaction was finished, the reaction mixture was cooled down to ambient temperature, filtered through celite to remove the black solid and molecular sieves, and eluted with dioxane. Dioxane was removed by rotary evaporation and the remained yellowish oil was re-dissolved in ethyl acetate (200 mL), washed with brine (20 mL), water (20 mL), saturated potassium carbonate solution (20 mL) and dried over $MgSO_4$. The product solution was evaporated to give a crude product as a sticky yellow oil, which was used in the next step without further purification. (115 mg (69%) of pure product in the mixture evaluated by NMR integration)

TLF R_f = 0.50 (silica, 2:1, hexane/ethyl acetate)

1H NMR (400 mHz, $CDCl_3$) δ 9.58 (s, **CH**O, 1H) 9.08 (d, *J* = 9 Hz, quinolone **CH**, 1H), 8.14 (d, *J* = 8.5 Hz, quinolone **CH**, 1H), 7.95 (d, *J* = 9 Hz, quinolone **CH**, 1H), 7.80-7.20 (m, diphenyl, 10H), 7.18 (d, *J* = 8.5 Hz, quinolone **CH**, 1H), 2.74 (s, 2N**CH$_3$**, 6H), 1.21 (s, tert-butyl, 9H)

8-tert-butyldiphenylsilyloxy-5-(N,N-dimethyl)sulfamoyl-2-(hydroxymethyl)quinoline (6)

Sodium borohydride (12 mg, 0.317 mmol, purchased from Junsei) was dissolved in absolute

ethanol and cooled to 0 ^{O}C. Crude 8-tert-butyldiphenylsilyloxy-5-(N,N-dimethyl)sulfamoyl-2-formylquinoline (**5,** 0.322 mmol) was dissolved in dry dichloromethane and added dropwise to the cooled sodium borohydride solution. The reaction mixture was stirred for 15 minutes. Then the reaction solution was diluted with diethyl ether (200 mL), washed with saturated ammonium chloride (40 mL), water (40 mL x2), and brine (40 mL) and dried over $MgSO_4$. The solvent was removed by rotary evaporation to yield a pale yellow sticky solid. The product was purified by silica gel column chromatography (2:1 of hexane and ethyl acetate). (88%)

TLC R_f = 0.3 (2:1, hexane/ethyl acetate)

^{1}H NMR (400 MHz, $CDCl_3$) δ 9.00 (d, *J* = 8,9 Hz, 1H), 7.97 (d, *J* = 8,3 Hz, 1H), 7.87-7.64 (m, 4H), 7.50-7.28 (m, 6CH in diphenyl + 1CH in quinolone, 7H), 7.09 (d, J = 8.3 Hz, 1H), 4.63 (s, **CH_2**OH, 2H), 2.71 (s, N**$(CH_3)_2$**, 6H), 1.19 (s, tert-butyl, 9H)

2-bromomethyl-8-tert-butyldiphenylsilyloxy-5-(N,N-dimethyl)sulfoamoylquinoline (Sox-Br, 7)

8-tert-butyldiphenylsilyloxy-5-(N,N-dimethyl)sulfamoyl-2-(hydroxymethyl)quinolone (**6**, 100mg, 0.192 mmol) was dried over P_2O_5 for 15 hours in a desiccator and dissolved in 1 mL of dry dichloromethane under nitrogen. The solution was cooled to 0 ^{O}C. N-bromosuccinimide (NBS) and triphenylphosphine were pre-mixed in dichloromethane and added into the cooled solution. The reaction solution was stirred for 4 hours at 0 ^{O}C. The reaction mixture was diluted with 1200 mL of diethyl ether, washed with water (150 mL) and brine (100 mL) and dried over $MgSO_4$. The solvent was evaporated and the residue was purified by column chromatography (florisil, 100-200 mesh, 1:9 of ethyl acetate/hexane). (55.9 mg, 50%)

TLC R_f = 0.7 (2:1, hexane/ethyl acetate)

^{1}H NMR (400 MHz, $CDCl_3$) δ 8.93 (d, *J* = 8,9 Hz, 1H), 8.02 (d, *J* = 8,3 Hz, 1H), 7.73 (dd, J = 8.0, 1.4 Hz, 4H), 7.51 (d, J = 9.0 Hz, 1H), 7.40-7.21 (m, 6H), 7.15 (d, J = 8.3 Hz, 1H), 4.12 (s, **CH_2**Br, 2H), 2.72 (s, N**$(CH_3)_2$**, 6H), 1.17 (s, tert-butyl, 9H)

^{13}C NMR (101 MHz, $CDCl_3$) δ 157.15, 155.42, 140.29, 134.93, 134.59, 133.37, 132.42, 129.65, 127.58, 125.36, 123.81, 122.72, 115.75, 37.33, 32.71, 26.58, 20.17

3-(tritylthio)propionic acid (trt-MPA, 8)

In an air-dried flask, 3-mercaptopropionic acid (1mL, 11 mmol, purchased from Alfa Aesar) was dissolved in 20 mL of dichloromethane. Trityl chloride (3.14 g, 11 mmol) dissolved in tetrahydrofuran was slowly added into the reaction mixture at room temperature. After 15 minutes, a white solid became formed and the reaction mixture was stirred for 14 hours at room temperature. When the reaction was finished, the reaction mixture was filtered and washed with

dichloromethane three times. The filtered white solid gave desired product (3.73 g, 95%).

^{1}H NMR (400 MHz, $CDCl_3$) δ 7.42 (dt, *J* = 8.7 Hz, 5H), 7.32 – 7.17 (m, 10H), 2.46 (t, *J* = 7.3 Hz, 2H), 2.2.4 (t, *J* = 7.3 Hz, 2H)

N-(2-(1H-imidazol-5-yl)ethyl)-3-(tritylthio)propanamide (trt-MPA-histamine, 9)

3-(tritylthio)propionic acid (**8**, 380 mg, 1.1 mmol), N,N'-dicyclohexylcarbodiimide (DCC) and triethylamine were dissolved in 15 mL of N,N-dimethylformamide. Histamine dihydrochloride (200 mg, 1.1 mmol) were added and the reaction solution was stirred overnight at 40 ^{O}C. The reaction mixture was filtered, evaporated, extracted by dichloromethane and dried over $MgSO_4$. The organic layer was evaporated and the residue was purified by silica gel column chromatography. (10:1 of ethyl acetate/Methanol) (337 mg, 70%).

TLC R_f = 0.2 (10:1, ethyl acetate/methanol)

^{1}H NMR (400 MHz, Chloroform-*d*) δ 7.39 (d, *J* = 7.4 Hz, **5H** in trityl group + **1H** in imidazole group, 6H), 7.32 – 7.18 (m, trityl group, 10H), 6.75 (s, imidazole, 1H), 5.99 (s, CO**NH**, 1H), 3.46 (q, *J* = 6.1 Hz, CONH**CH$_2$**, 2H), 2.77 (t, *J* = 6.3 Hz, CONHCH$_2$**CH$_2$**, 2H), 2.52 (t, *J* = 7.2 Hz, **CH$_2$**CO, 2H), 1.93 (t, *J* = 7.2 Hz, trt-S**CH$_2$**, 2H).

^{13}C NMR (101 MHz, Chloroform-*d*) δ 171.13, 144.62, 134.60, 129.57, 127.94, 126.73, 109.99, 77.20, 66.79, 39.23, 25.63, 27.91, 26.71

N-(2-(1H-imidazol-5-yl)ethyl)-3-mercaptopropanamide (MPA-histamine, 10)

To a solution of N-(2-(1H-imidazol-5-yl)ethyl)-3-(tritylthio)propanamide (**9**, 110 mg, 0.250 mmol) in 10 mL of dichloromethane was added triethylsilane (TES, purchased from Alfa Aesar, 60 μL, 0.38 mL) followed by trifluoroacetic acid (5 mL). The initially developed yellow color disappeared within a few seconds and the colorless reaction mixture was stirred at r.t for 2 hours. The volatiles were evaporated *in vacuo* and the residue was washed with hexane. Hexane was removed by suction carefully and the product was yellow-like liquid not mixed with hexane and heavier than hexane. (39.7 mg, 80%)

TLC R_f = 0.2 (5:1, ethyl acetate/methanol)

^{1}H NMR (400 MHz, Methanol-d_4) δ 9.77 (s, imidazole, 1H), 8.85 (s, CO**NH**, 1H), 8.21 (s, imidazole, 1H), 4.14 (q, *J* = 6.5 Hz, CONH**CH$_2$**, 2H), 3.57 (t, *J* = 6.8 Hz, CONHCH$_2$**CH$_2$**, 2H), 3.41 (q, *J* = 7.2 Hz, HS**CH$_2$**, 2H), 3.14 (t, *J* = 6.9 Hz, HSCH$_2$**CH$_2$**, 2H), 3.02 (td, *J* = 8.0, 1.7 Hz, **SH**, 1H).

N-(2-(1H-imidazol-5-yl)ethyl)-3-(((8-hydroxy-5-(N,N-dimethylsulfamoyl)quinolin-2-yl)-methyl)thio)propanamide (12)

N-(2-(1H-imidazol-5-yl)ethyl)-3-mercaptopropanamide (**10**, 20 mg, 0.1 mmol) was well-dried and dissolved in N,N-dimethylformamide (DMF, 2 mL). 1,1,3,3-Tetramethylguanidine (TMG) was added into the solution of **10**, and Sox-Br (**7**, 30 mg, 0.05 mmol) was subsequently added and reacted for 1 hour at room temperature. The reaction solution was evaporated under low pressure, and product was extracted by ethyl acetate and washed with distilled water. The collected organic layer was dried over $MgSO_4$ and solvent was evaporated. The product was purified by HPLC. (7 mg, 30%)

HPLC: 100% solvent A (clean H_2O with 0.1% TFA) to 30% solvent A and 70% solvent B (9:1 of MeCN and H_2O with 0.1% TFA) in 15 min., T_R=13.1 min.

^{1}H NMR (400 MHz, Deuterium Oxide) δ 9.03 (d, *J* = 9.0 Hz, quinoline, 1H), 8.41 (s, imidazole, 1H), 8.04 (d, *J* = 8.4 Hz, quinoline, 1H), 7.78 (d, *J* = 9.1 Hz, quinoline, 1H), 7.21 (d, *J* = 8.4 Hz, quinoline, 1H), 7.05 (s, imidazole, 1H), 4.02 (s, quinoline-**CH$_2$**S, 2H), 3.25 (t, *J* = 6.7 Hz, CONH**CH$_2$**, 2H), 2.69 (t, *J* = 6.6 Hz, CONHCH$_2$**CH$_2$**, 2H), 2.65-2.61 (m, **CH$_2$**CO + N**(CH$_3$)$_2$**, 6H), 2.33 (t, *J* = 6.7 Hz, S**CH$_2$**CH$_2$CO, 2H).

^{13}C NMR (101 MHz, D_2O) δ 174.05, 162.77, 158.17, 146.56, 137.47, 133.57, 132.94, 130.57, 124.81, 124.30, 120.54, 116.09, 111.39, 37.74, 36.74, 35.57, 35.14, 27.05, 23.93.

Boc-glycine-OH (14)

Boc_2O (1.53 mL, 7 mmol) was added dropwise to L-glycine (3 g, 40 mmol) and 1 N NaOH (6 mL) at 0 ^{O}C for 30 minutes with stirring. Thereafter, temperature was raised up to 35 ^{O}C and the reaction solution was stirred for 2.5 hours. The reaction mixture was poured into hexane and the product was extracted by aqueous layer (25 mL of H_2O x2, and 25 mL of Na_2CO_3 solution x2). The collected aqueous layer was adjusted into pH 1 using $KHSO_4$. Product was extracted by ethyl acetate (25 mL x2) from the aqueous solution. The collected organic layer was dried over Na_2SO_4 and the solvent was removed by rotary evaporator to leave product. (5.3 g, 30 mmol, 75%)

TLC R_f = 0.5 (65:24:4 of Chloroform/methanol/water)

^{1}H NMR (400 MHz, Chloroform-*d*) δ 9.50 (bs, **COOH**,1 H), 6.72 (bs, **NH**, 1H), 5.09 (bs, **NH**, 1H), 3.98 (s, **C*H$_2$**, 2H),1.46 (s, Boc, 9H)

N-(2-(1H-imidazol-5-yl)ethyl)-2-(Boc)aminoacetamide (Boc-Gly-histaime, 15)

Boc-Glycine was dissolved in DMF and triethylamine (1.9 g, 18.8 mmol) and HBTU (2.16 g, 5.70 mmol). A few minutes later, histamine dihydrochloride (1.15 g, 6.267 mmol) was added into the mixture and stirred at room temperature for 1.5 hours. DMF was removed by rotary evaporator and the residue was diluted in ethyl acetate, washed with water and brine, and dried over Na_2SO_4. Solvent was removed and the product was purified by silica gel column chromatography (5:1 of

$CHCl_3$/MeOH). (1.223 g, 4.558 mmol, 80%).

^{1}H NMR (400 MHz, D2O) δ 7.56 (s, imidazole, 1H), 6.79 (s, imidazole, 1H) 3.56 (s, **C*H$_2$**, 2H), 3.33 (t, *J* = 6.6 Hz, 2H), 2.66 (t, *J* = 6.4 Hz, 2H), 1.29 (s, Boc, 9H)

N-(2-(1H-imidazol-5-yl)ethyl)-2-aminoacetamide (Gly-histamine, 16)

Boc-Gly-Histamine (**15**) was dissolved in DCM and TES was added. Trifluoroacetic acid (TFA) was added and stirred for 10 minutes. Solvent was removed and ether was added. Precipitated solid was washed by ether three times.

^{1}H NMR (400 MHz, Deuterium Oxide) δ 8.47 (s, imidazole, 1H), 7.15 (s, imidazole, 1H), 3.64 (s, **C*H$_2$**, 2H), 3.43 (t, *J* = 6.7 Hz, 2H), 2.84 (t, *J* = 6.8 Hz, 2H).

Glycine-methyl ester (Gly-CH_3, 27)

4.354 mL of thionyl chloride (60 mmol) was added dropwise into 60 mL of ice-cold MeOH with stirring. 3 g of glycine (40 mmol) was added and stirred at room temperature for 4 hours. Solvent was removed by rotary evaporation. The residue was re-dissolved in MeOH and re-evaporated, repeating three times. It was dissolved in ether and evaporated another three times. The product was recrystallized in 1:9 of MeOH/ether. 4.3885 g of product (87%) was obtained as a white solid.

^{1}H NMR (400 MHz, Deuterium Oxide) δ 3.80 (s, 2H), 3.71 (s, 3H)

Trt-MPA-Gly-CH_3 (28)

3-(tritylthio)propionic acid (**8**, 293 mg, 0.84 mmol), DIPEA (103.4 mg, 0.8 mmol) and HBTU (303.4 mg, 0.8 mmol) were dissolved in DMF. A couple of minutes later, glycine-methyl ester (**27**, 100 mg, 1.1 mmol) was added and stirred at room temperature for 1.5 hours. After reaction was finished, solvent was evaporated and the residue was diluted with DCM, washed with water and brine, and dried over $MgSO_4$. Dried organic layer was evaporated and product was purified by silica gel column chromatography (25:1 of DCM/MeOH). Product was 300 mg (0.72 mmol, 90%).

^{1}H NMR (400 MHz, Chloroform-*d*) δ 7.42 (d, *J* = 7.4 Hz, 6H), 7.34 – 7.16 (m, 9H), 6.20 (bs, CO**NH**, 1H) 3.93 (d, *J* = 5.2 Hz, 2H), 3.69 (s, **CH$_3$**COO, 3H), 2.78 (s, CONH**CH$_2$**, 2H), 2.50 (t, *J* = 7.4 Hz, 2H), 2.06 (t, *J* = 7.4 Hz, 2H).

^{13}C NMR (101 MHz, Chloroform-*d*) δ 171.18, 170.28, 162.54, 144.65, 129.57, 127.93, 126.68, 66.80, 52.26, 41.18, 38.60, 36.46, 35.12, 31.41, 27.46

Trt-MPA-Gly-OH (29)

800 mg of trt-MPA-Gly-Me (**28**, 800 mg, 1.91 mmol) was dissolved in 5 mL of methanol, and 13 mL of 1N sodium hydroxide solution (13 mmol) was added with stirring at room temperature for

30 minutes. Thereafter, it was titrated into neutral pH using hydrochloric acid, and solvent was removed by rotary evaporator. The residue was re-dissolved in water and pH was set to 3 with hydrochloric acid. The product was extracted with ethyl acetate, dried over Na_2SO_4, and evaporated. (688 mg, 1.70 mmol, 89%)

^{1}H NMR (400 MHz, Chloroform-*d*) δ 7.42 (d, *J* = 8.1 Hz, 6H), 7.32 – 7.13 (m, 9H), 5.98 (bs, NH, 1H) 3.97 (t, 2H), 2.51 (td, *J* = 7.3, 1.5 Hz, 2H), 2.05 (t, 2H).

Trt-MPA-Gly-histamine (17)

328 mg of trt-MPA-Gly-OH (**29**, 327.6 mg, 0.809 mmol) was dissolved in 1 mL of DMF, and 0.706 mL of DIPEA (4.04 mmol) and 304 mg of HBTU (0.801 mmol) were added. A couple of minutes later, 156 mg of histamine dihydrochlorde (0.850 mmol) was added and stirred at room temperature for 2 hours. Solvent was removed by rotary evaporation. The residue was diluted into ethyl acetate, washed with water, dried over Na_2SO_4, evaporated. The product was purified by silica gel column chromatography (5:1 of $CHCl_3$/MeOH).

^{1}H NMR (400 MHz, Methanol-d_4) δ 7.59 (s, 1H), 7.43 – 7.17 (m, 15H), 6.82 (s, 1H), 3.76 (s, 2H), 3.38 (t, *J* = 7.1 Hz, 2H), 2.73 (t, *J* = 7.1 Hz, 2H), 2.45 (t, *J* = 7.3 Hz, 2H), 2.27 (t, *J* = 7.3 Hz, 2H).

MPA-Gly-histamine (18)

226 mg of trt-MPA-Gly-histamine (0.45 mmol) was dissolved in 4 mL of dichloromethane, and TES (261 mg, 2.25 mmol) and 1 mL of TFA were added, with stirring at room temperature for 1 minute. Solvent was removed by rotary evaporator, and residue was washed with hexane.

^{1}H NMR (400 MHz, Methanol-d_4) δ 8.77 (s, 1H), 7.34 (s, 1H), 3.79 (s, 2H), 3.50 (t, *J* = 6.5 Hz, 2H), 2.92 (t, *J* = 6.4 Hz, 2H), 2.76 (t, *J* = 6.8 Hz, 2H), 2.57 (t, *J* = 6.8 Hz, 2H).

Sox-MPA-Gly-histamine (23)

^{1}H NMR (400 MHz, Deuterium Oxide) δ 8.90 (d, *J* = 9.0 Hz, 1H), 8.35 (s, 1H), 7.99 (d, *J* = 8.4 Hz, 1H), 7.70 (d, *J* = 9.0 Hz, 1H), 7.14 (d, *J* = 8.4 Hz, 1H), 6.90 (s, 1H), 4.01 (s, 1H), 3.60 (s, 2H), 3.19 (t, *J* = 6.6 Hz, 2H), 2.72 (t, *J* = 6.7 Hz, 2H), 2.60 (s, 8H), 2.46 (t, *J* = 6.7 Hz, 2H).

^{13}C NMR (101 MHz, Chloroform-*d*) δ 174.56, 171.23, 157.53, 153.84, 140.84, 134.43, 132.87, 132.22, 130.41, 125.22, 124.69, 120.92, 116.02, 112.88, 42.40, 37.82, 36.66, 34.77, 27.03, 23.84

2.5 Experimental Data

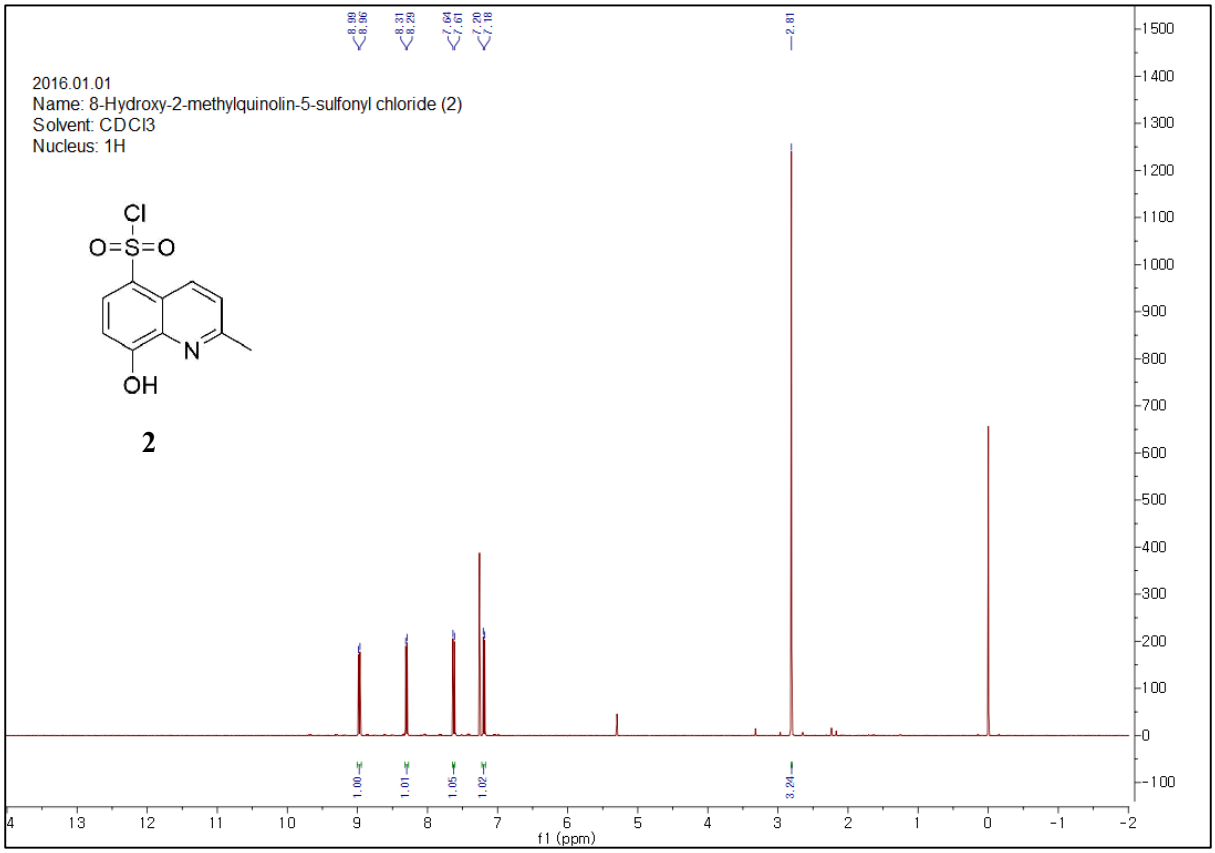

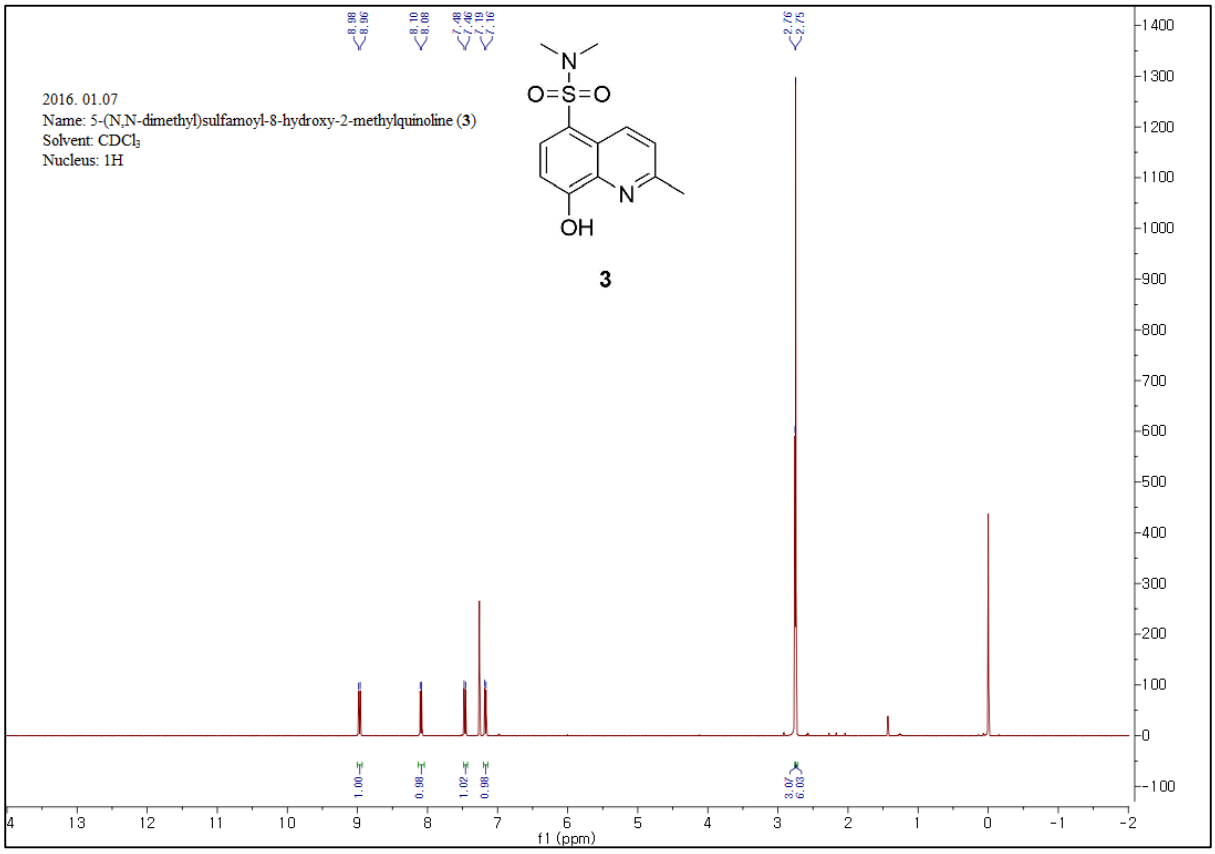

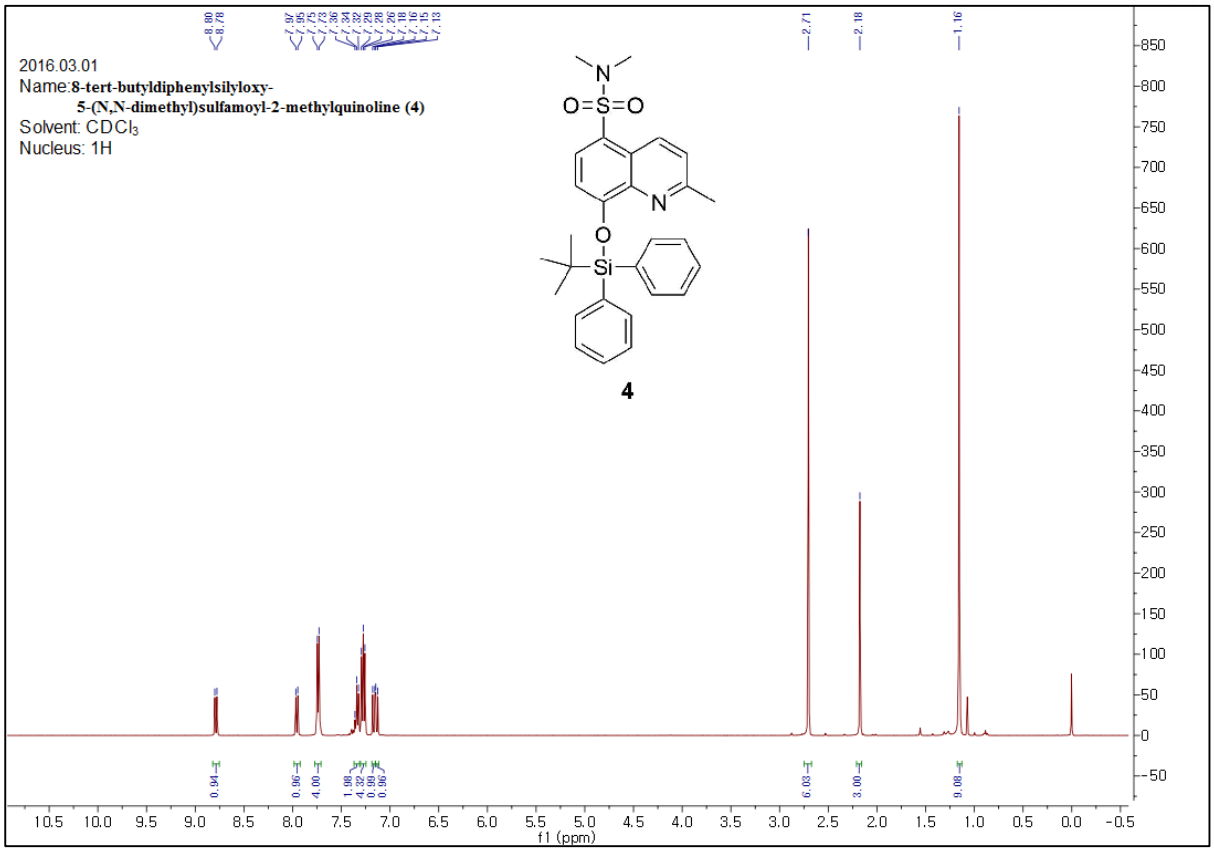

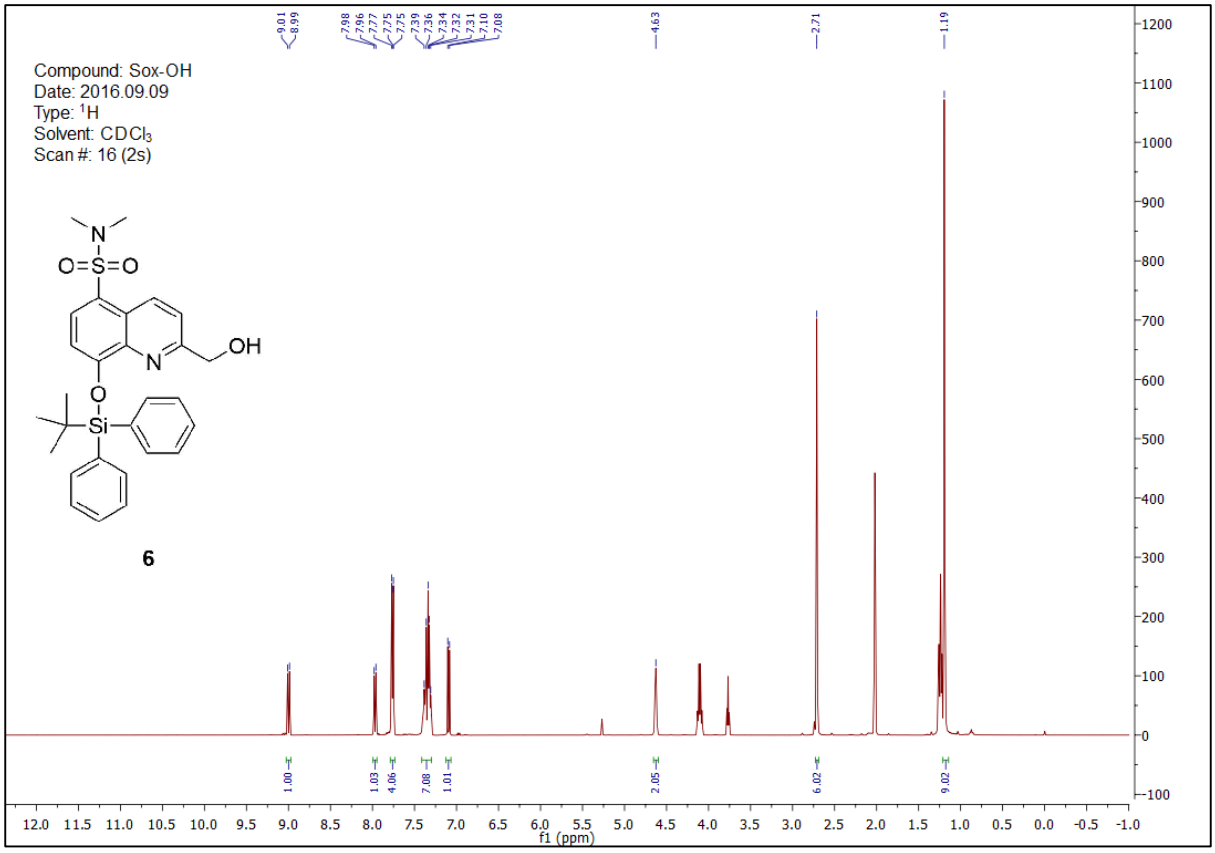

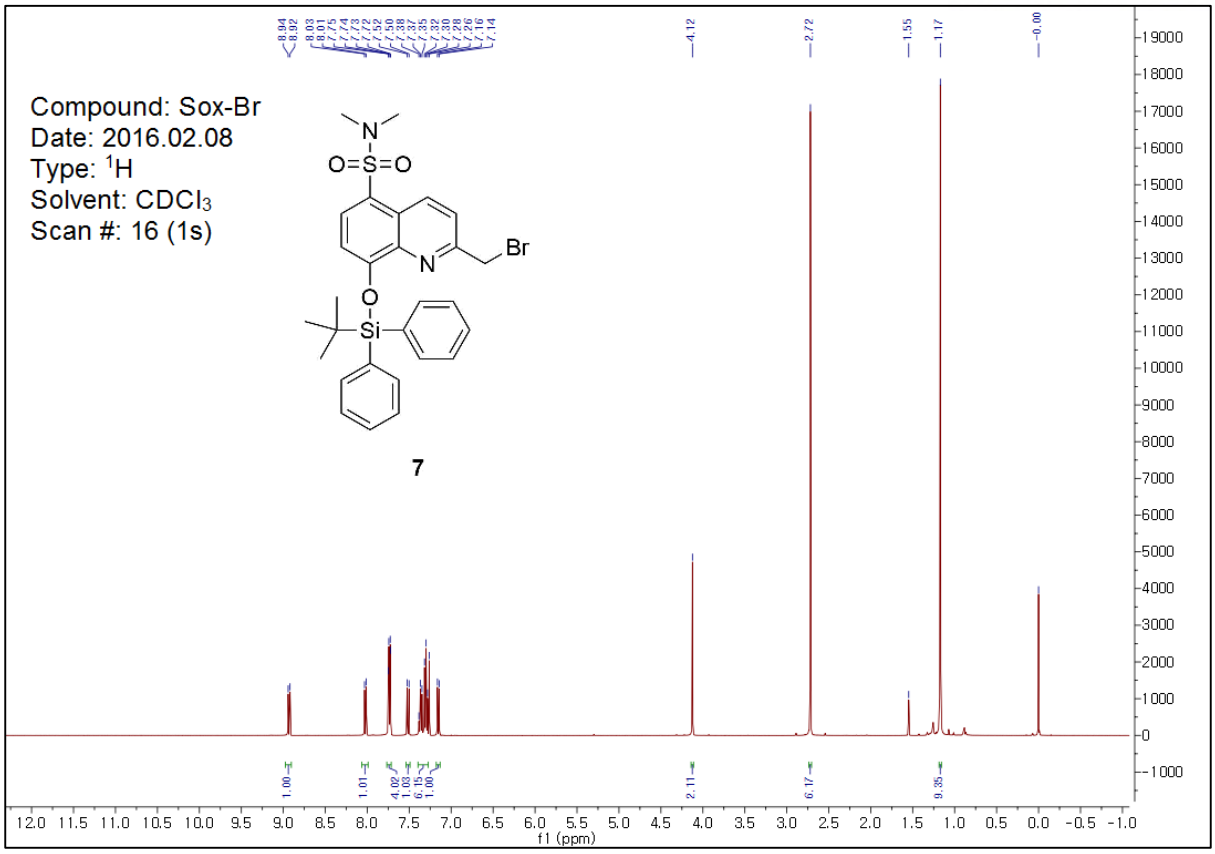

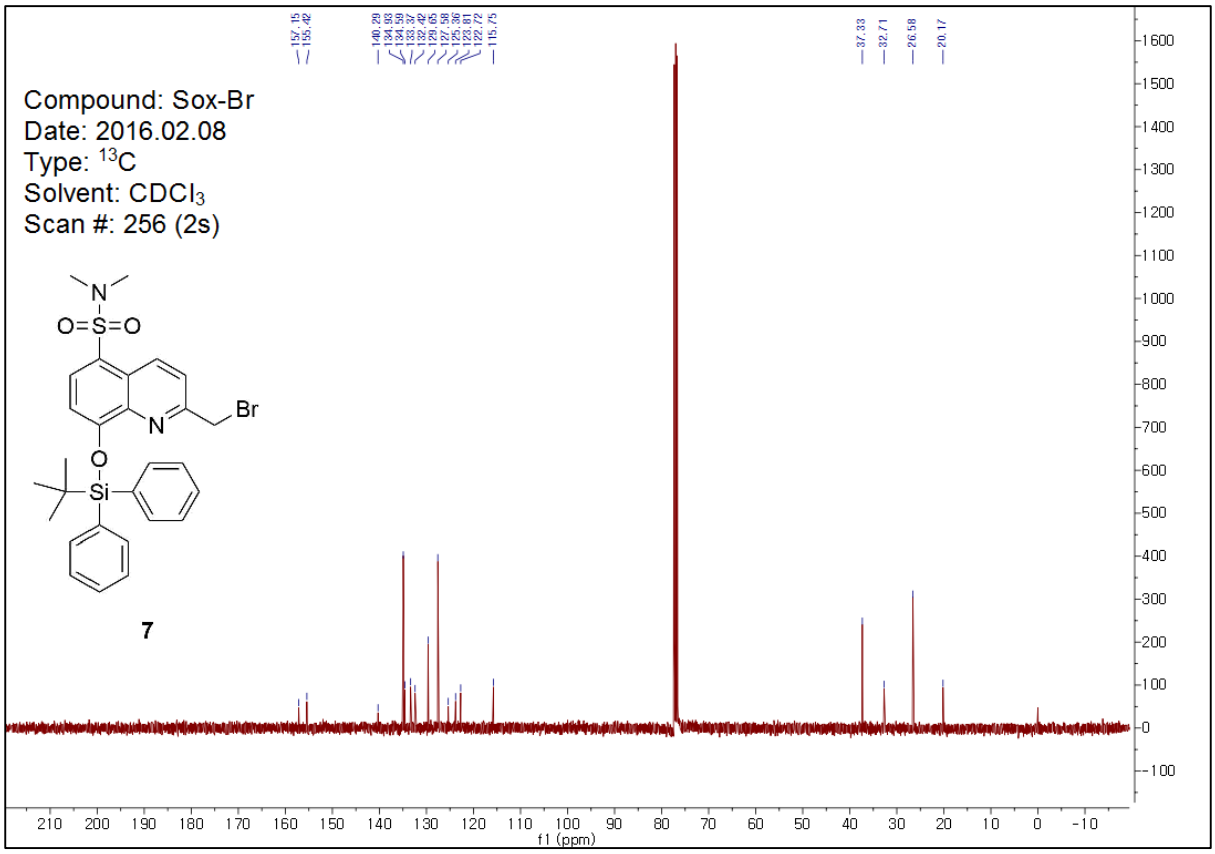

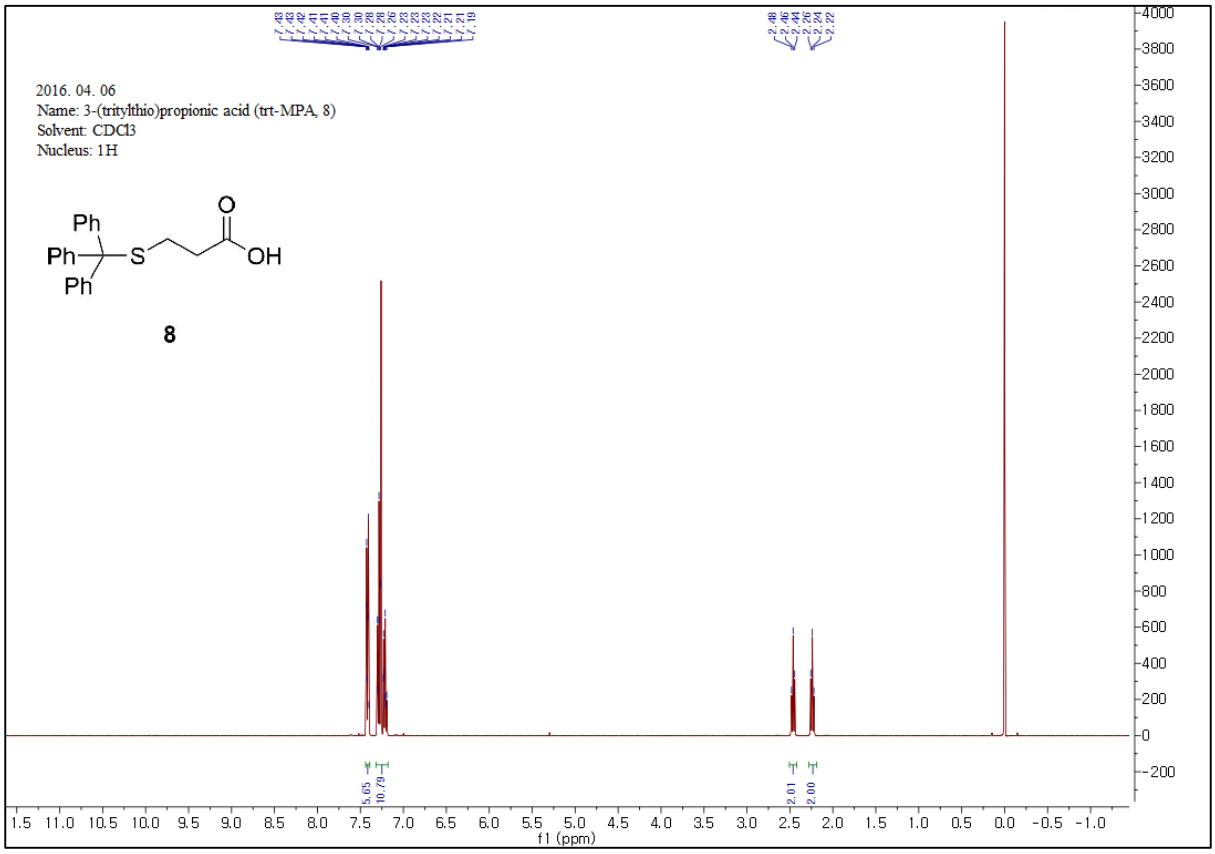

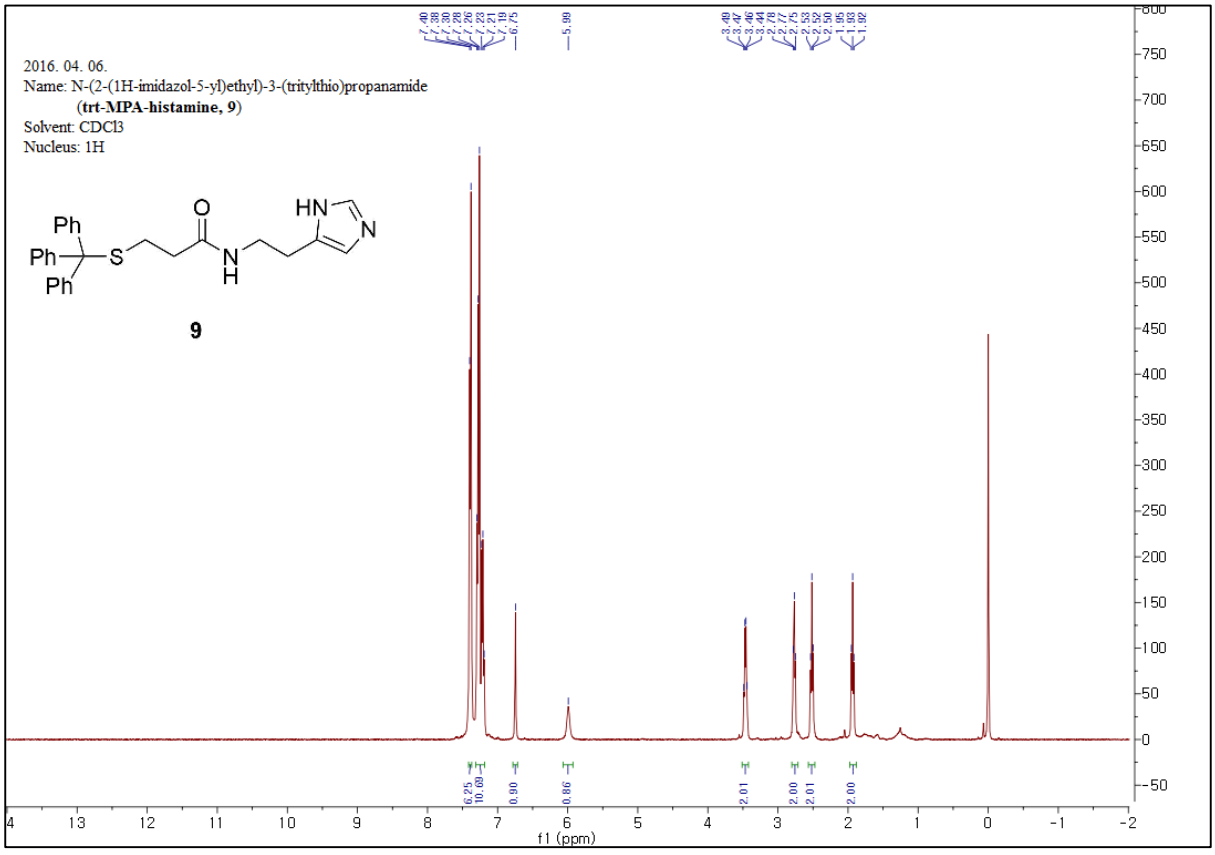

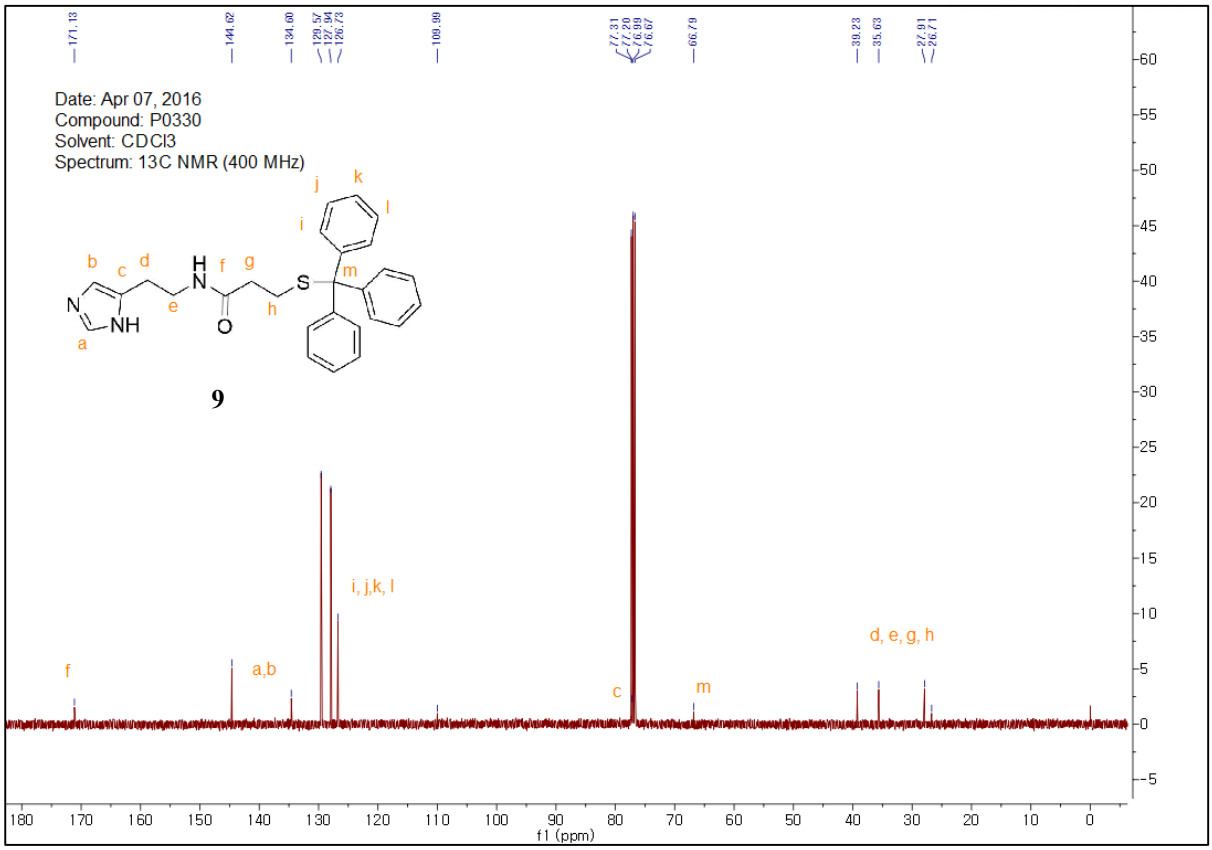

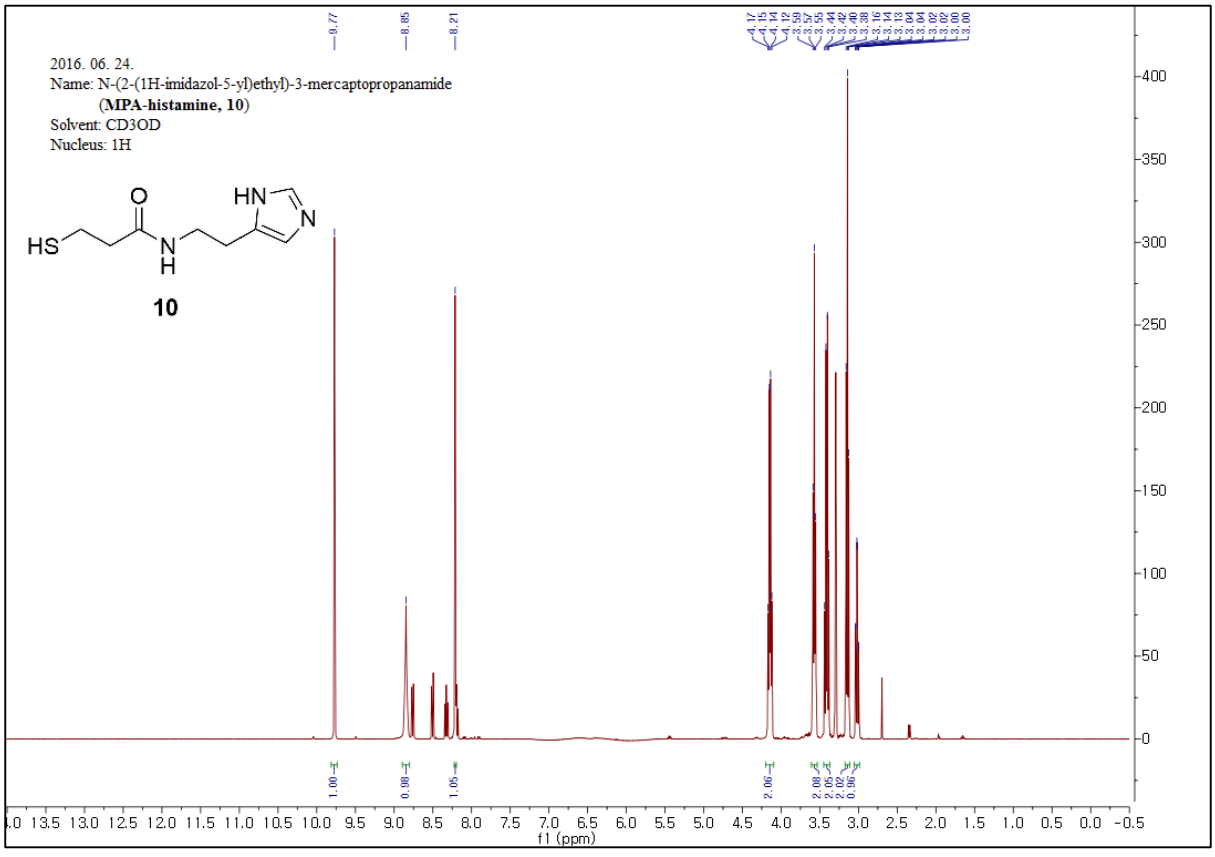

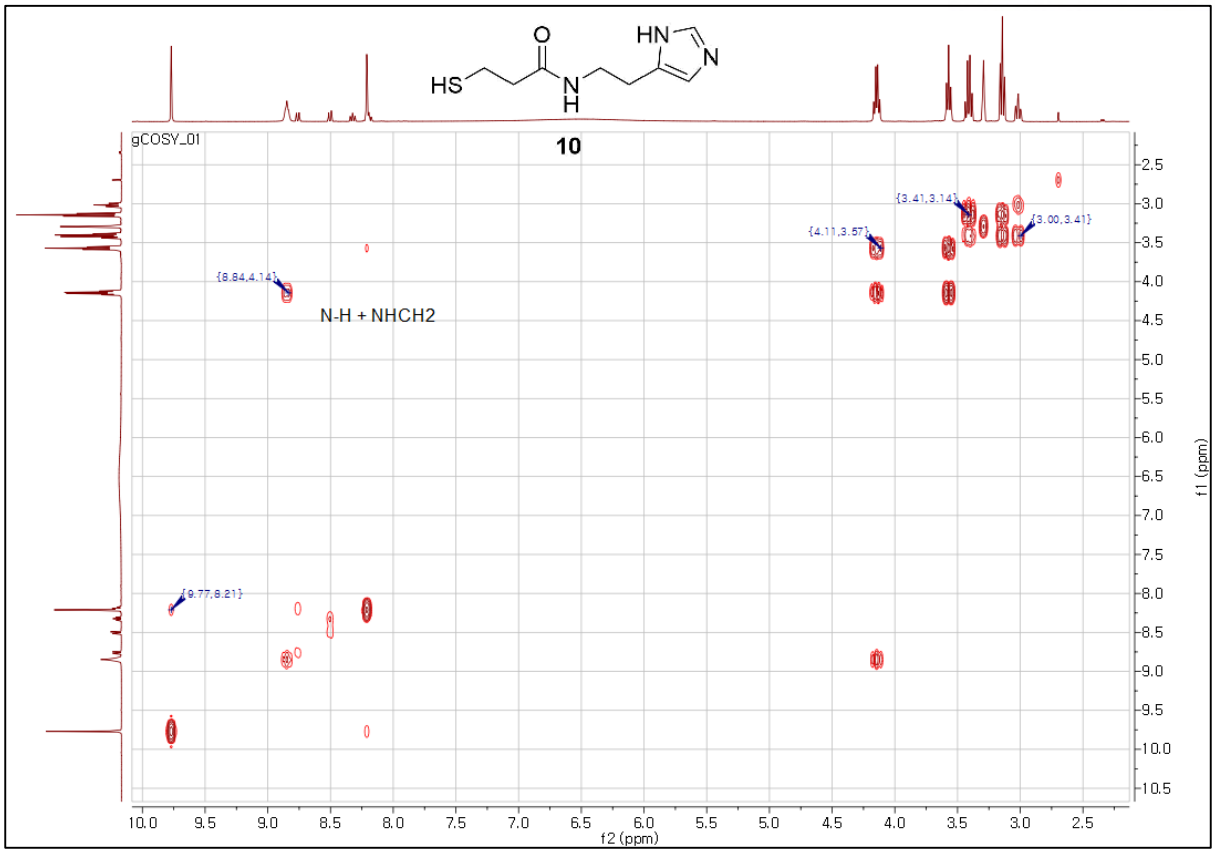

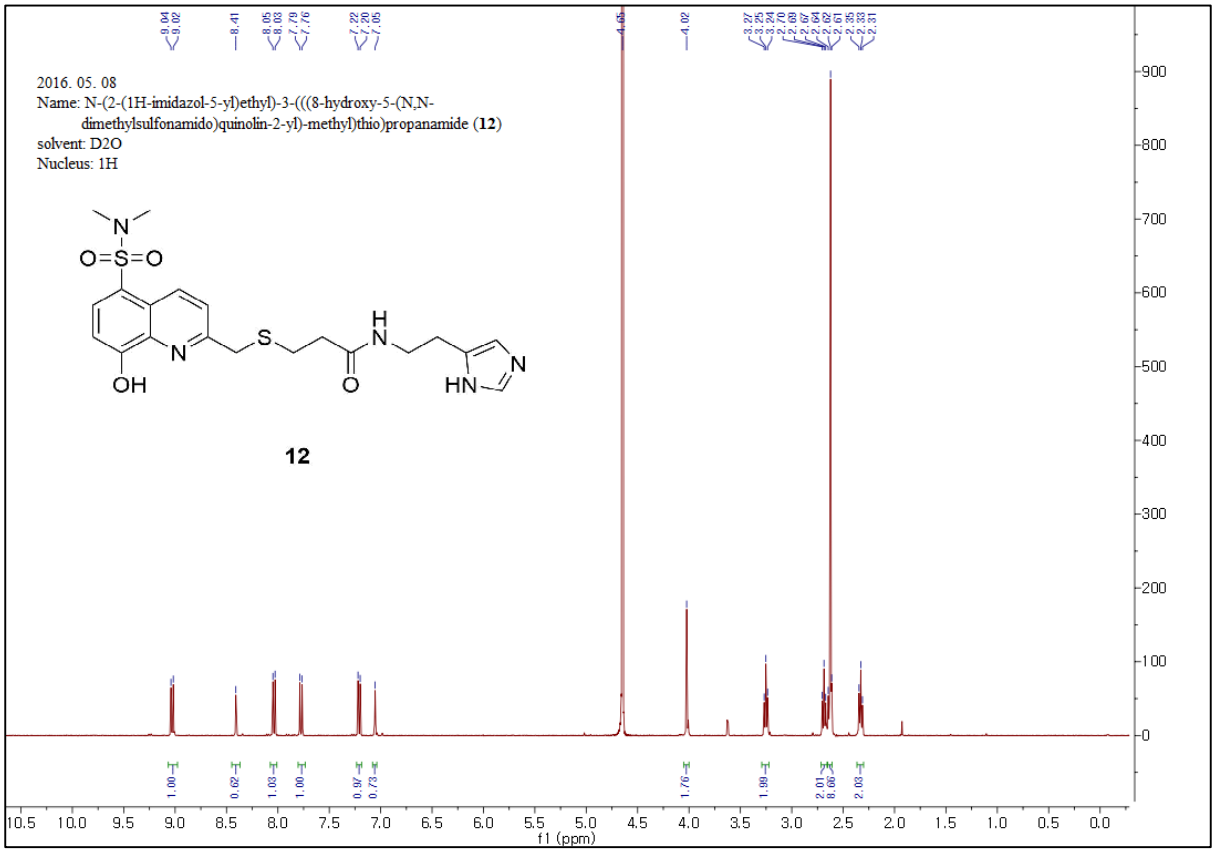

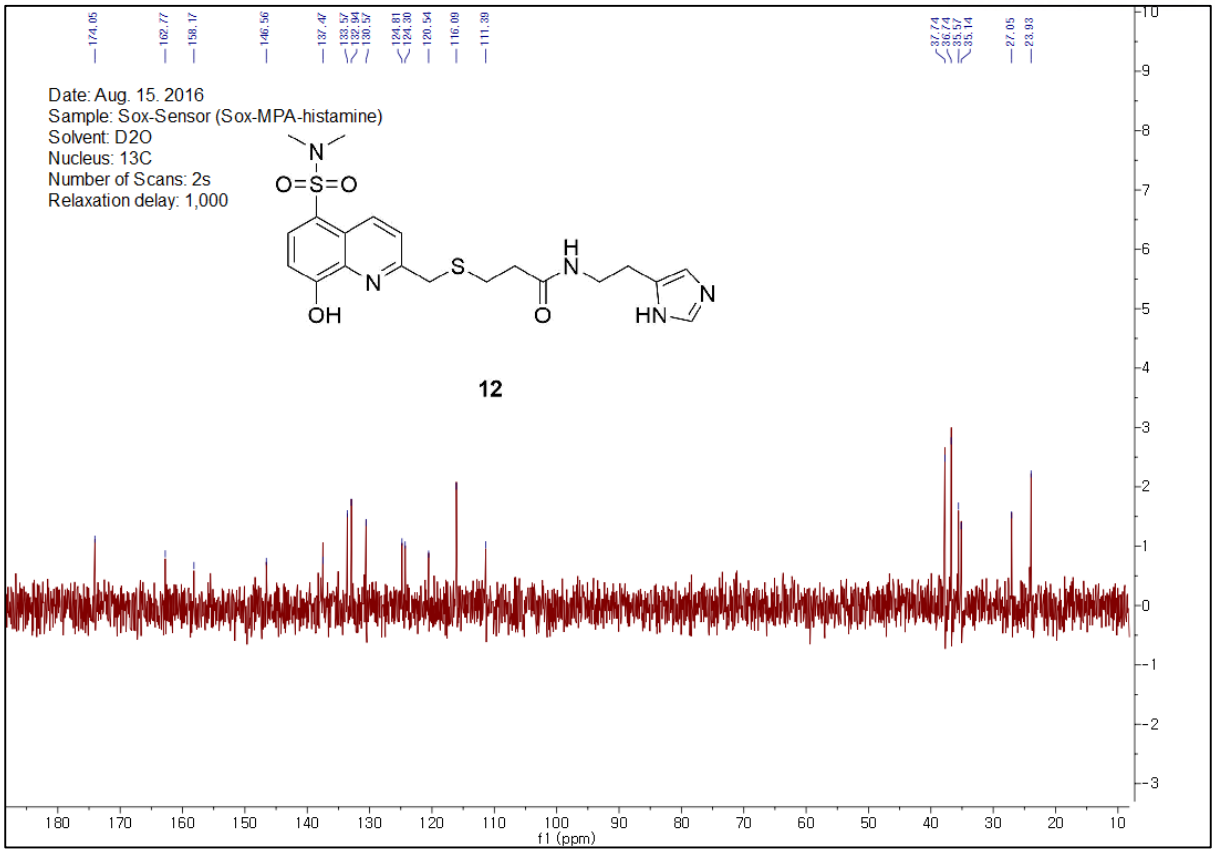

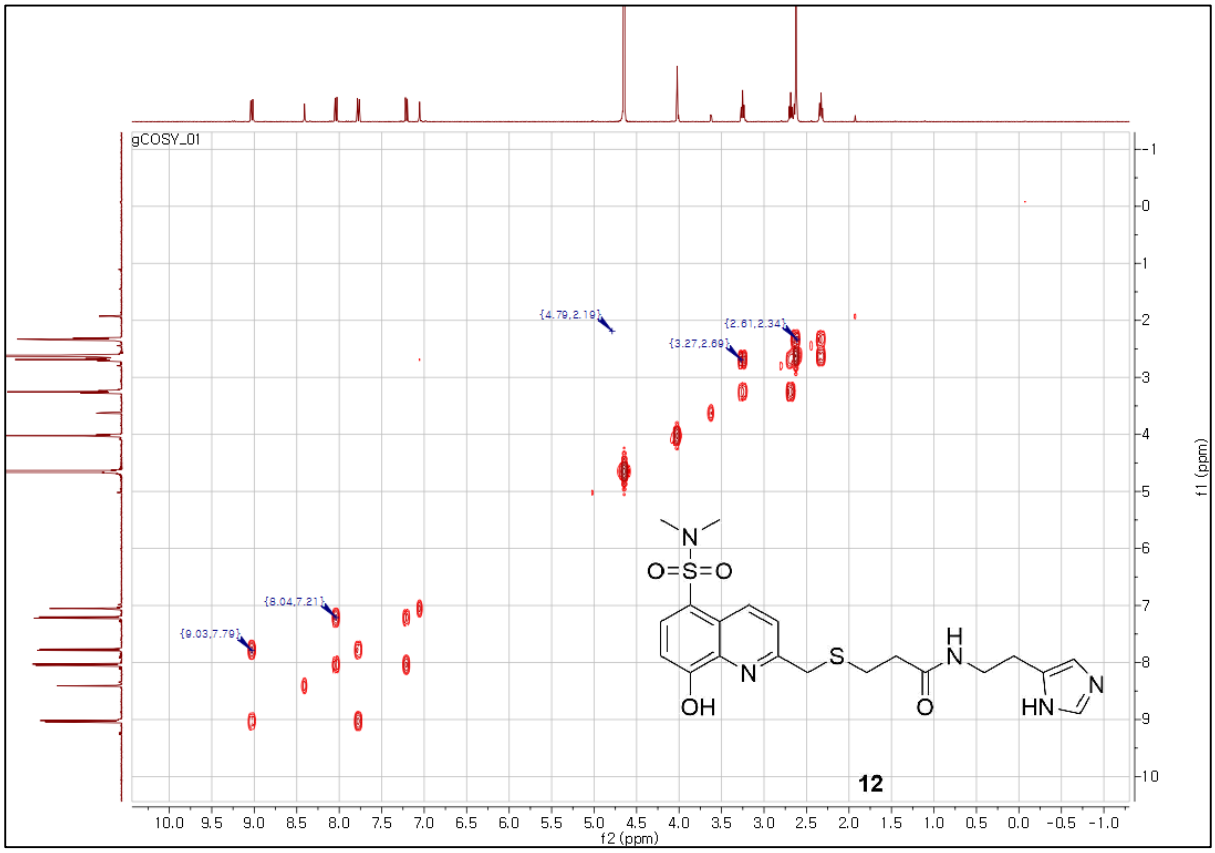

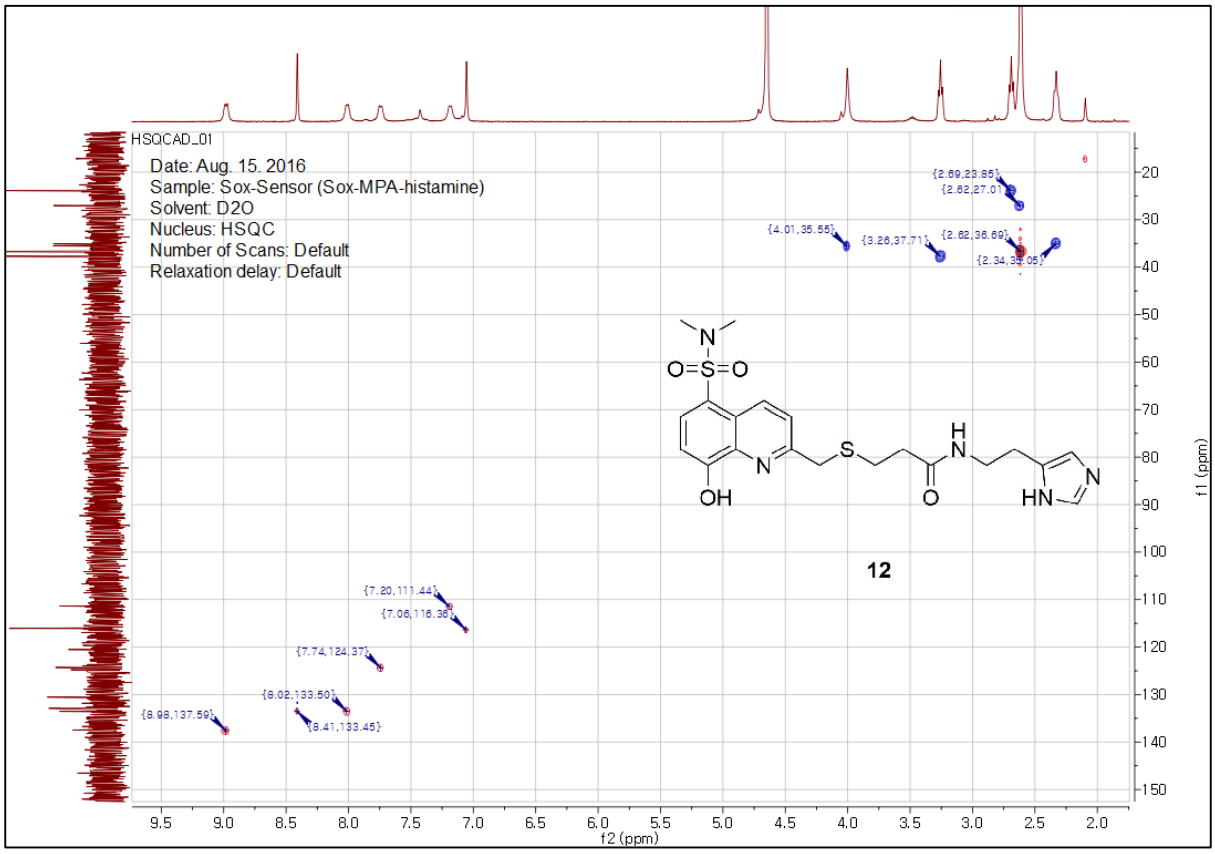

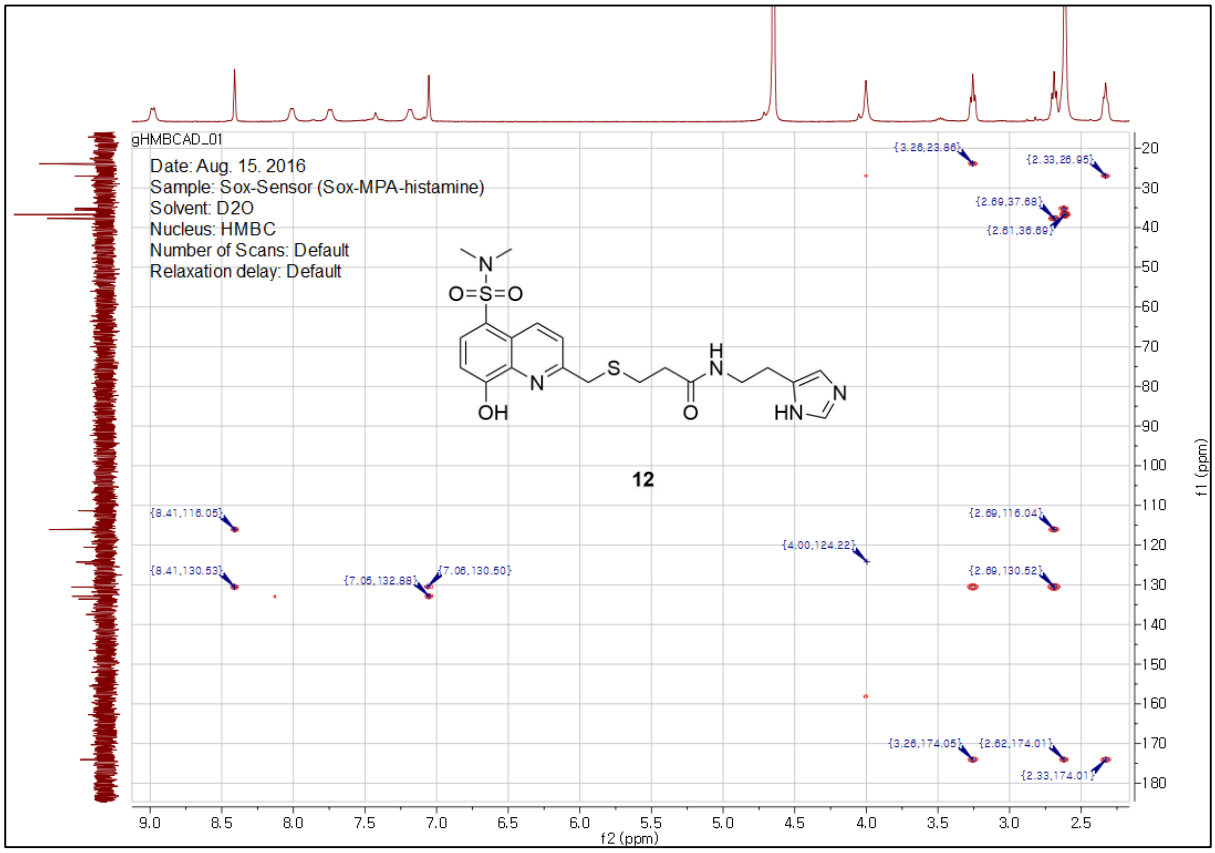

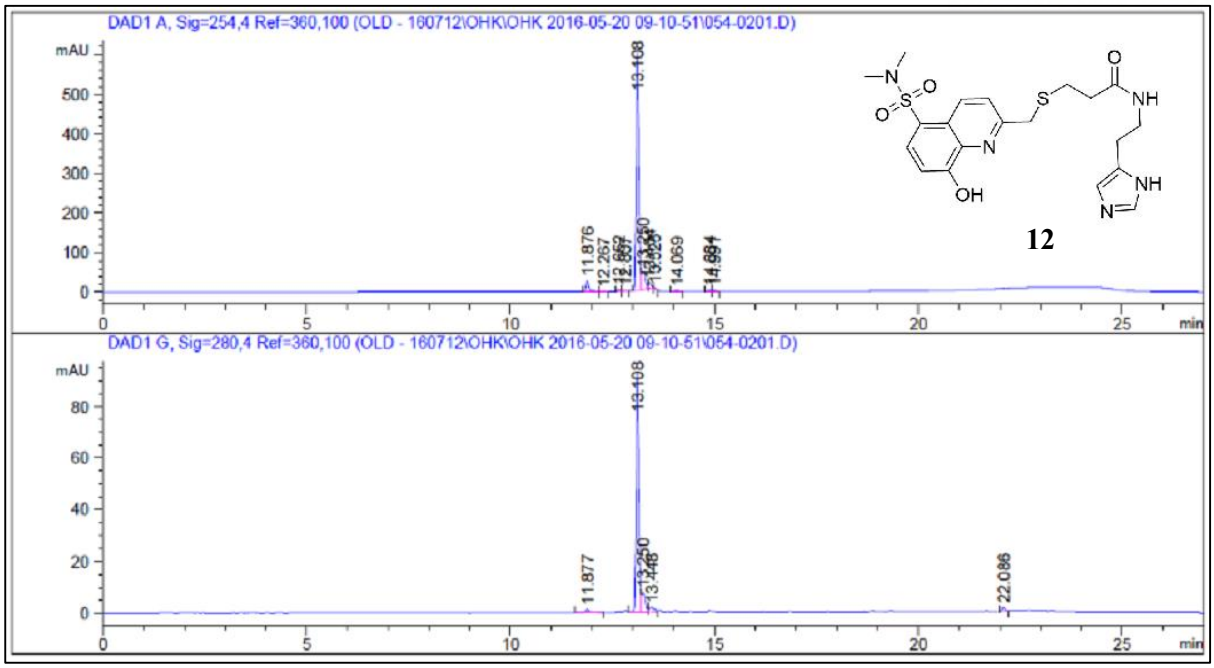

12

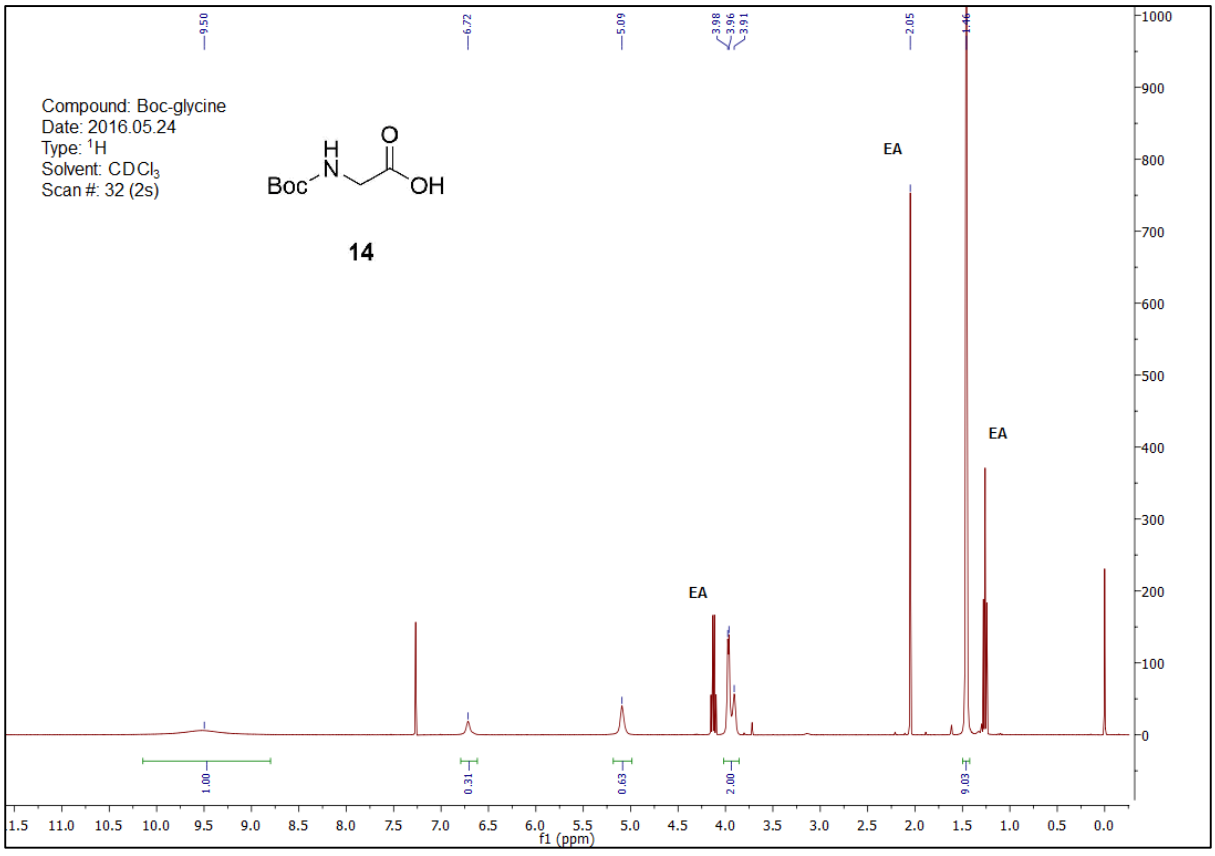

14

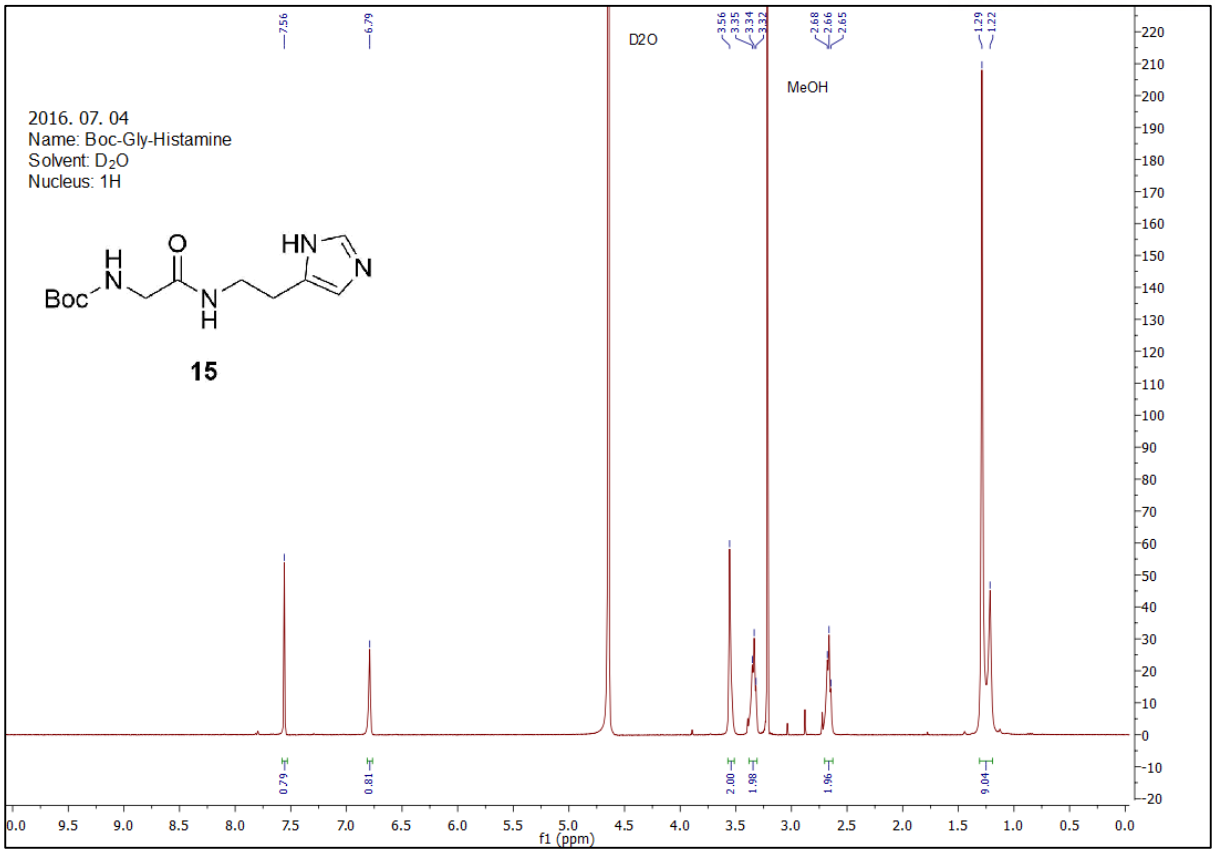

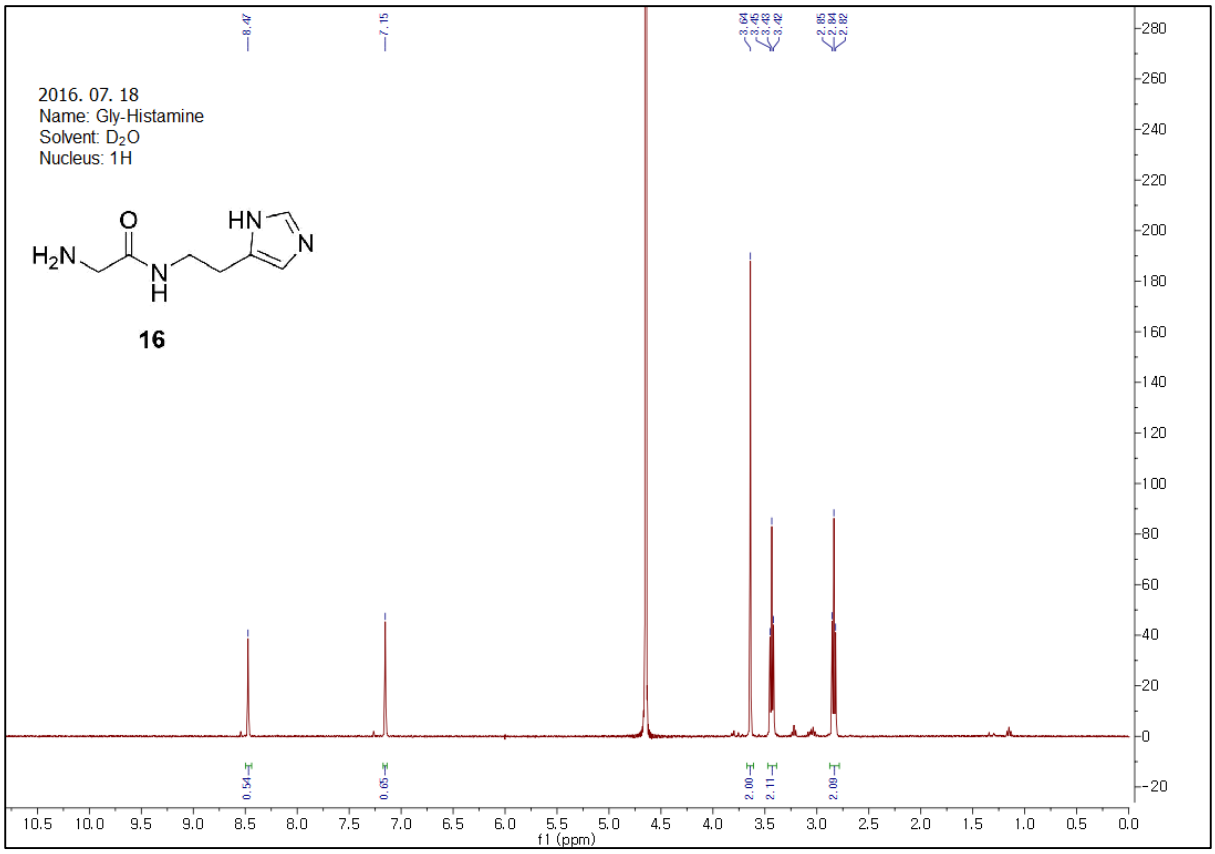

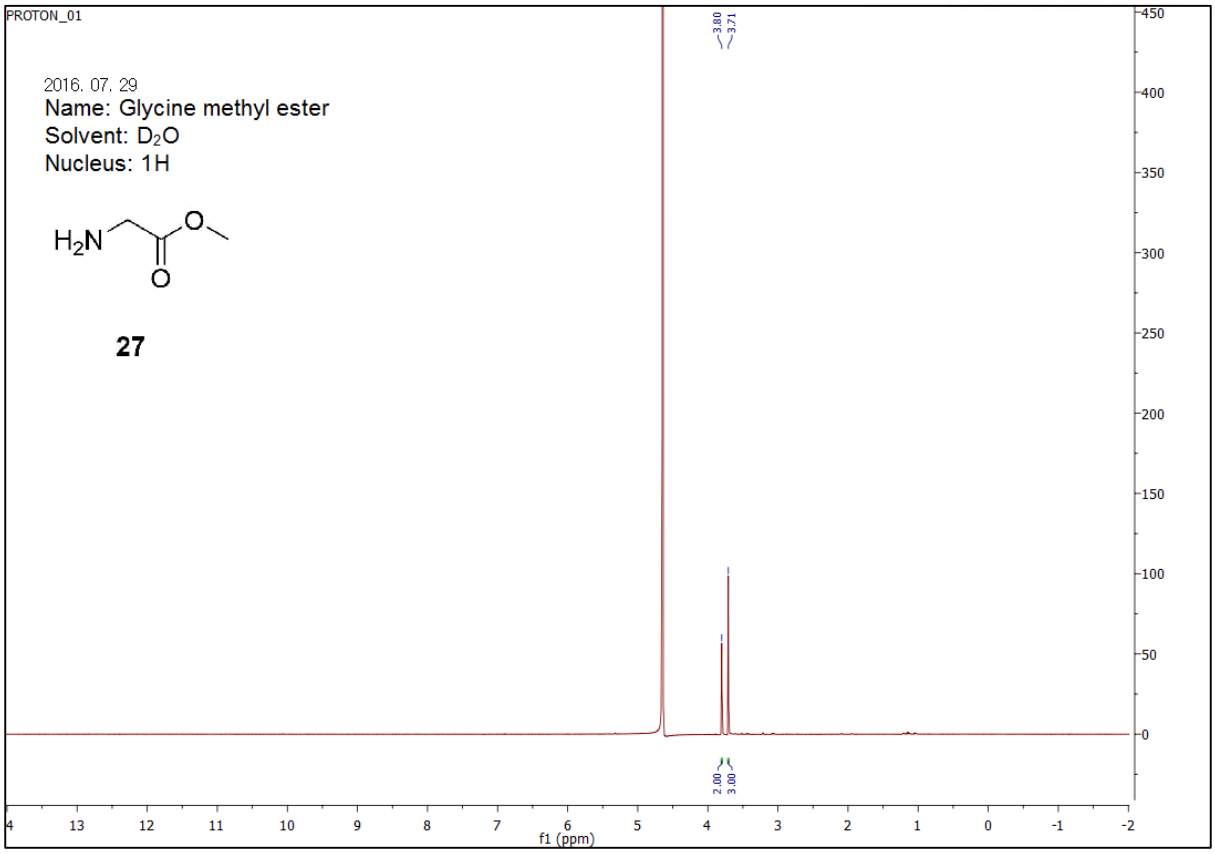

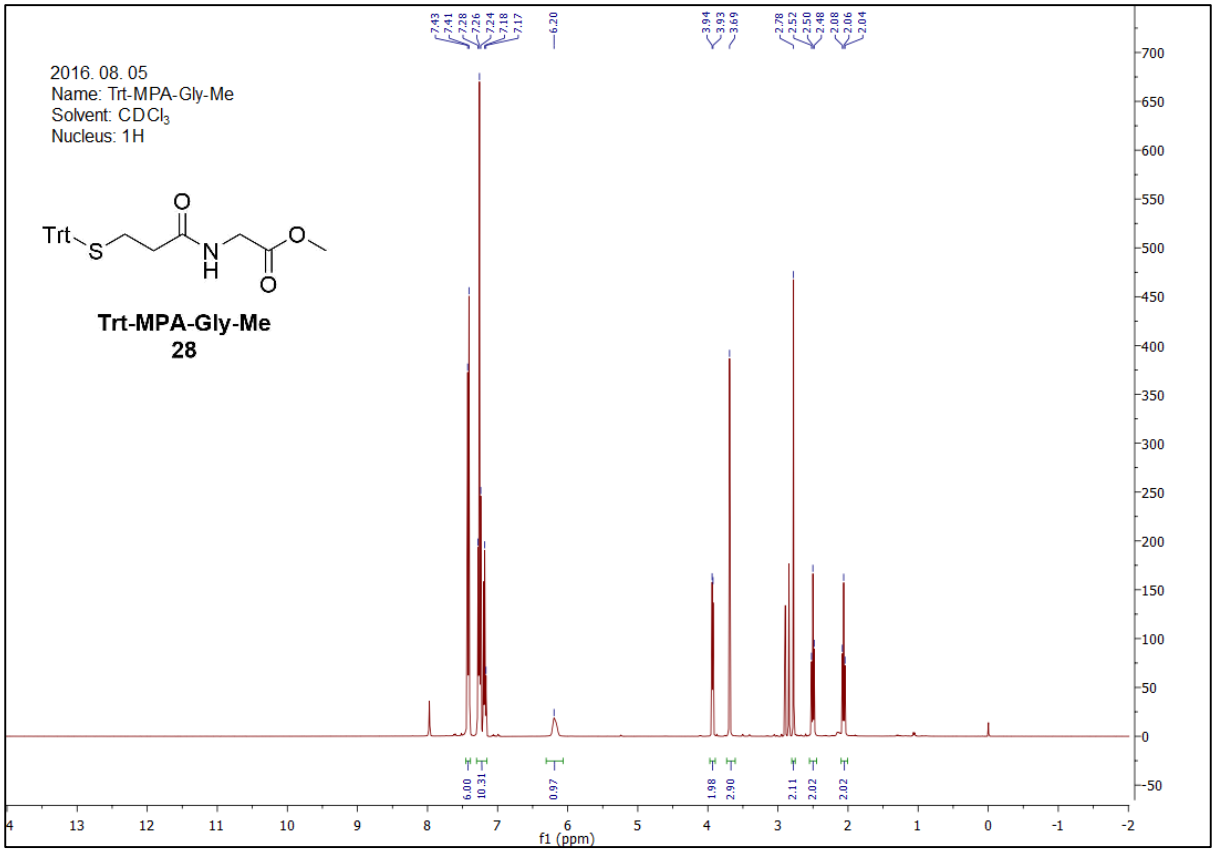

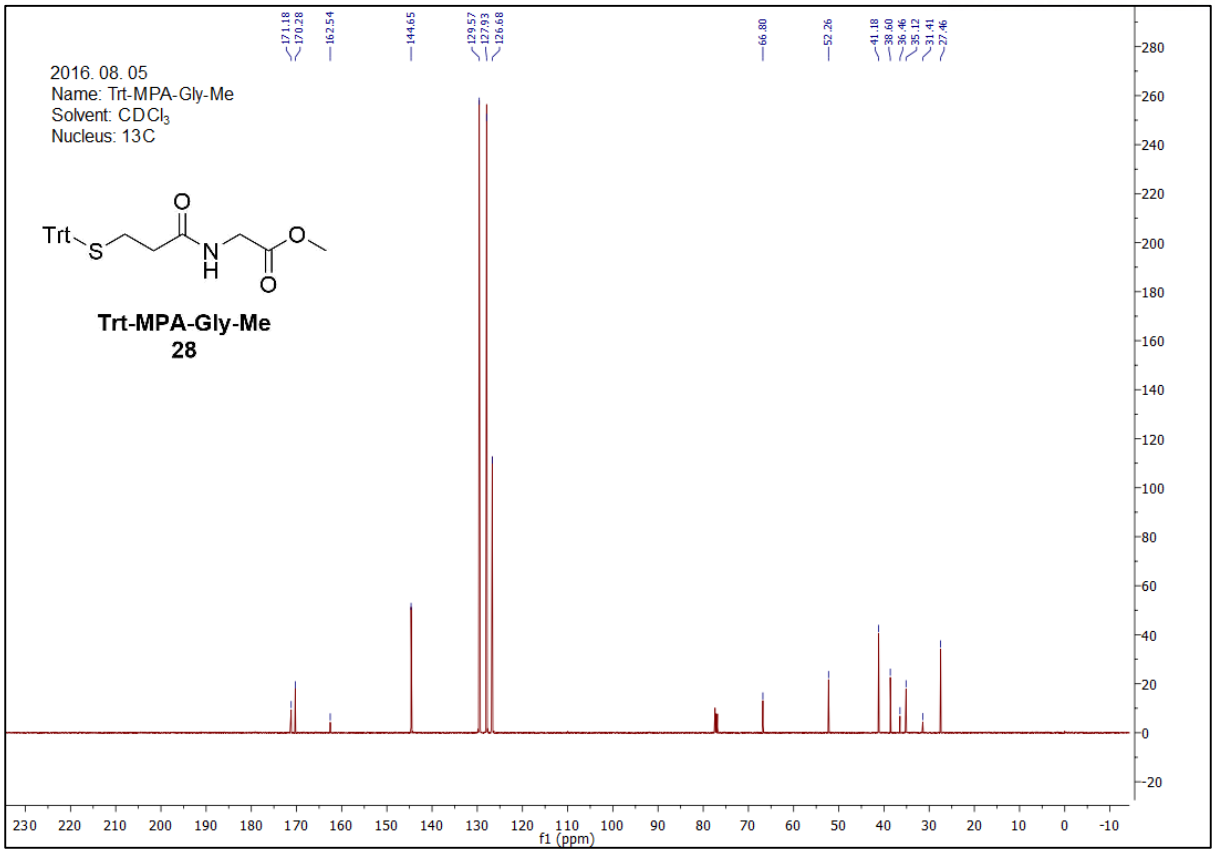

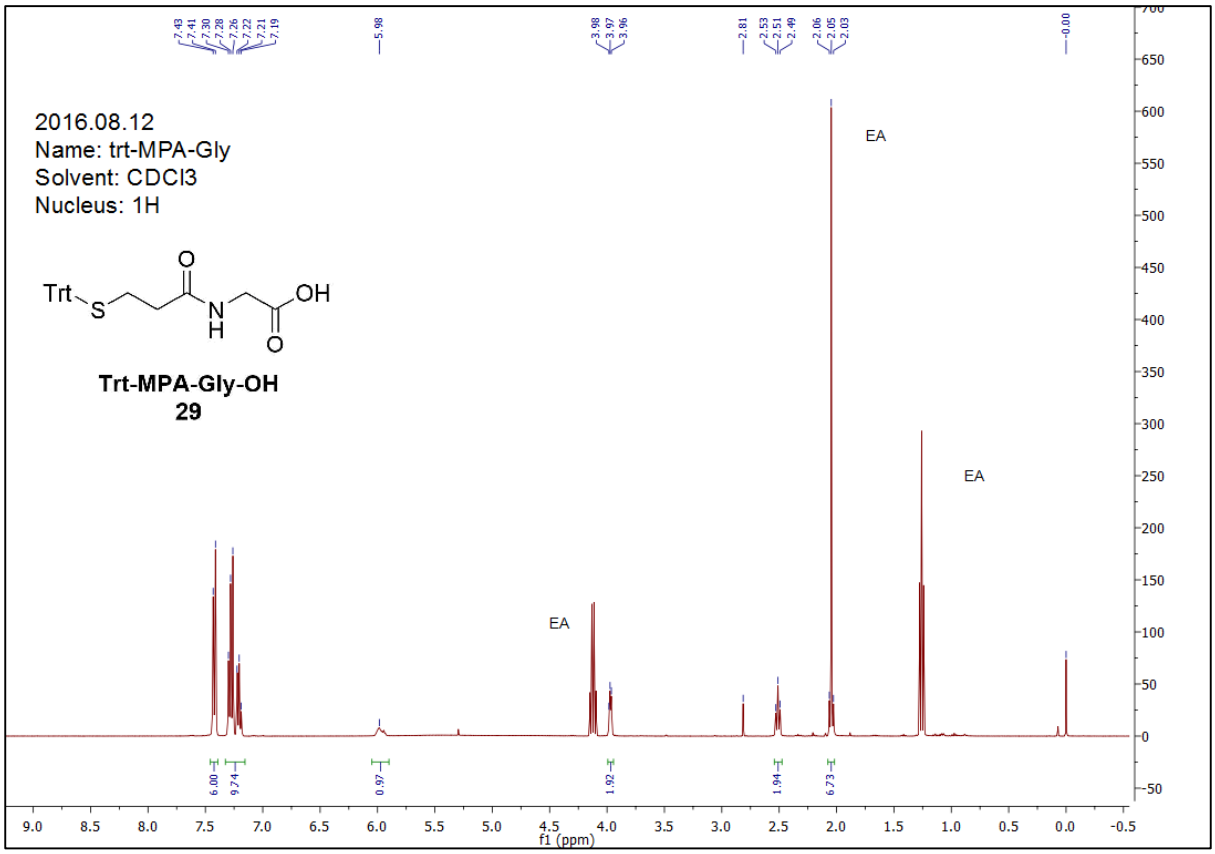

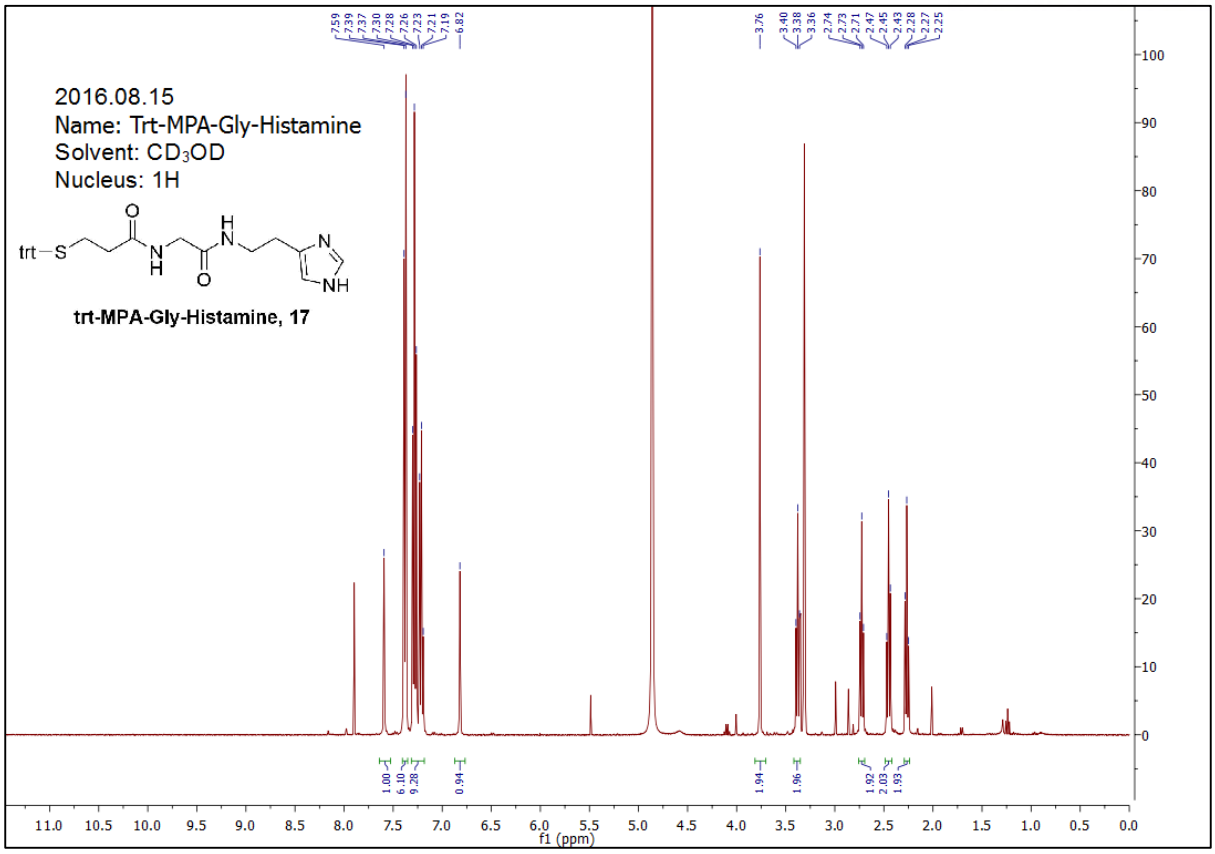

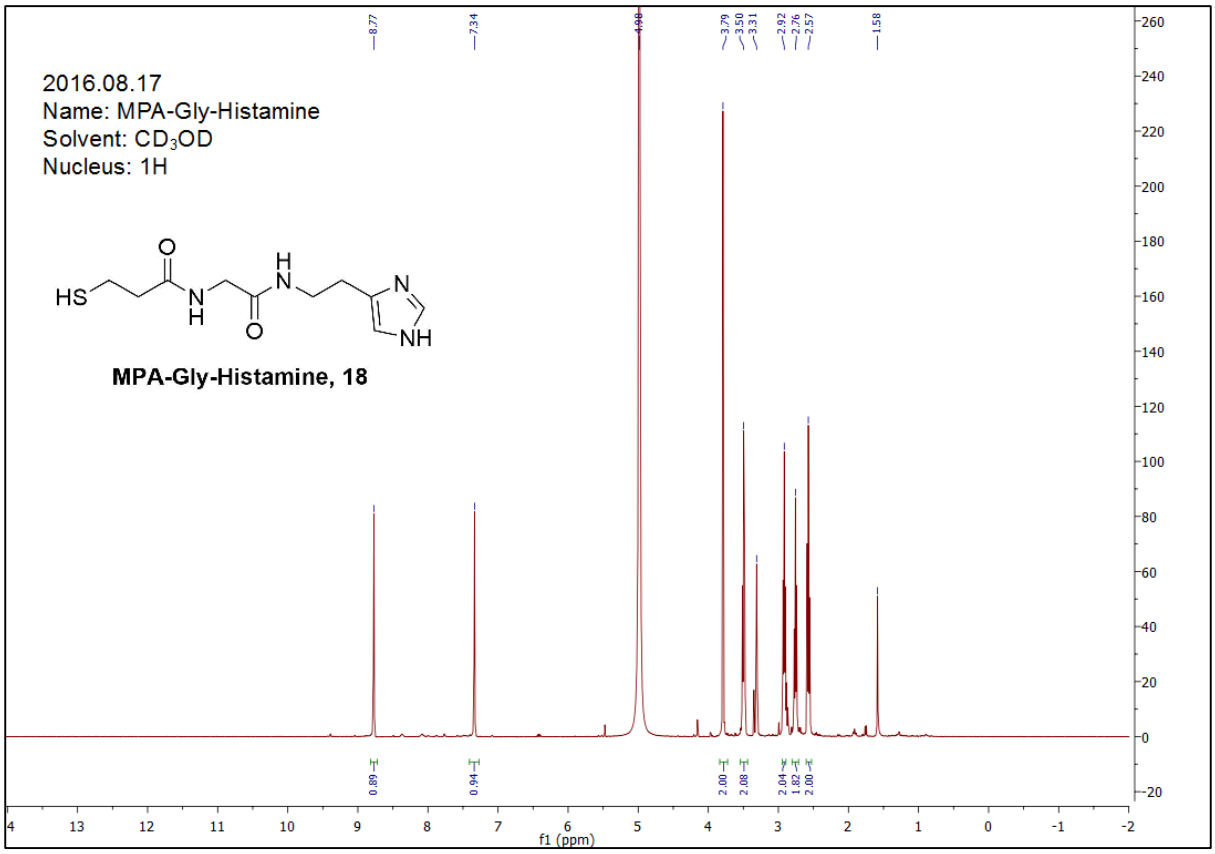

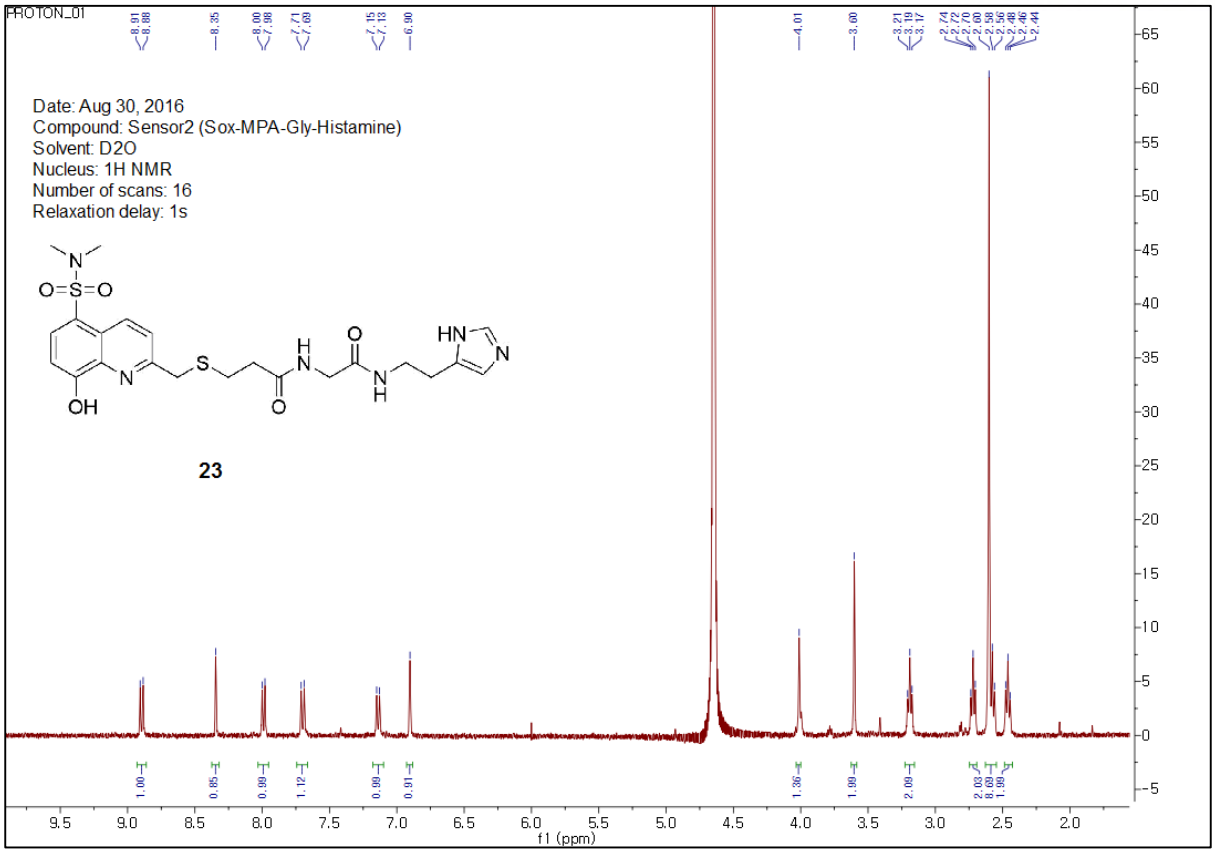

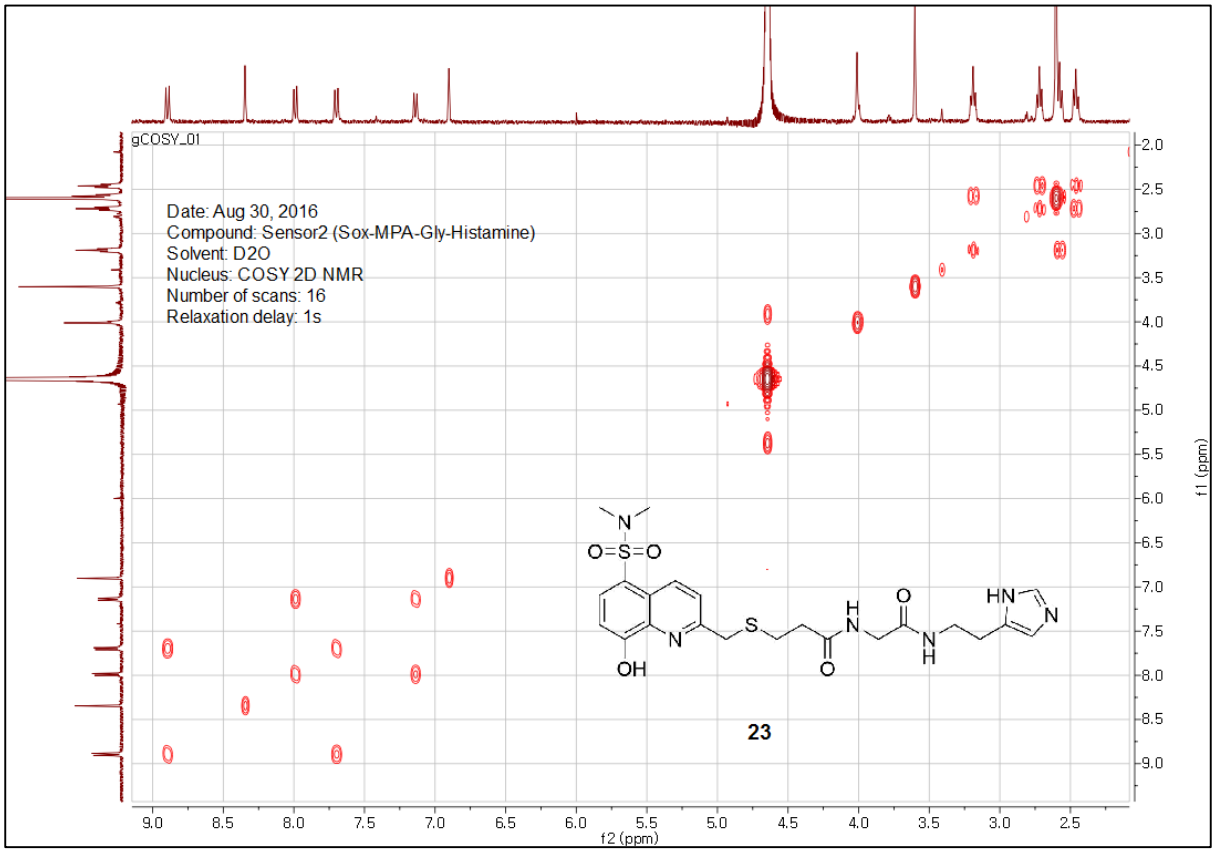

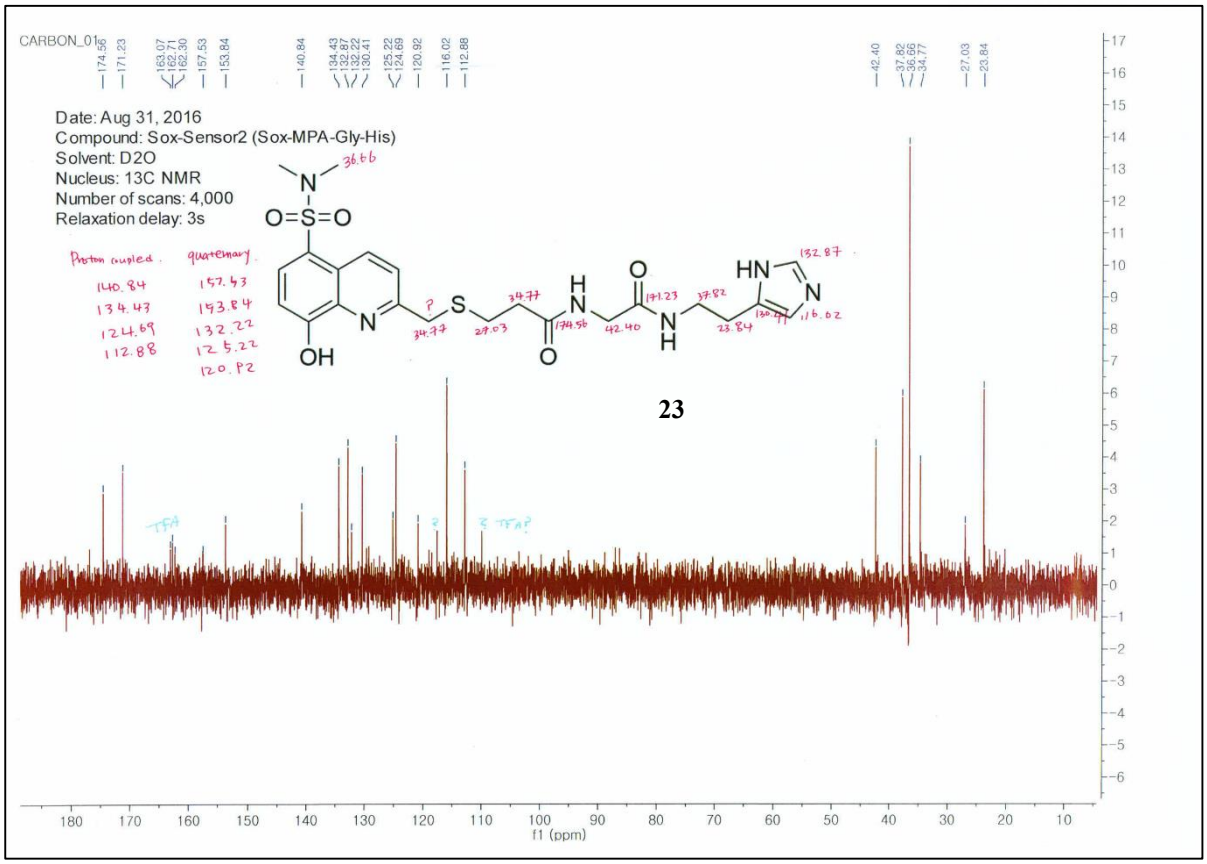

Fluoroscence (AFU)	D.I. water	1 mM Sensor	1 mM Sensor + 10 mM $MgCl_2$	1 mM Sensor + 100 mM PPA	1 mM Sensor + 100 mM PPA + 10 mM $MgCl_2$
	1	2	3	4	5
data 1	72	3277	38284	2541	47178
data 2	67	4163		3162	47186
data 3	69			3107	
average	69.33333333	3720	38284	2936.666667	47182

Table 2-1. Numerical data of Figure 2-8. Fluorescence assay of model kinase sensor;
1) Distilled water (control); 2) 1 mM sensor molecule;
3) 1mM sensor molecule and 10 mM $MgCl_2$; 4) 1mM sensor molecule and 100 mM PPA;
5) 1mM sensor molecule, 100 mM PPA and 10mM $MgCl_2$.

	1	2	3	4
not phosphorylated sensor (mM)	0.1	0.25	0.5	1
$MgCl_2$ (mM)	0	0	0	0
Fluorescence (AFU)	338	558	671	1097
	310	737	1066	1648
average	324	647.5	868.5	1372.5

Table 2-2. Numerical data of Figure 2-9.

Fluorescence change by sensor molecule concentration

Sensor (mM)	$MgCl_2$ (mM)	d1	d2	d3	Average
0.1	0	349	394	313	352
0.1	1	342	410	388	380
0.1	2	410	428	384	407.33333
0.1	5	483	421	483	462.33333
0.1	10	581	584	532	565.66667
0.1	20	757	848	830	811.66667
0.1	50	1727	1785	1782	1764.6667
0.1	100	3975	3839	4022	3945.3333
0.1	200	10260	9787	10057	10034.667
0.1	400	30322	29595	27545	29154
0.1	800	59493	58204		58848.5
0.1	1000	Overrange Limitation of equipment			
0.1	1500				

Table 2-3. Numerical data of Figure 2-10. The fluorescence change in dependence of magnesium ion.

0.1 mM Sensor	0.1 mM Sensor + 10 mM PPA	0.1 mM Sensor + 10 mM $MgCl_2$	0.1 mM Sensor + 10 mM PPA + 10 mM $MgCl_2$
3347	3639	8804	22070
3367	3122	8594	18156
3357	3380.5	8699	20113

Table 2-4. Numerical data of Figure 2-11. Phosphorylation and fluorescence of the 100 μM sensor molecule with 10 mM $MgCl_2$. pH 7.5 100 mM phosphate buffer

2.6 References

1. Hunter, T. Signaling—2000 and Beyond *Cell* **2000**, *100*, 113-127
2. Manning, G.; Whyte, D. B.; Martinez, R.; Hunter, T.; and Sudarsanam, S. The Protein kinase complement of the human genome, *Science* **2002**, *298*, 192-1934
3. Graves, J. D.; and Krebs, E. G. Protein phosphorylation and signal transduction, *Pharmacol. Ther.* **1999**, *82*, 111-121
4. Hunter, T. Protein kinases and phosphatases: The yin and yang of protein phosphoyrylation and signaling, *Cell* **1995**, *80*, 225-236
5. Rothman, D. M.; Shults, M. D.; and Imperiali, B. Chemical approaches for investigating phosphorylation in signal transduction networks. *Trends in Cell Biol.* **2005**, *15*, 502-510
6. Leonard, H. A. Human pyruvate kinases. Role of the divalent cation in the catalytic mechanism of the red cell enzyme. *Biochemistry*, **1972**, *11* (23), 4407-4414
7. Kanpe, M. J.; Ahuja, L. G.; Bertinetti, D.; Burghardt, N. C.; Zimmermann, B.; Talyor, S. S.; and Herberg, F. W. Divalent metal ions Mg^{2+} and Ca^{2+} have distinct effects on protein kinase A activity and regulation. *ACS Chem. Biol.* **2015**, *10* (10), 2303=2315
8. Nowak, T.; and Suelter, C. Pyruvate kinase: activation by and catalytic role of the monovalent and divalent cations. *Mol. Cell Biochem.* **1981**, *35*(2), 65-75
9. Williams, R. L.; Oren, D. A.; Muñoz-Dorado, J.; Inouye, S.; Inouye, M.; and Arnold, E. Crystal structure of *Myxococcus xanthus* nucleoside diphosphate kinase and its interaction with a nucleotide substrate at 2.0 Å resolution. *J. Mol. Biol.* **1993**, *234*, 1230–1247.
10. Matte, A.; Tari, L. W.; and Delbaere, L. T. J. How do kinases transfer phosphoryl groups? *Structure* **1998**, *6* (4), 413-419
11. Auerbach, G.; Huber, R.; Grättinger, M.; Zaiss, K.; Schurig, H.; Jaenicke, R.; and Jacob, U. Closed structure of phosphoglycerate kinase from *Thermotoga maritima* reveals the catalytic mechanism and determinants of thermal stability, *Structure* **1997**, *5*, 1475-1483
12. Blume-Jensen, P.; and Hunter, T. Oncogenic kinase signaling. *Nature* **2001**, *411*, 355-365
13. Yarden, Y.; and Sliwkowski, M. X. Untangling the ErbB signaling network, *Nat. Rev.Mol. Cell. Biol.* **2001**, *2*, 127-137
14. Ortutay, C.; Väliaho, J.; Stenberg, K.; and Vihinen, M. KinMutBase: A registry of disease-causing mutations in protein kinase domains. *Hum. Mutat.* **2005**, *25*, 435-442
15. Mendelsohn, J.; and Baselga, J. Epidermal growth factor receptor targeting in cancer, *Semin. Oncol.* **2006**, *33*, 369-385
16. Skorski, T. Oncogenic tyrosine kinases and the DNA-damage response. *Nat. Rev. Cancer* **2002**, *2*, 351-360

17. Cohen, P. Protein kinases — the major drug targets of the twenty-first century? *Nat. Rev. Drug Discovery* **2002**, *1*, 309-315
18. Daub, H. Kinase inhibitors: Narrowing down the real targets. *Nat. Chem. Biol.* **2010**, *6*, 249-250
19. Opar, A. Kinase inhibitors attract attention as oral rheumatoid arthritis drugs. *Nat. Rev. Drug Discovery* **2010**, *9*, 257-258
20. Zhang, J.; Yang, P. L.; and Gray, N. S. Targeting cancer with small molecule kinase inhibitors. *Nat. Rev. Cancer* **2009**, *9*, 28-39
21. Saywers, C. Targeted cancer therapy. *Nature* **2004**, *432*, 294-297
22. Dancey, J.; and Sausville, E. A. Issues and progress with protein kinase inhibitors for cancer treatement, *Nat. Rev. Drug Discovery* **2003**, *2*, 296-113
23. Scapin, G. Protein Kinase Inhibition: Different Approaches to Selective Inhibitor Design. *Curr. Drug Targets* **2006**, *7*, 1443-1454
24. Van, T. N. N.; and Morris, M. C. *Fluorescent Sensors of Protein Kinases: From Basics to Biomedical Applications*, 1st ed.; Elsevier Inc., 2013; Vol. 113, pp 217–274.
25. González-Vera, J. A. Probing the Kinome in Real Time with Fluorescent Peptides. *Chem. Soc. Rev* **2012**, *41* (5), 1652
26. Beck, J. R.; Peterson, L. B.; Imperiali, B. and Stains, C. I. Quantification of Protein Kinase Enzymatic Activity in Unfractionated Cell Lysates Using CSox-Based Sensors, *Curr. Protoc. Chem. Biol.* **2014**, *6*(3), 135-156
27. Stains, C. I.; Tedford, N. C.; Walkup, T. C.; Lukovic, E.; Goduen, B. N.; Griffith, L. G.; Lauffenburger, D. A.; and Imperiali, B. Interrogating Signaling Nodes Involved in Cellular Transformations Using Kinase Activity Probes. *Chem. Biol.* **2012**, *19*, 210-217
28. Shults, M. D.; Pearce, D. A.; and Imperiali, B. Modular and tunable chemosensor scaffold for divalent zinc. *J. Am. Chem. Soc.* **2003**, *125*(35), 10591-10597
29. Shults, M. D.; and Imperiali, B. Versatile Fluorescence Probes of Protein Kinase Activity. *J. Am. Chem. Soc.* **2003**, *125*(35), 14248-14249
30. Shults, M. D.; Carrico-Moniz, D.; and Imperiali, B. optimal Sox-based fluorescent chemosensor design for serine/threonine protein kinases. *Anal. Biochem.* **2006**, *352*, 198-207
31. Luković, E.; González-Vera, J. A.; and Imperiali, B. Recognition-Domain Focused Chemosensors: Versatile and Efficient Reporters of Protein Kinase Activity. *J. Am. Chem. Soc.* **2008**, *130* (38), 12821–12827
32. Luković, E.; Vogel Taylor, E.; and Imperiali, B. Monitoring Protein Kinases in Cellular Media with Highly Selective Chimeric Reporters. *Angew. Chem. Int. Ed* **2009**, *48* (37), 6828–6831
33. Shults, M. D.; Janes, K. A.; Lauffenburger, D. A.; and Imperiali, B. A multiplexed

homogeneous fluorescence-based assay for protein kinase activity in cell lysates. *Nat. Method* **2005**, *2*(4), 277-283

Chapter 3. Proteomic Labeling Strategy through Desthiobiotin with Conjugation of Isotope-Labeled Tyramine using APEX System

3.1 Introduction

To understand the function of a protein, it is crucial to know its intracellular localization. The conventional method to identify proteins in certain organelles or compartments of cells is the fractionation of the organelle from cells, followed by mass spectrometry (MS)-based proteomics[1]. Using this technique, lots of proteins could be detected, although the limited specificity and loss of materials during the fractionation were limitation. Also, it could not be applied into live cells.

To overcome these problems, localized protein tagging strategies have been used recently. For example, green fluorescent proteins (GFP) has been widely used for target protein imaging. GFP is genetically fused to the target protein and visualized. A problem of GFP is that it is quite large and it may affect the localization of small proteins. And it is tedious to carry out the genetic manipulation one by one.

Biotin is also a very useful tag. It has a specific strong interaction with streptavidin, and it is possible to enrich biotin-tagged proteins using streptavidin-bead or visualized them with streptavidin-fluorophore in imaging system. Biotin-tagging in live cells has been successfully achieved using genetically encoded labeling enzymes which tag its neighboring proteins, but not too distant proteins preserving spatial relationships. Promiscuous biotin ligases[2-4], activate biotin into biotin-adenylate ester, but it is a relatively long-lasting intermediate (a half-life of minutes) and low-specific spatial labeling in wide region.

Recently, an engineered ascorbate peroxidase (APEX)[5,6], which is active in cell and oxidizes various phenol derivatives to phenoxy radicals has been utilized. The radicals are short-lived (1< ms) and have a small labeling region[7-9]. Also, radicals can make covalent bonds with amino acids including Tyr, His and Cys[10-13]. Thus, biotin labeling strategy has been developed, in which a biotin-labeled phenol derivative is tagged to the proteome of interest through radical reaction by genetically encoded APEX. However, it was discovered that thioether of biotin was oxidized into sulfoxide group during the radical reaction by APEX and it complicated the MS analyses[14,15].

To address this, desthiobiotin was chosen to replace biotin; desthiobiotin is not oxidized during the radical reaction and it also had a strong affinity for streptavidin ($K_d = 10^{-11}$M)[16]. It was revealed that desthiobiotin performed better than biotin[17], and we decided to apply desthiobiotin in this approach. In addition, non-radioactive stable isotopes were incorporated in desthiobiotin-phenol derivatives to apply in multiplex MS analyses instead of SILAC analyses.

3.2 Design of Isotope-labeled Desthiobiotinyl Tyramide

To prepare desthiobiotin-phenol derivative, the tagged substrates for APEX, desthiobiotin was previously coupled with tyramine to give desthiobiotinyl tyramide (DBT). This time, it was necessary to prepare tyramine containing non-radioactive stable isotopes, which are 13-carbons and 15-nitrogens. By controlling the number of isotopes, we designed four kinds of DBTs with mass difference of three daltons. Its different molecular weight of tags will make it possible to distinguish target proteins in a same sample.

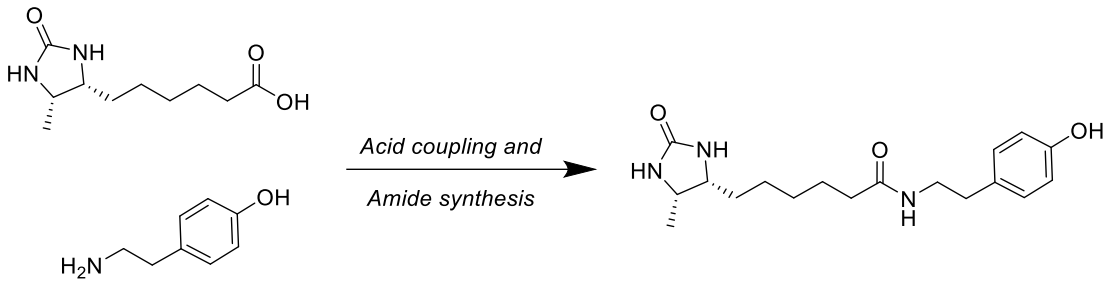

Scheme 3-1. *Synthesis of desthiobiotinyl tyramide*

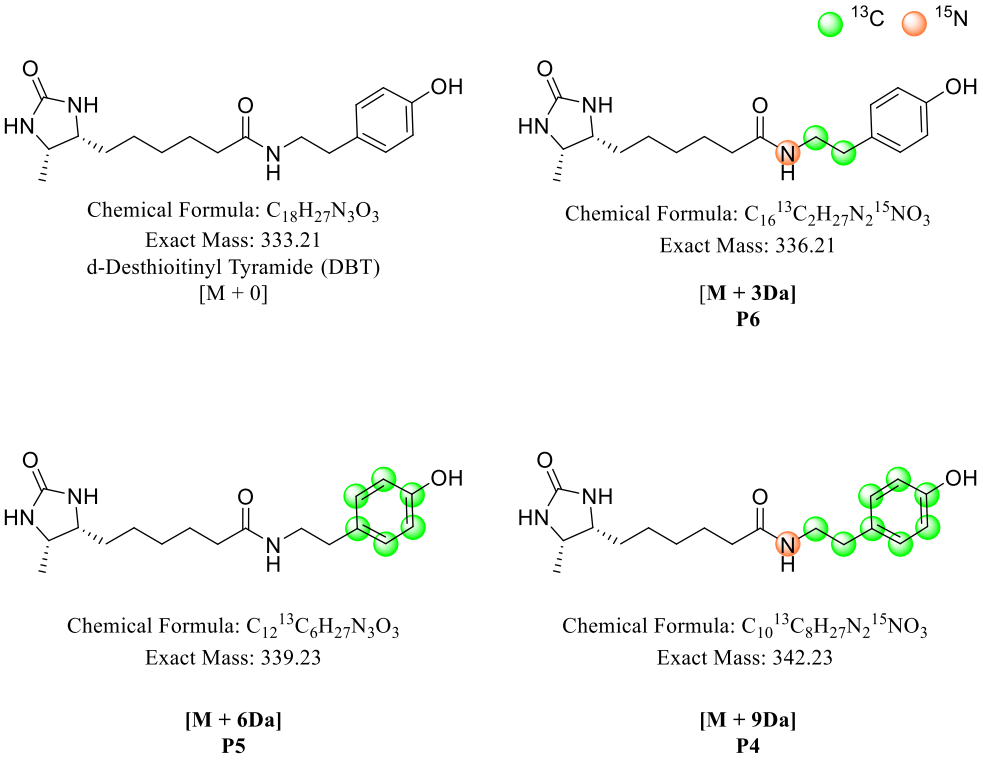

Figure 3-1. Isotope-labeled desthiobiotinyl tyramide tags

3.3 Results and Discussion

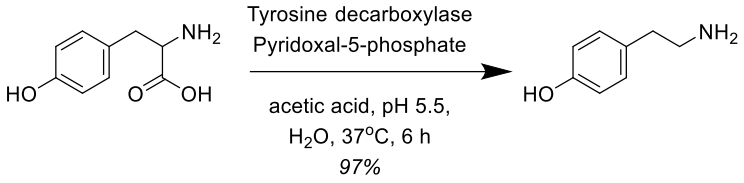

Scheme 3-2. *Tyrosine decarboxylation*

Isotope-labeled tyramines were prepared by decarboxylation of commercial isotope-labeled tyrosine by enzymatic reaction of tyrosine decarboxylase[18,19]. Pyridoxal-5-phosphate was used as a cofactor for tyrosine decarboxylase. After reaction was finished, the reaction solution was removed by rotary evaporator and the residue was re-dissolved in water and passed through cation exchange column. As tyramine contained primary amine and was captured by column, it was eluted by 1 mM HCl solution, to give tyramine HCl salt after lyophilization.

Since the product could contain other inorganic salts, the product was exactly quantified using NMR comparing integration values with 1M 1,4-dioxane as internal standard. Tyramine and dioxane peaks were evaluated with their integration values and compared the ratio. 1,4-Dioxane had a single peak (eight hydrogens) in NMR and it was assigned to 8.00 integration value. The tyramine peak having one proton was 0.22 integration value, which means tyramine's concentration was 0.22 M in NMR sample. Since we know the concentration of added dioxane, we could calculate the amount of tyramine. Three kinds of Isotope-containing tyrosine were purchased and converted to isotope-containing tyramines as shown below.

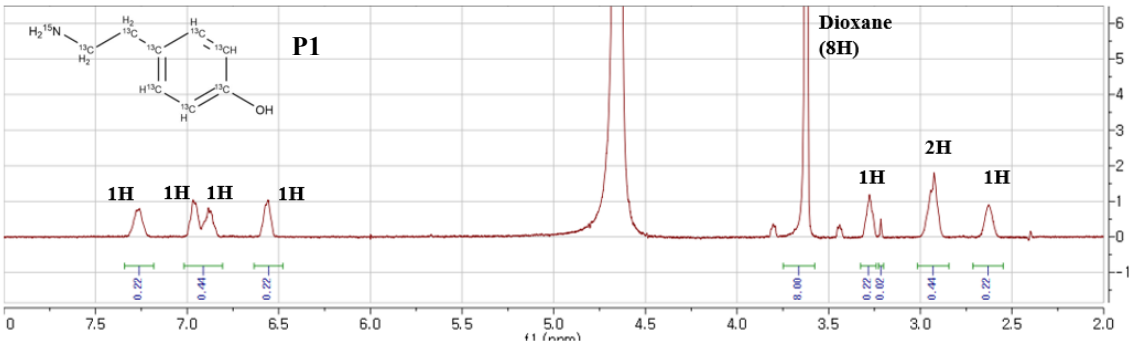

Calculation
1 M dioxane's 1H = 1.0 integration
Tyramine: 0.22 integration = 0.22 M in 3 mL water
Actual concentration = 0.22 x3 = 0.66 M

Figure 3-2. Tyramine Quantification using NMR Integration

Three kinds of Isotope-containing tyrosine were purchased and converted to isotope-containing tyramines which we wanted.

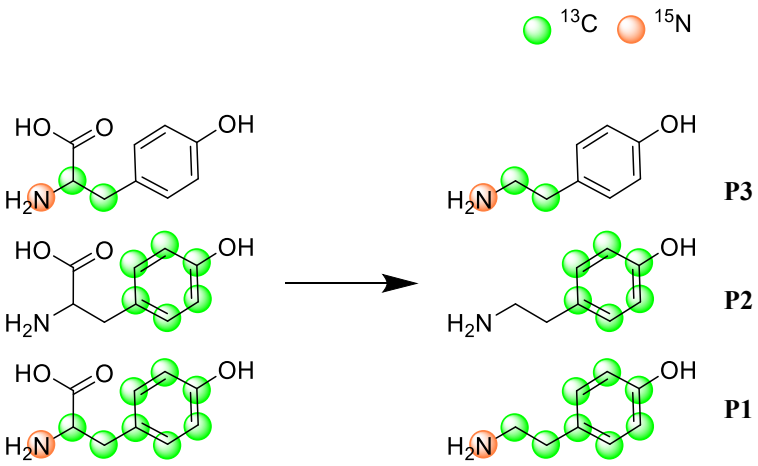

Scheme 3-3. *Isotope-labeled tyrosine*

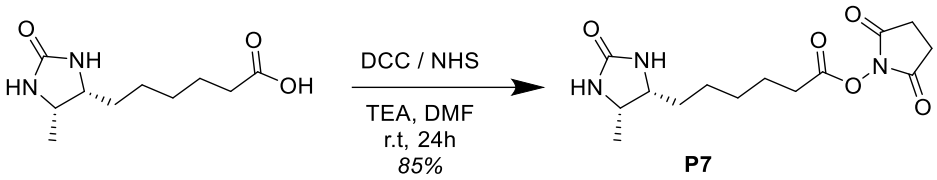

Scheme 3-4. *Carboxylic acid activation via NHS ester*

Synthesis of d-desthiobiotin-NHS ester was referred to the synthesis of biotin-NHS ester using DCC as the coupling agent. In case of biotin-NHS ester, it was not soluble in isopropanol whereas other compounds such as DCC, DCU, NHS (unreacted and remained), TEA (base) and DMF solvent were dissolved in isopropanol. So biotin-NHS ester was easily purified by precipitation in isopropanol. However, desthiobiotin-NHS ester was also soluble in isopropanol and another method was required.

When the reaction was finished, the precipitated solid (DCU) was removed by filtration and the solvent was evaporated. The residue was dissolved in ethyl acetate and worked up using ethyl acetate and NH_4Cl acidic solution. As NHS-activated ester is stable in mild acid, d-desthiobiotin-NHS ester was remaining in the organic phase and other mixtures were extracted into the aqueous phase. The organic layer was collected and evaporated to leave white powder. d-Desthiobiotin-NHS ester was obtained with good purity and good yield.

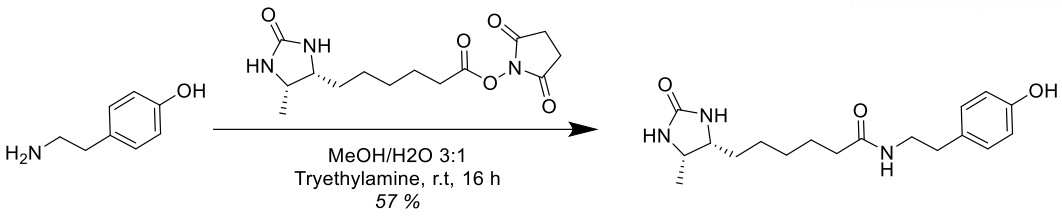

Scheme 3-5. *Synthesis of desthiobiotinyl tyramide*

As a test, non-labeled was reacted with d-desthiobiotin-NHS ester in a mixture of methanol and water. Reaction was monitored by TLC, and when the reaction was finished, solvent was removed by rotary evaporation. The product was easily separated from the reaction mixture using HPLC. (C_{18}-column, 100% water to 75% water and 25% acetonitrile in 5 min, and 75% water and 25% acetonitrile to 60% water and 40% acetonitrile in 40 min. All solvent contained 0.1% TFA.) Isotope-labeled tyramines were also conjugated with desthiobiotin-NHS ester to produce three kinds of isotope-labeled DBT products.

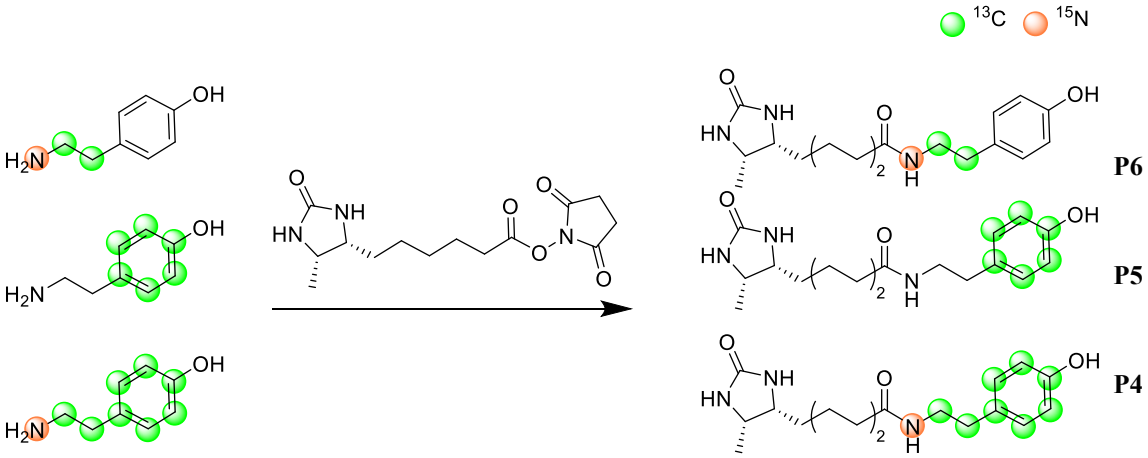

Scheme 3-6. *Isotope-labeled desthiobiotinyl tyramide*

3.4 Conclusion

APEX is a good engineered enzyme and applicable in biological experiments. A series of isotope-labeled tyrosine were converted to tyramine, and the subsequent desthiobiotin conjugation were successful. Desthiobiotin-tyramide tags were appropriate substrates for APEX system. In MS-based proteomics, their small difference of molecular weight can be distinguished, so isotope-labeled tags will be working effectively, since their chemical and physical properties are identical, but definitely identified by MS analysis.

3.5 Methods and Experimental Data

Synthesis of **[$^{13}C_8$, ^{15}N]tyramine** (**P1**).

The protocol for decarboxylation of d_4-tyrosine as described by Ntai *et al*[18] was followed with a few modifications. [$^{13}C_9$, ^{15}N]tyrosine (100 mg) was dissolved in 100 mL H_2O by microwave heating with little boiling until tyrosine was dissolved at all. The tyrosine solution was cooled to room temperature and a suspension of enzyme tyrosine decarboxylase from *Streptococcus faecalis* (2 mg, 0.05 unit/mg) and pyridoxal-5-phosphate (7 mg) in acetate buffer (4 mL, 0.1 M, pH 5.5) was added. The mixture was incubated at 37 ºC for 6 hours with stirring. The reaction was stopped by heating the mixture to boiling. The reaction mixture was concentrated in vacuo and passed through Dowex 50WX cation exchange (hydrogen form) resin. The tyramine product was eluted from the resin with approximately 50 mL of 1 mM HCl and the solvent was evaporated to give [$^{13}C_8$, ^{15}N]tyramine as a tan powder (74 mg, 97% yield).

TLC R_f = 0.5 (Methanol with 5% v/v NH_4OH solution)

^{1}H NMR (400 MHz, Deuterium Oxide) δ 7.09 (dd, *J* = 153.6, 8.4 Hz, ring 2**^{13}CH,** 2H), 6.77 (dd, *J* = 158.0, 6.3 Hz, ring 2**^{13}CH,** 2H), 3.12 (d, *J* = 134.0 Hz, **$^{13}CH_2$**$^{15}NH_2$, 2H), 2.79 (d, *J* = 120.9 Hz, ^{13}C**$^{13}CH_2$**, 2H) ppm.

^{13}C NMR (101 MHz, Deuterium Oxide) δ 154.44 (td, *J* = 65.3, 8.7 Hz), 130.22 (t, *J* = 54.4 Hz), 128.40 (m), 115.67 (td, *J* = 64.0, 62.8, 3.6 Hz), 40.68 (dd, *J* = 35.0, 4.0 Hz), 31.81 (td, *J* = 39.3, 4.4 Hz) ppm.

HRMS (ESI) Calcd. for $^{13}C_8H_{12}{}^{15}NO^+$; 147.1152 m/z (M+H), Observed; 147.1151 m/z (M+H)

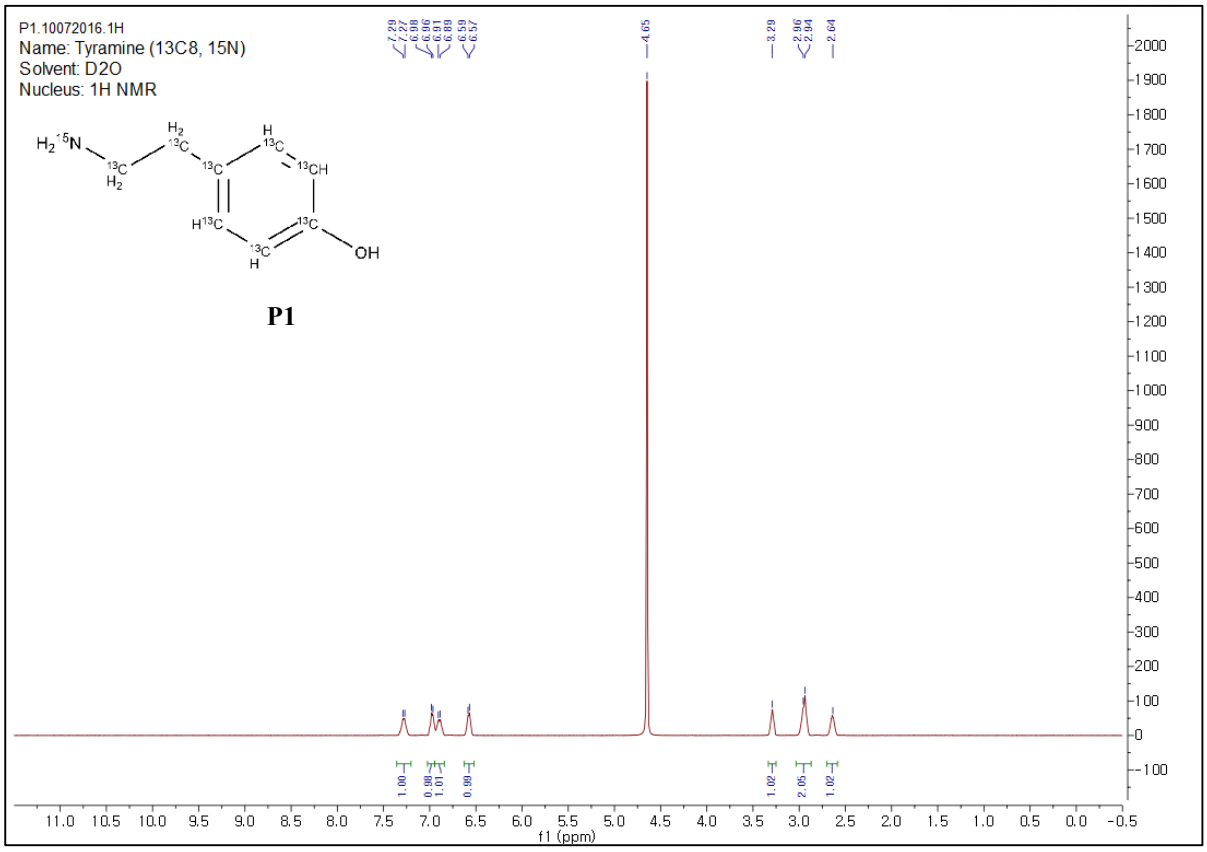

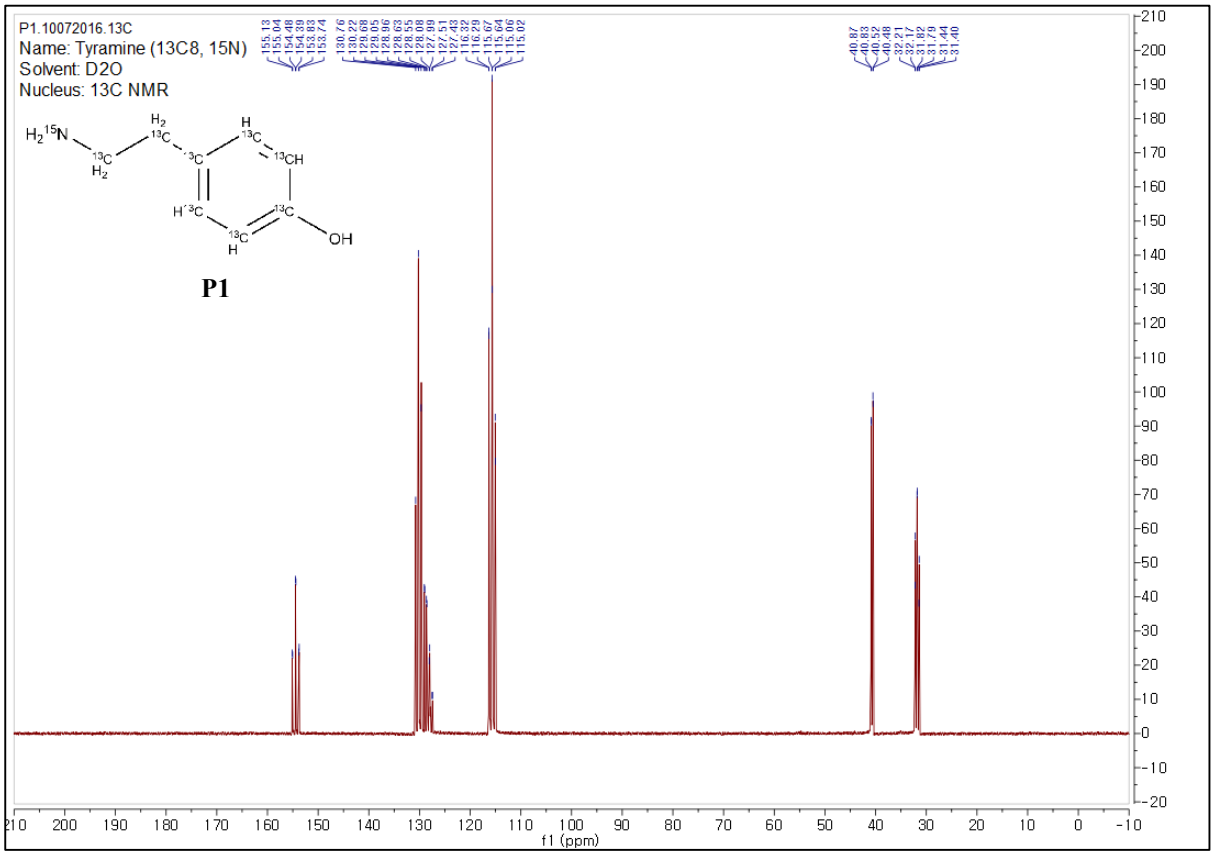

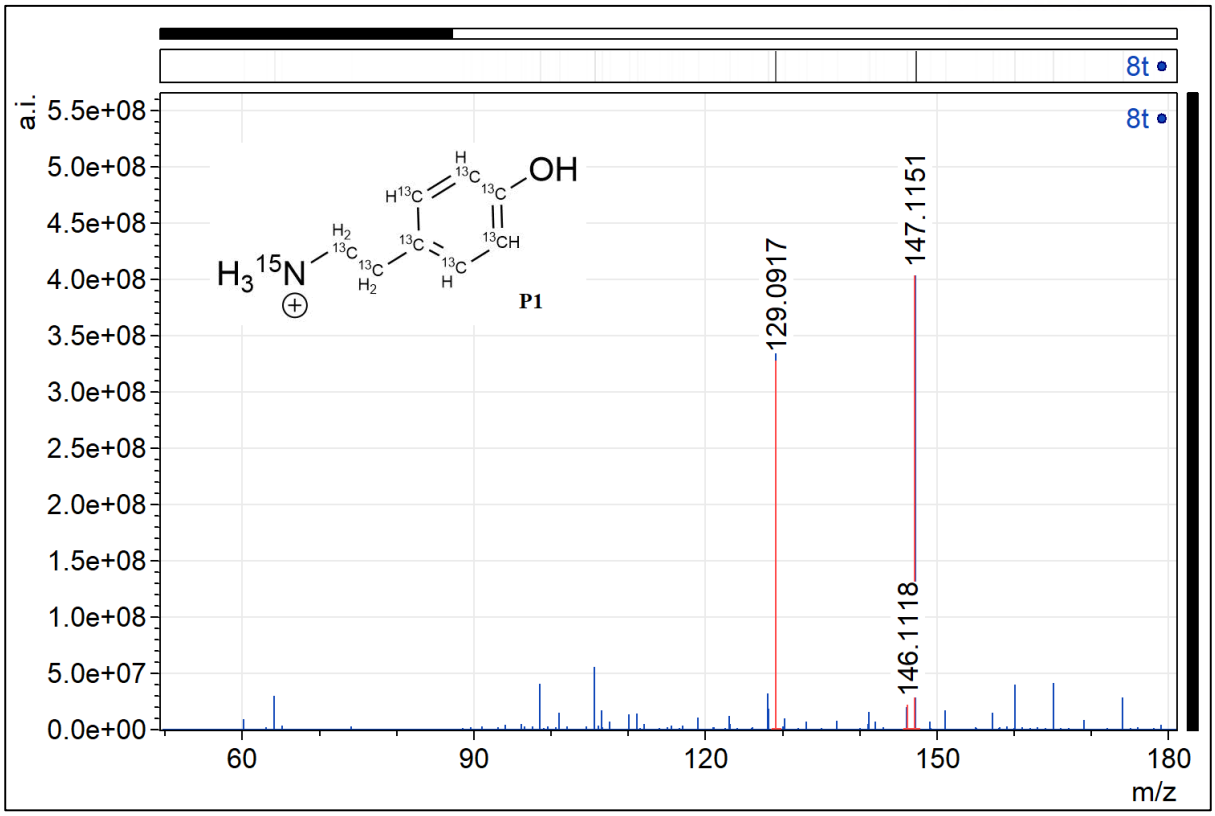

Synthesis of **[ring-$^{13}C_6$]tyramine** (**P2**).

The protocol was identical with the synthesis of [$^{13}C_8$, ^{15}N]tyramine (P1), except for the use of [ring-$^{13}C_6$]tyrosine as the starting material.

^{1}H NMR (400 MHz, Deuterium Oxide) δ 7.08 (dd, *J* = 156.0, 6.6 Hz, ring 2^{13}**CH**, 2H), 6.77 (dd, *J* = 157.4, 7.0 Hz, ring 2^{13}**CH**, 2H), 3.11 (s, **CH$_2$**NH$_2$, 2H), 2.80 (d, *J* = 7.3 Hz, ^{13}C**CH$_2$**, 2H) ppm.

^{13}C NMR (101 MHz, Deuterium Oxide) δ 154.44 (td, *J* = 65.4, 8.7 Hz), 130.24 (t, *J* = 52.2 Hz), 128.36 (dd, *J* = 65.4, 62.5 Hz), 115.65 (m), 40.70, 31.80 (d, *J* = 43.6 Hz) ppm.

HRMS (ESI) Calcd. for $C_2{}^{13}C_6H_{12}NO^+$; 144.1115 m/z (M+H), Observed; 144.1114 m/z (M+H)

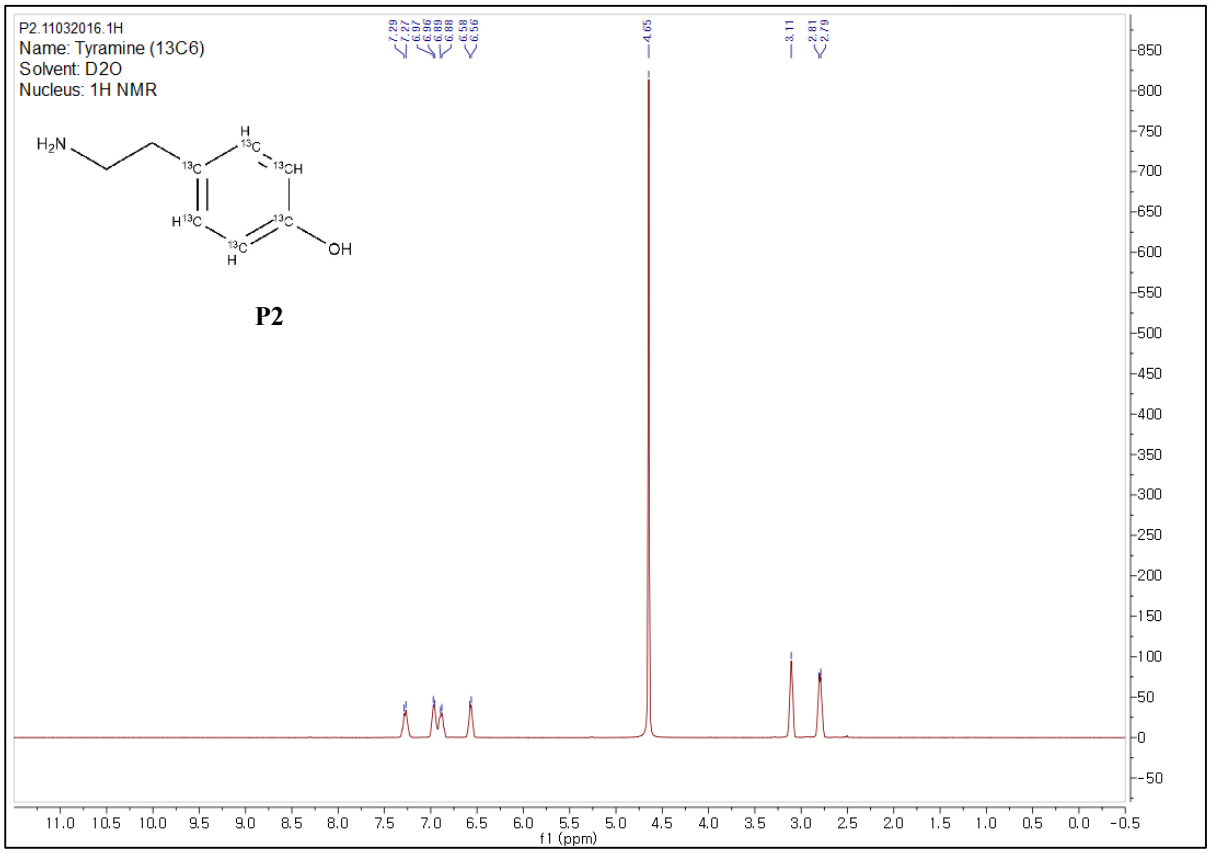

P2

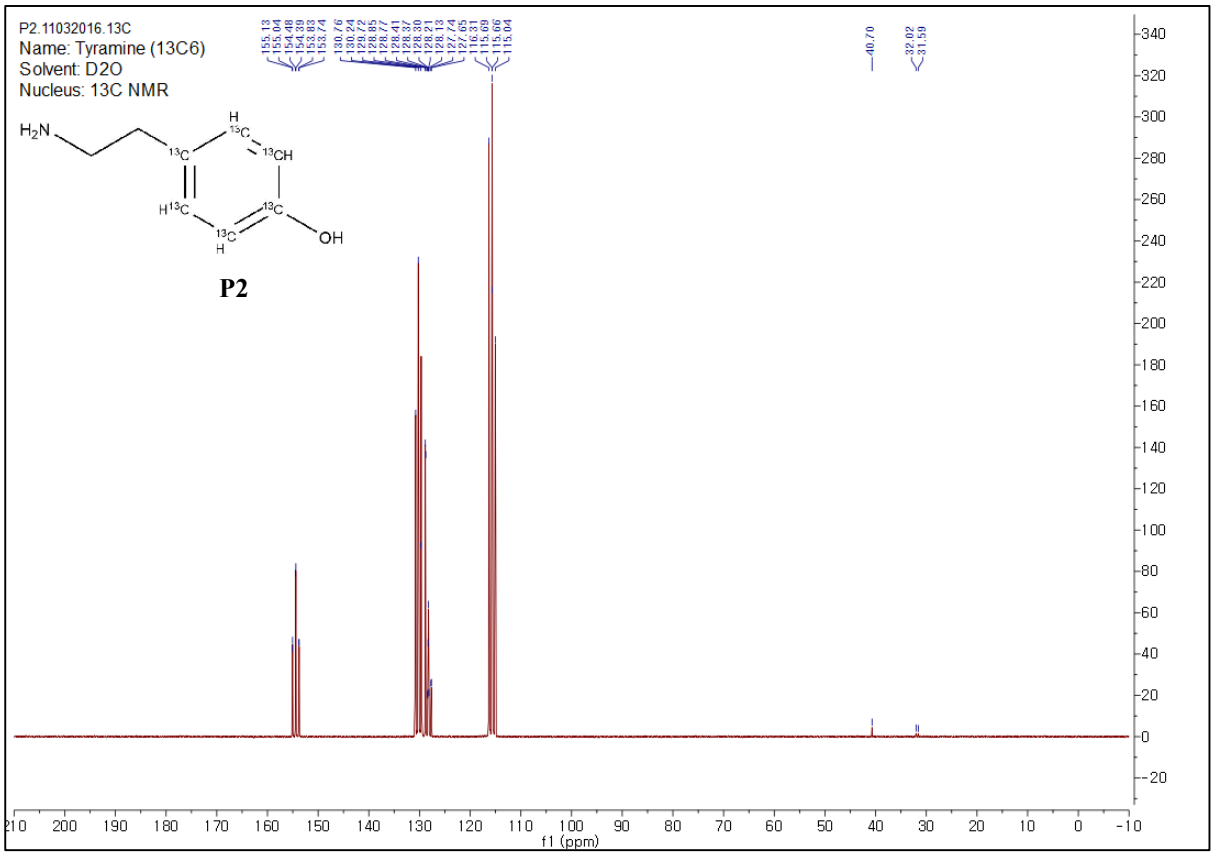

P2

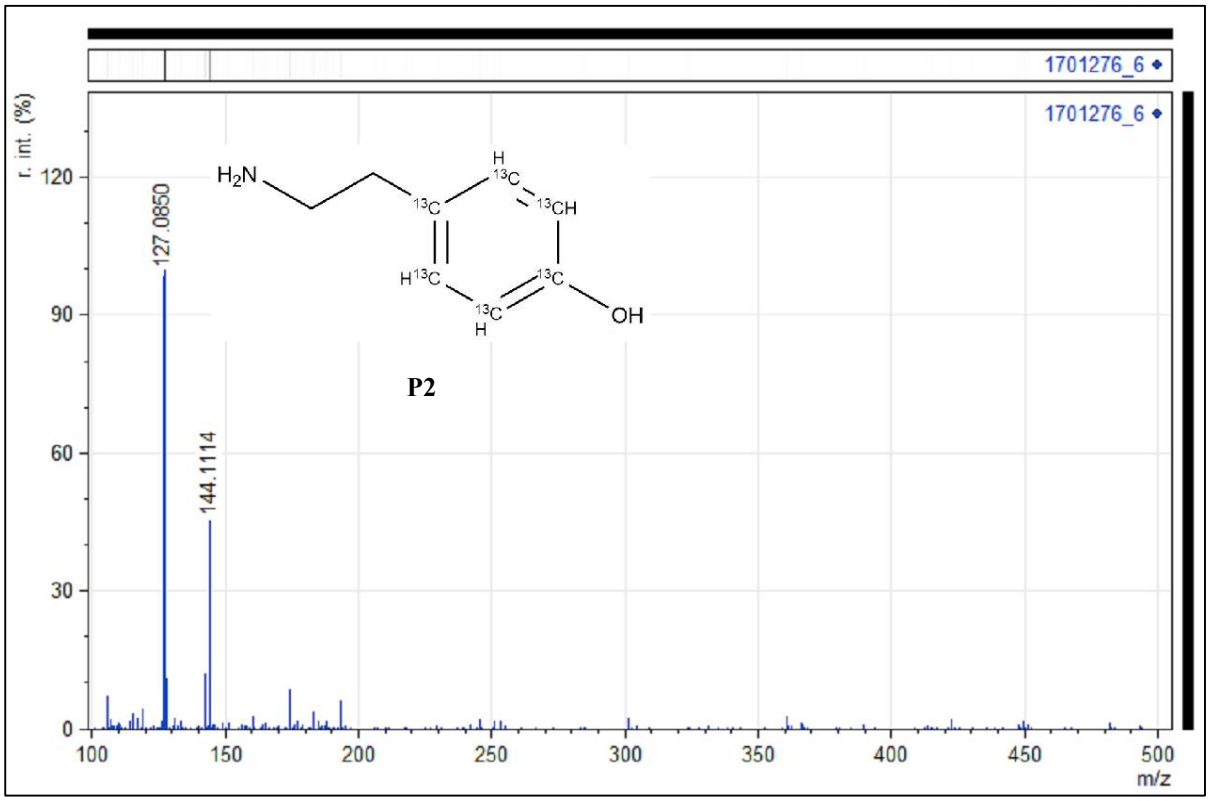

Synthesis of **[$^{13}C_2$, ^{15}N]tyramine** (**P3**).

The protocol was identical with the synthesis of [$^{13}C_8$, ^{15}N]tyramine (P1) except for the use of [$^{13}C_2$, ^{15}N]tyrosine as the starting material.

^1H NMR (400 MHz, Deuterium Oxide) δ 7.09 (dd, *J* = 8.3, 4.0 Hz, ring 2**CH,** 2H), 6.77 (dd, *J* = 8.4 Hz, ring 2**CH**, 2H), 3.12 (dd, *J* = 130.8, 4.1 Hz, **$^{13}CH_2$**$^{15}NH_2$, 2H), 2.79 (dd, *J* = 121.9, 7.1 Hz, C**$^{13}CH_2$**, 2H) ppm.

^{13}C NMR (101 MHz, Deuterium Oxide) δ 154.46, 130.20, 128.33 (d, *J* = 46.3 Hz), 115.70, 40.64 (dd, *J* = 34.9, 5.0 Hz), 31.79 (d, *J* = 34.9 Hz) ppm.

HRMS (ESI) Calcd. for $C_6{}^{13}C_2H_{12}{}^{15}NO^+$; 141.0951 m/z (M+H), Observed; 141.0950 m/z (M+H)

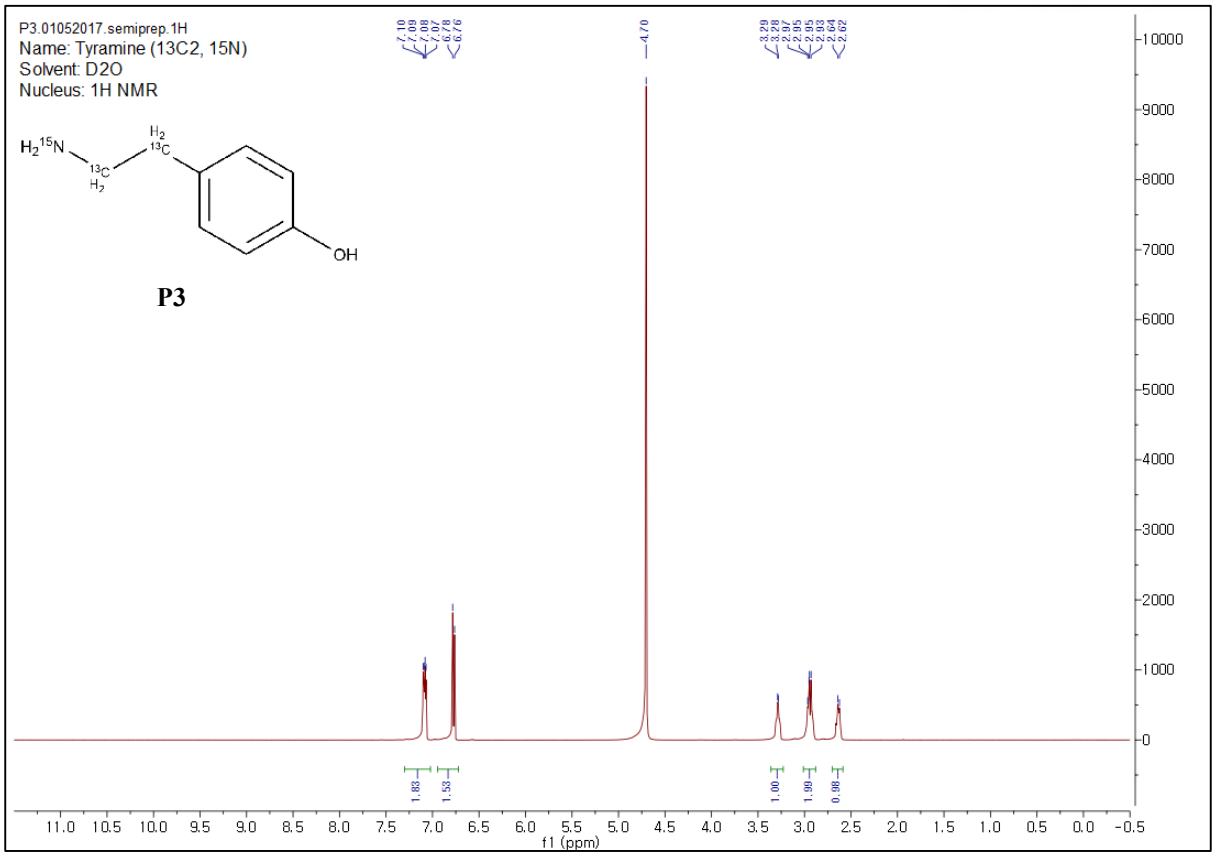

P3

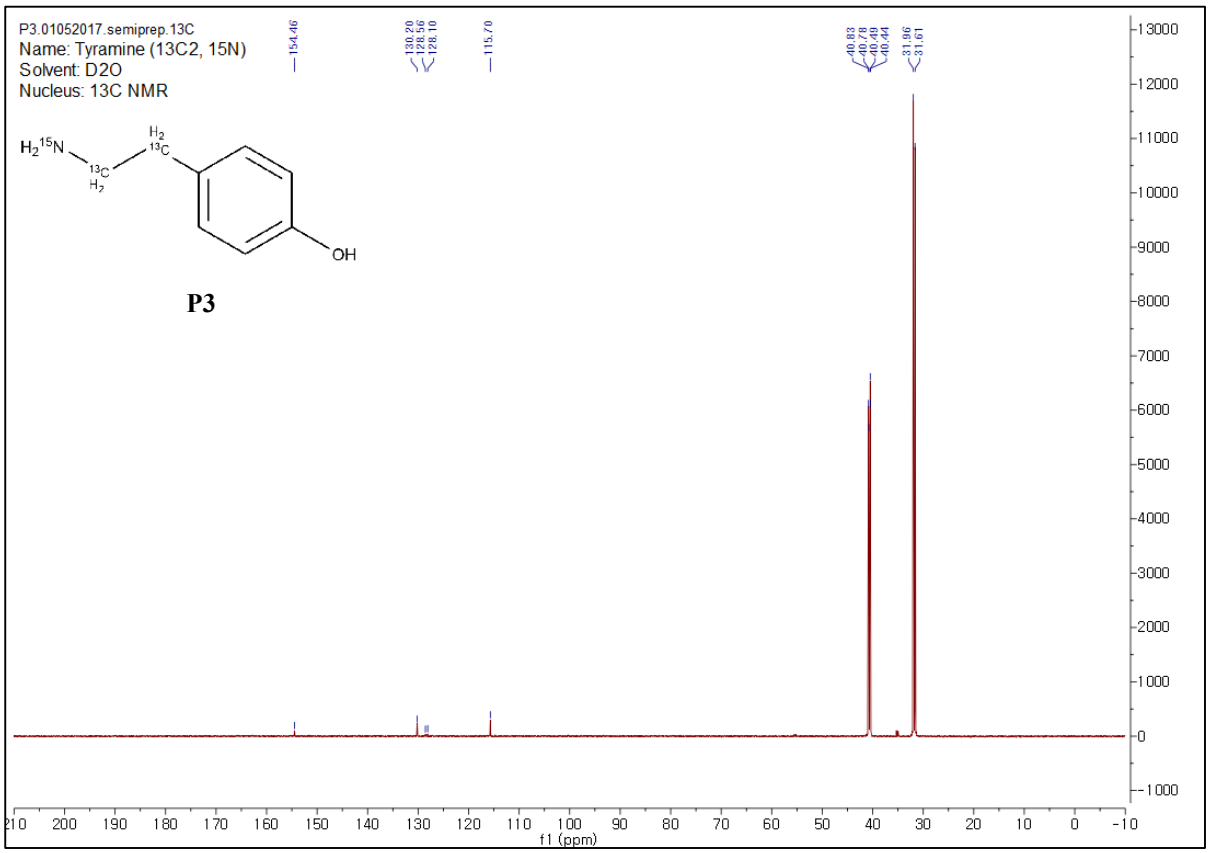

P3

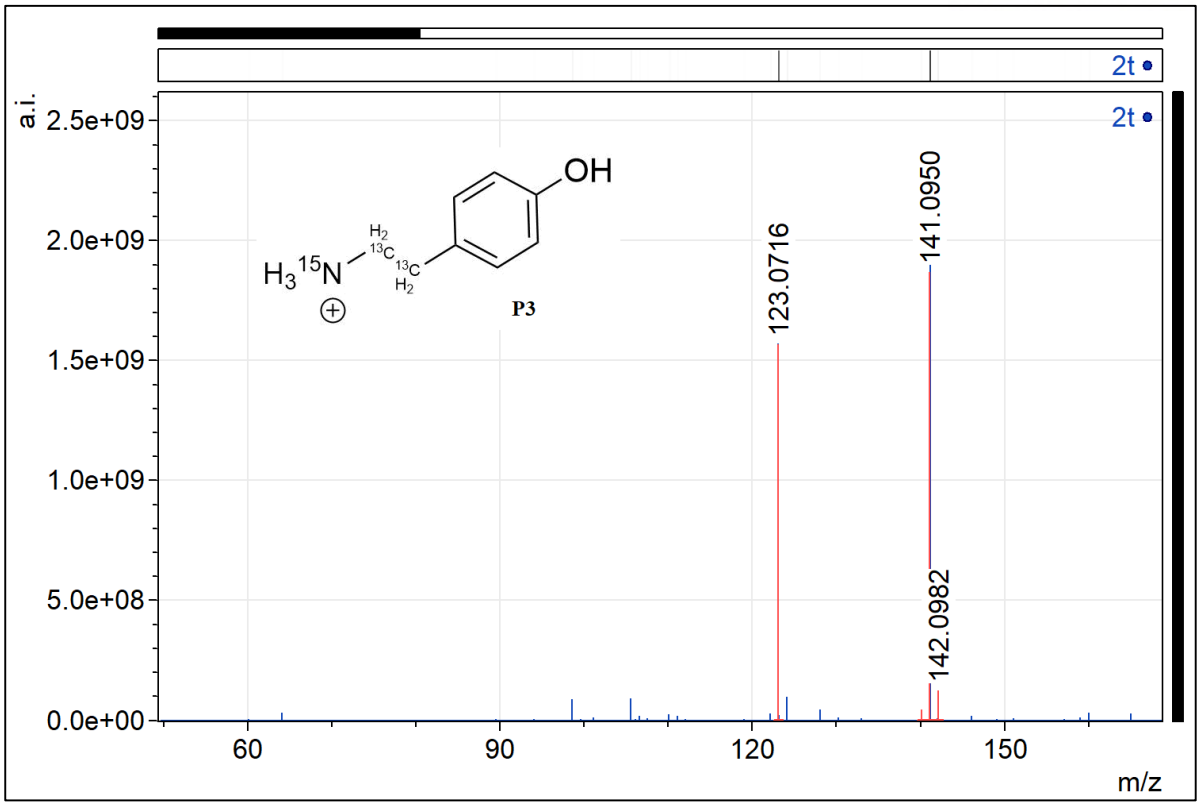

Synthesis of **d-Desthiobiotinyl[$^{13}C_8$, ^{15}N]tyramine** (**P4**).

The protocol was referred to the synthesis of d-biotinyl tramide[21]. [$^{13}C_8$, ^{15}N]tyramine (190.8 mg, 1.32 mmol) was dissolved in 5 mL of methanol/water (3:1). d-Desthiobiotinyl-NHS ester (**P7**, 450.1 mg, 1.44 mmol) and triethylamine (209 μL, 1.44 mmol) were added to the tyramine solution. 5 mL of methanol was added and the resulting solution was stirred at room temperature for 16 hours. The reaction mixture was concentrated *in vacuo* and the residue was extracted by ethyl acetate (50 mL x 8 times) from water (50 mL). The collected organic phase was dried over magnesium sulfate, filtered, and concentrated *in vacuo*. The crude product was purified by reverse-phase HPLC (C_{18} column, 10 mL/min, 15 to 35% acetonitrile/water over 40 min, retention time 10 min). The product was lyophilized to yield white powder. (250 mg, 0.75 mmol, 57%)

TLC R_f = 0.85 (3:1, ethyl acetate/methanol)

HPLC method: 20-40B, 15 min. 100% solvent A to 20% solvent A and 80% solvent in 2 minutes, and subsequent to 60% solvent A and 40% solvent B. T_R = 12.043 min.

Solvent A: clean water with 0.1% TFA

Solvent B: 9:1 of MeCN and water with 0.1% TFA

^{1}H NMR (400 MHz, Methanol-d_4) δ 7.02 (dd, *J* = 154.3, 6.7 Hz, ring 2^{13}**CH**, 2H), 6.70 (d, *J* = 158.6 Hz, ring 2^{13}**CH**, 2H), 3.81 (p, *J* = 6.5 Hz, **CH**CH_3, 1H), 3.67 (q, *J* = 6.9 Hz, **CH**CH_2CH_2,

1H), 3.35 (d, *J* = 138.8 Hz, $^{15}NH^{13}\mathbf{CH_2}$, 2H), 2.68 (d, *J* = 126.6 Hz, $C^{13}\mathbf{CH_2}$, 2H), 2.14 (t, *J* = 7.3 Hz, $\mathbf{CH_2}CONH$, 2H), 1.57 (t, *J* = 7.0 Hz, $CH\mathbf{CH_2}$, 2H), 1.49 – 1.28 (m, $CCH_2\mathbf{CH_2CH_2CH_2}$, 6H), 1.10 (d, J = 6.4 Hz, $CH\mathbf{CH_3}$, 3H) ppm.

^{13}C NMR (101 MHz, Methanol-d_4) δ 174.65 (d, *J* = 14.9 Hz), 164.77, 155.45 (td, *J* = 66.6, 8.3 Hz), 129.56 (ddd, *J* = 18.6, 12.2, 5.3Hz), 129.02 (m), 114.74 (ddd, *J* = 65.5 54.6, 11.8 Hz), 55.99, 51.29, 40.67 (dd, *J* = 35.0, 10.0 Hz), 35.57 (d, *J* = 7.1 Hz), 34.23 (ddt, *J* = 44.1 35.1, 7.5 Hz), 29.28, 28.72, 25.78, 25.47, 14.22 ppm.

HRMS (ESI) Calcd. for $C_{10}{}^{13}C_8H_{27}N_2{}^{15}NO_3$; 343.2364 m/z (M+H), 365.2183 m/z (M+Na) Observed; 343.2362 m/z (M+H) 365.2180 m/z (M+Na).

IR 3265.79, 2933.84, 1691.80, 1643.31, 1540.76, 1477.59, 1435.30, 1215.46

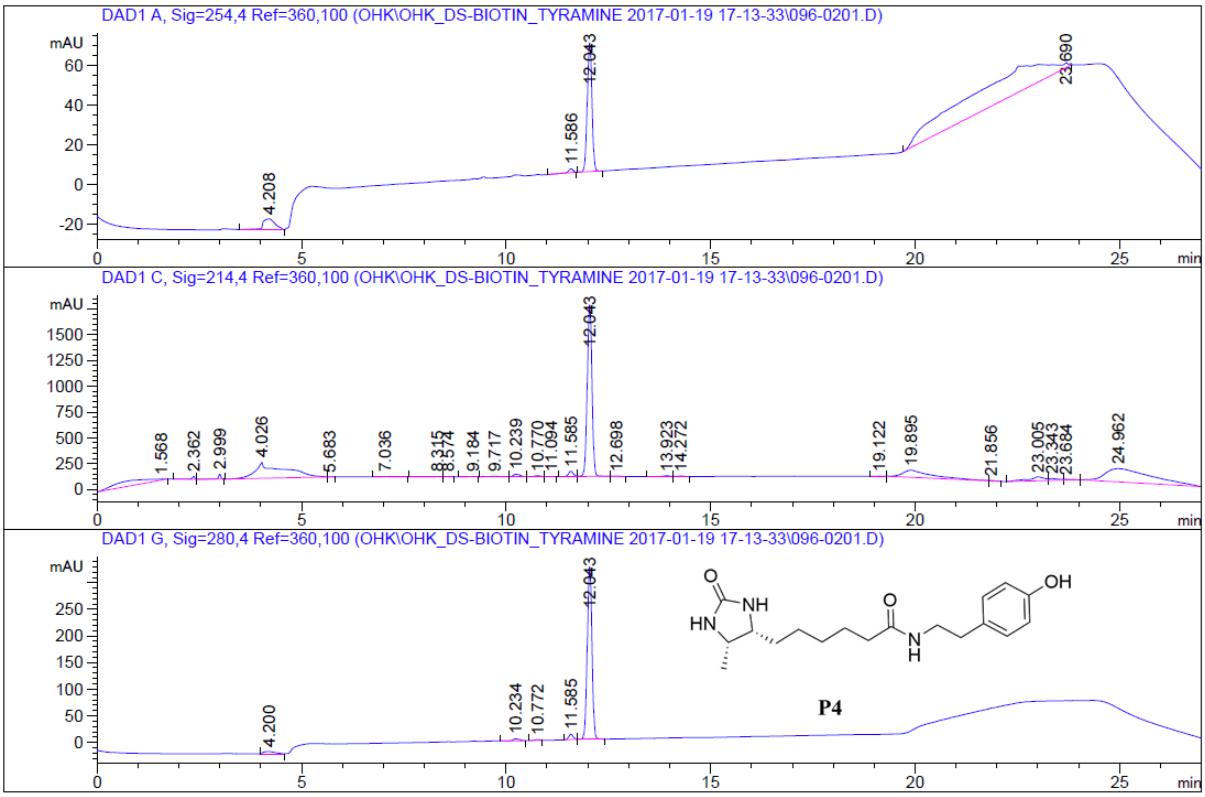

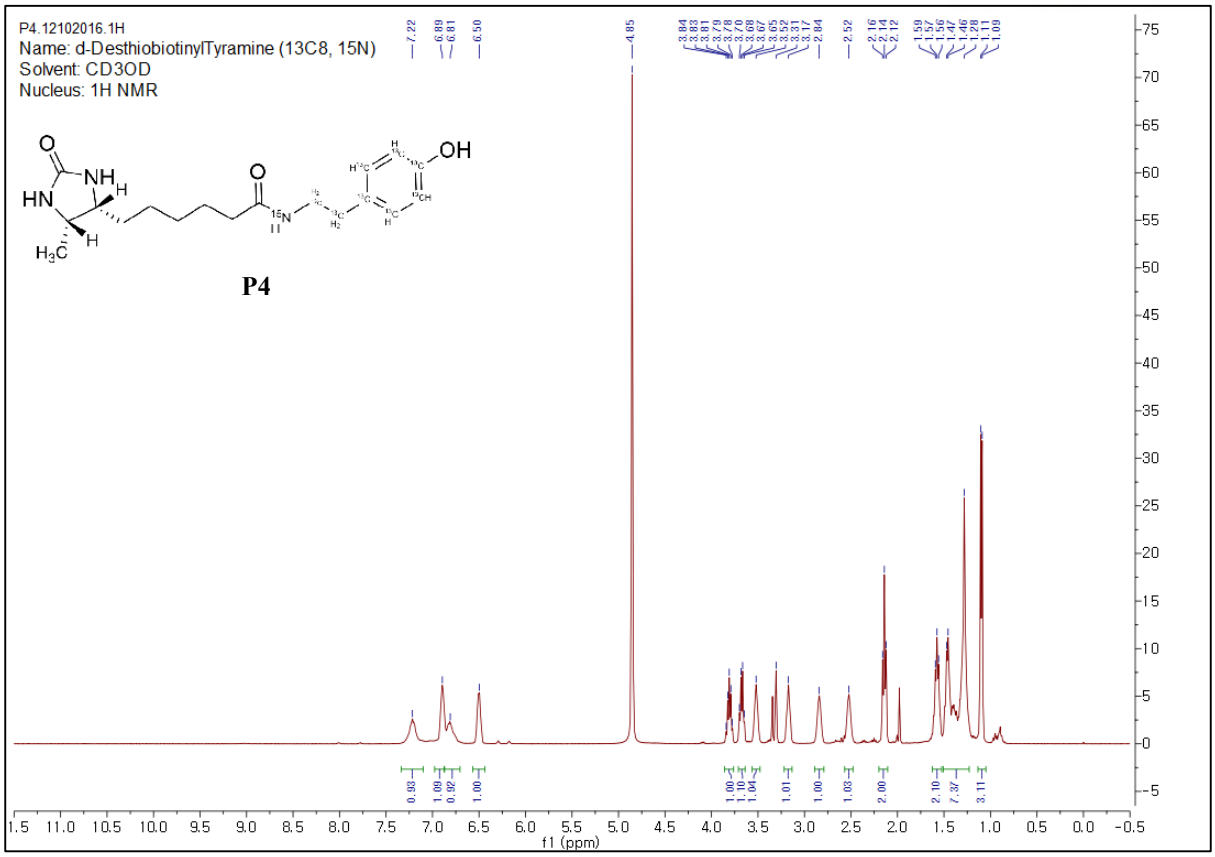

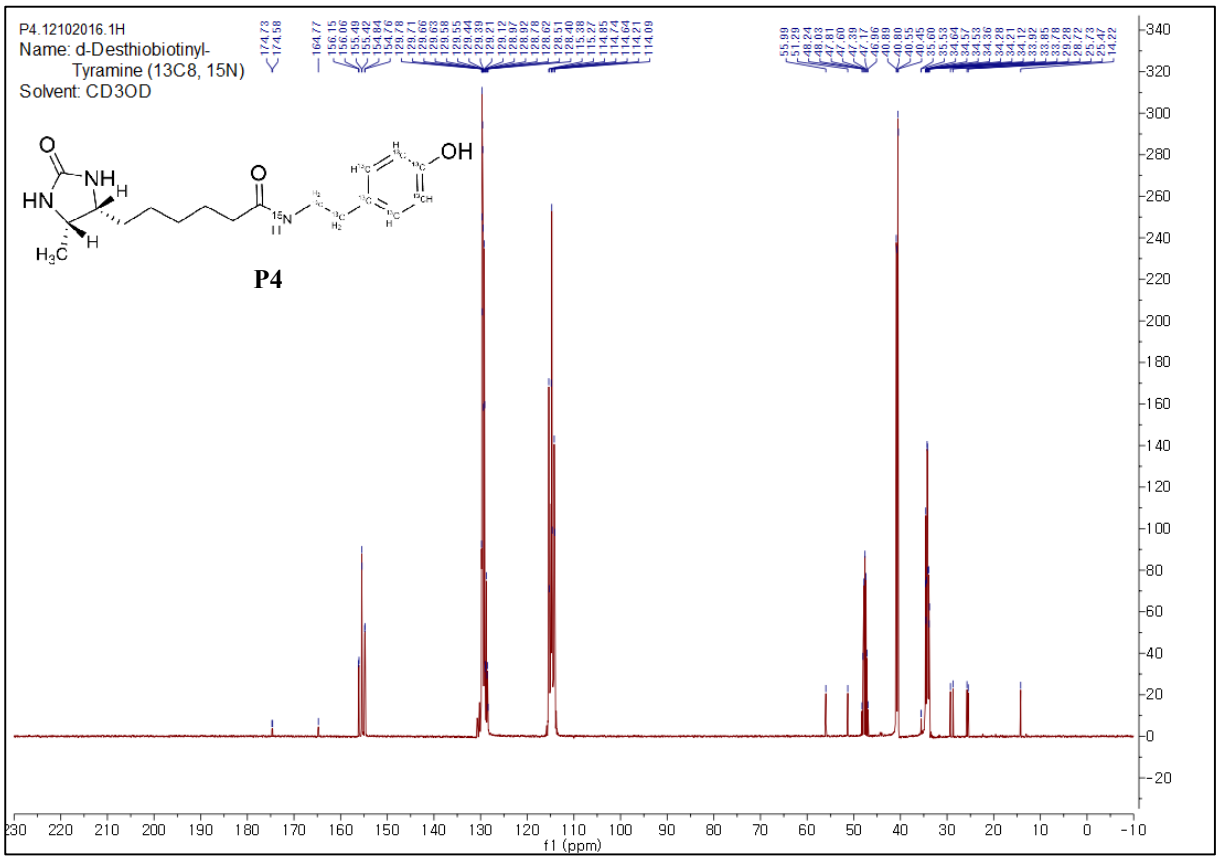

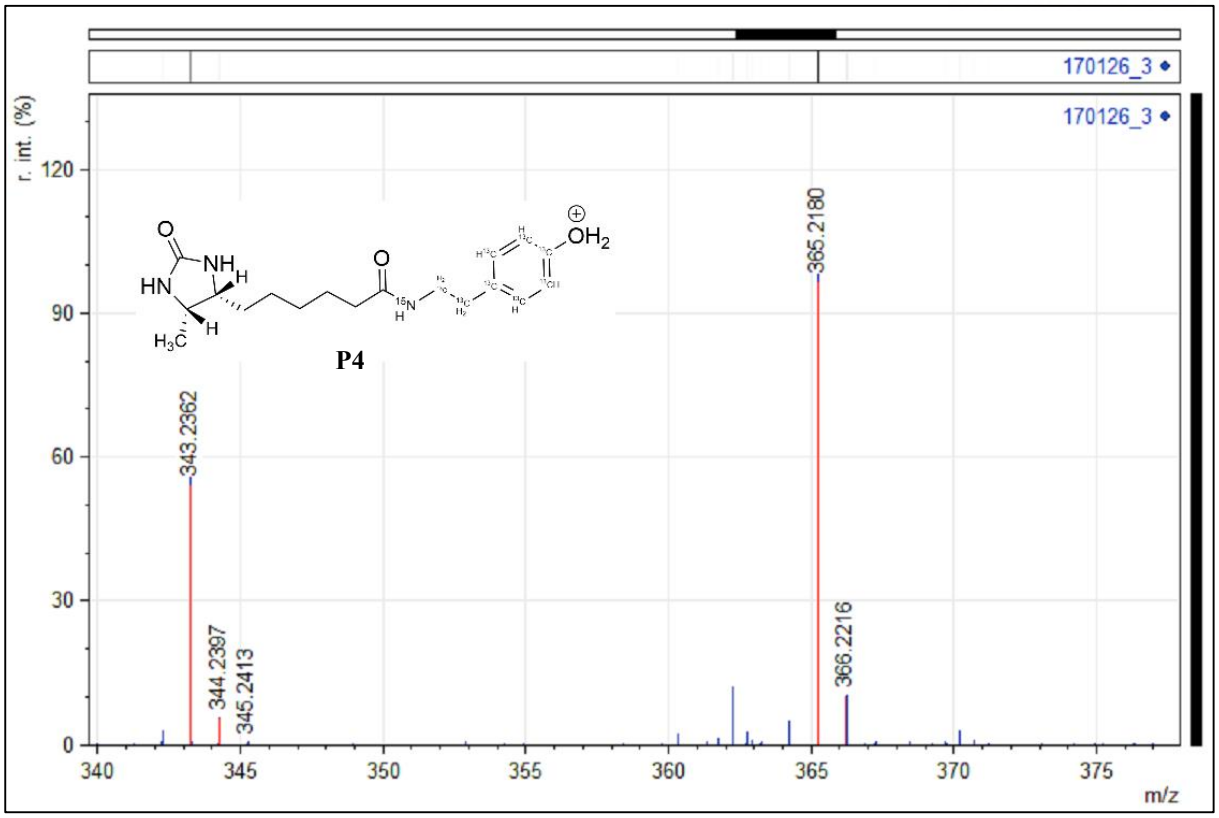

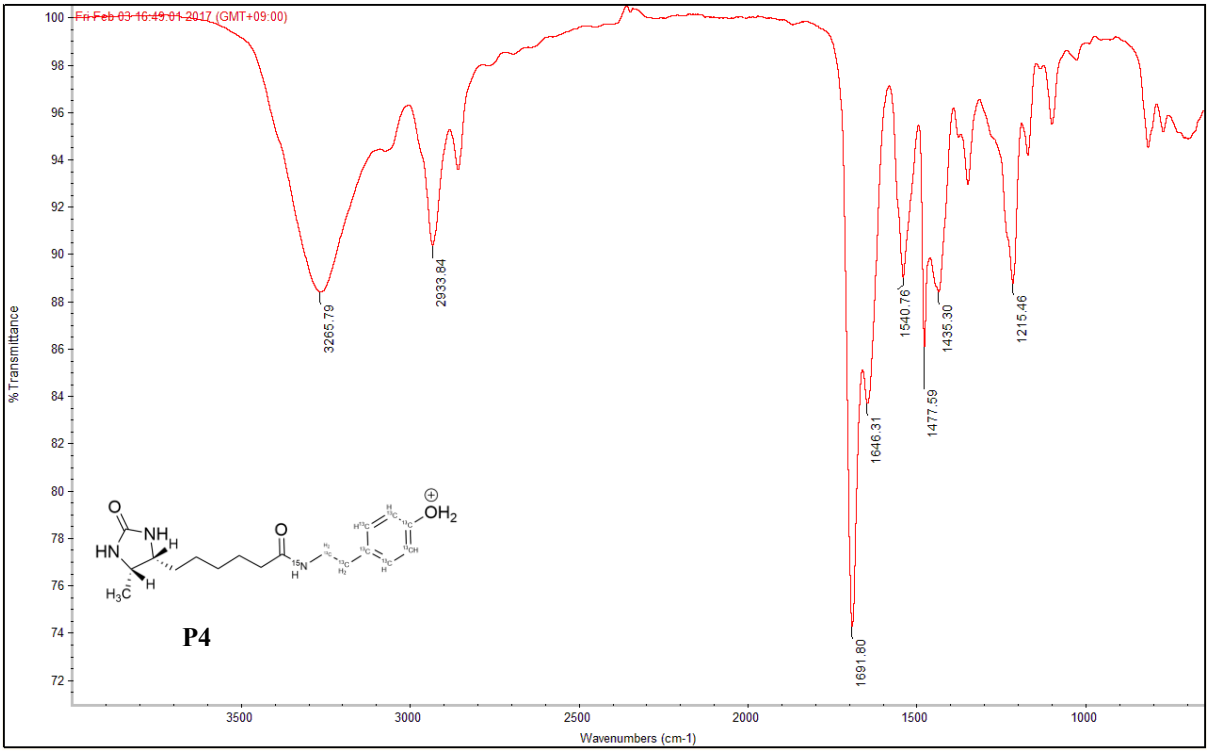

Synthesis of **d-Desthiobiotinyl[ring-$^{13}C_6$]tyramine** (**P5**).

The protocol was identical with synthesis of Synthesis of d-Desthiobiotinyl[$^{13}C_8$, ^{15}N]tyramine (**P4**).

^{1}H NMR (400 MHz, Methanol-d_4) δ 7.02 (dt, J = 163.7, 8.7 Hz, ring 2^{13}**CH**, 2H), 6.70 (d, J = 158.7 Hz, ring 2^{13}**CH**, 2H), 3.83 (p, J = 6.6 Hz, **CH**CH_3, 1H), 3.68 (dt, J = 14.0, 6.9 Hz, **CH**CH_2CH_2, 1H), 3.36 (t, J = 6.3 Hz, NH**CH$_2$**, 2H), 2.69 (s, C**CH$_2$**, 2H), 2.15 (t, J = 7.3 Hz, **CH$_2$**CONH, 2H), 1.58 (p, J = 7.1 Hz, CH**CH$_2$**, 2H), 1.52 – 1.23 (m, CCH_2**$CH_2CH_2CH_2$**, 6H), 1.10 (d, J = 6.4 Hz, CH**CH$_3$**, 3H)

^{13}C NMR (101 MHz, Methanol-d_4) δ 174.76, 164.76, 155.47 (td, J = 67.7, 8.5 Hz), 129.59 (dt, J = 12.7, 5.6 Hz), 129.13 (m), 114.75 (ddd, J = 62.6, 49.0, 11.1 Hz), 56.09, 51.40, 40.74, 35.57, 34.26 (d, J = 29.1 Hz), 29.26, 28.73, 25.75, 25.50, 14.22.

HRMS (ESI) Calcd for $C_{12}{}^{13}C_6H_{28}N_3O_3^+$; 362.2146 m/z (M+H) Observed; 362.2145 m/z (M+H).

IR 3277.00, 2936.69, 1691.29, 1647.66, 1543.74, 1477.65, 1438.09, 1216.10

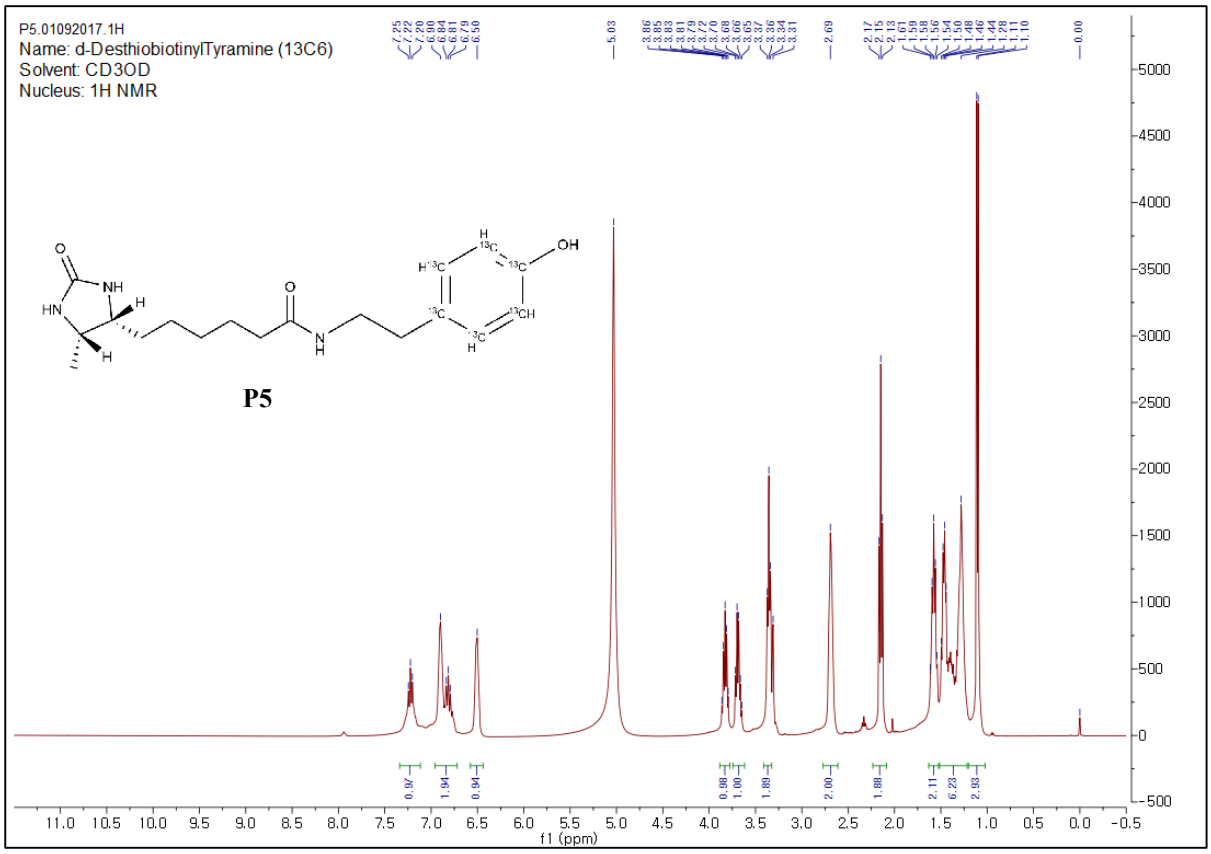

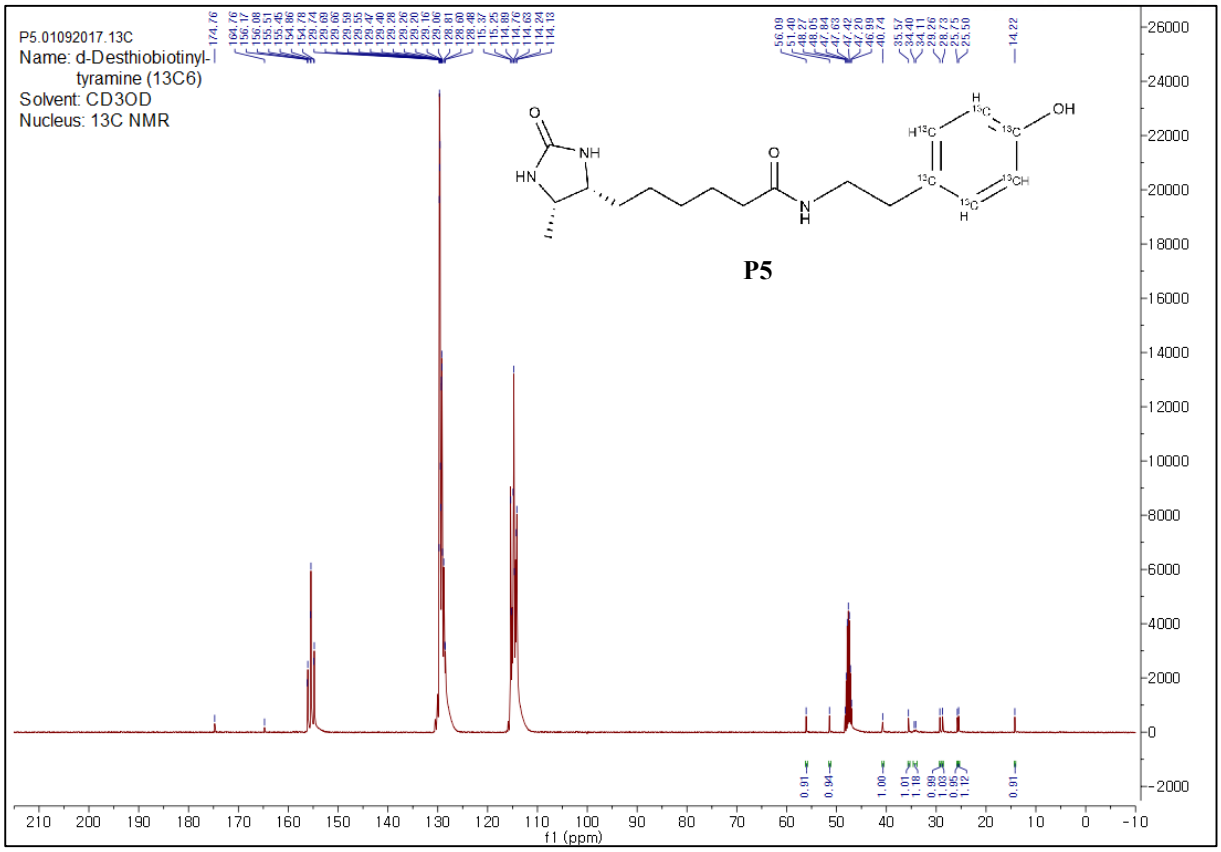

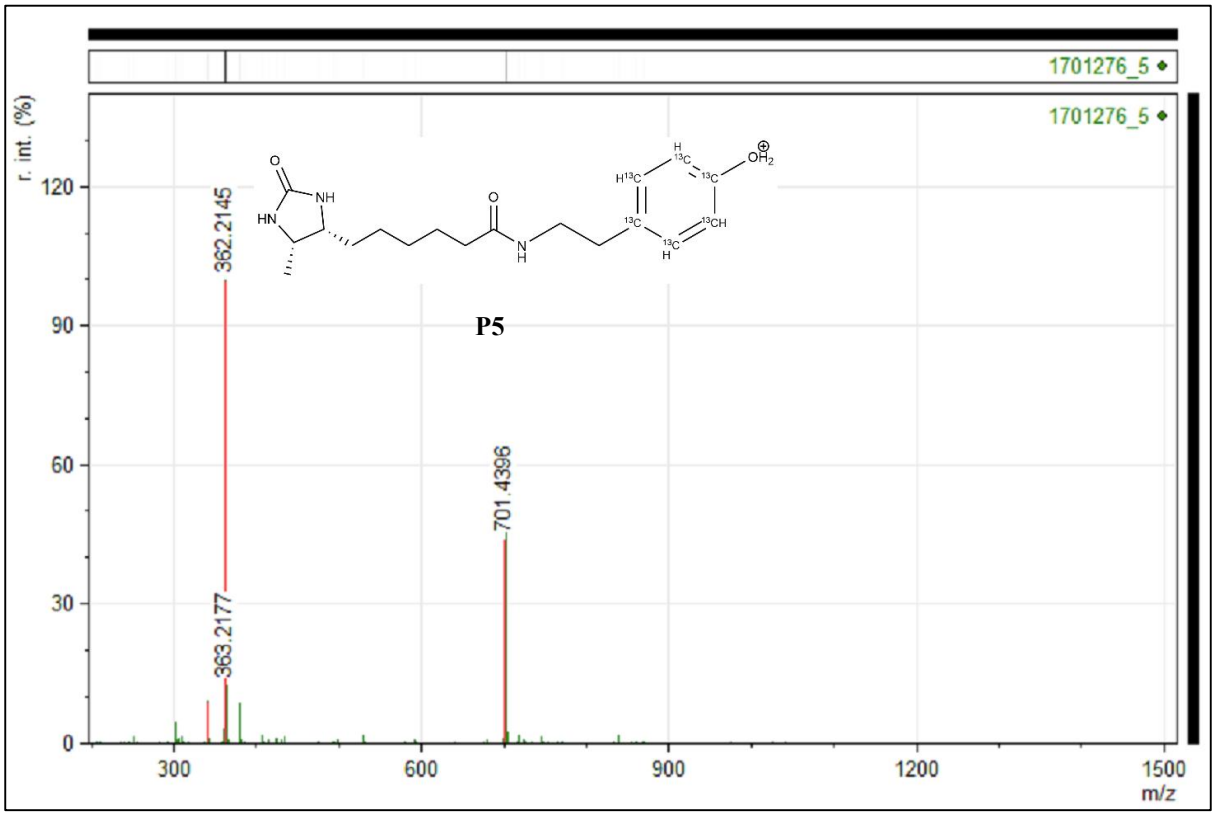

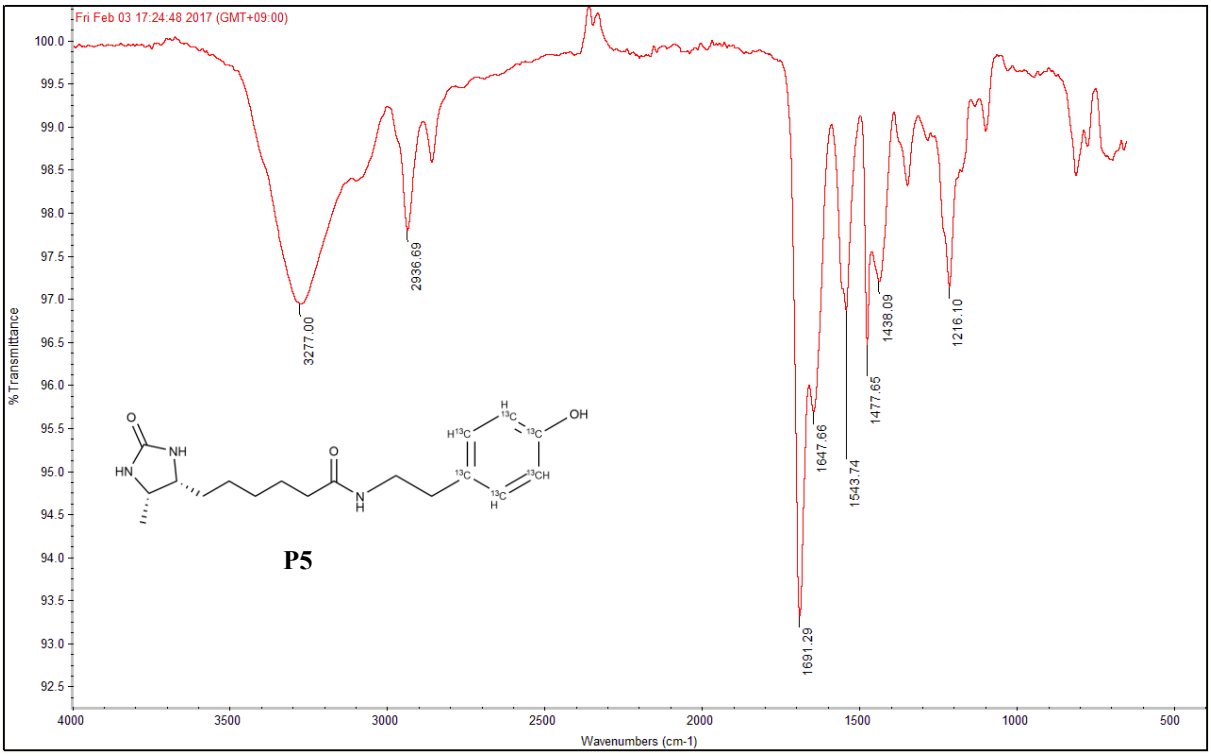

Synthesis of **d-Desthiobiotinyl[$^{13}C_2$, ^{15}N]tyramine** (**P6**).

The protocol was identical with synthesis of Synthesis of d-Desthiobiotinyl[$^{13}C_8$, ^{15}N]tyramine (**P4**).

^{1}H NMR (400 MHz, Methanol-d_4) δ 7.02 (dd, J = 8.5, 3.9 Hz, ring 2**CH**, 2H), 6.70 (d, J = 8.5 Hz, ring 2**CH,** 2H) 3.81 (m, **CH**CH_3, 1H), 3.68 (q, J = 7.4 Hz, **CH**CH_2CH_2, 1H), 3.35 (dtd, J = 139.0, 7.1, 3.0 Hz, ^{15}NH**^{13}CH$_2$**, 2H), 2.68 (dtdd, J = 127.4, 7.2, 5.1, 2.3 Hz, C**^{13}CH$_2$**, 2H), 2.14 (t, J = 7.1 Hz, **CH$_2$**CONH, 2H), 1.58 (p, J = 7.4 Hz, CH**CH$_2$**, 2H), 1.50-1.27 (m, CCH_2**$CH_2CH_2CH_2$**, 6H), 1.10 (d, J = 6. 5 Hz, CH**CH$_3$**, 3H)

^{13}C NMR (101 MHz, Methanol-d_4) δ 174.78, 164.49, 155.51, 129.79 (d, J = 44.9 Hz), 129.34, 114.78 (d, J = 3.8 Hz), 56.05, 51.35, 40.69 (dd, J = 35.2, 9.9 Hz), 35.57 (d, J = 7.2 Hz), 34.22 (d, J = 35.2 Hz), 29.28, 28.73, 25.76, 25.49, 14.20

HRMS (ESI) Calcd for $C_{16}{}^{13}C_2H_{28}N_2{}^{15}NO_3^+$; 337.2163 m/z (M+H), $C_{16}{}^{13}C_2H_{27}N_2{}^{15}NO_3Na^+$; 359.1982 m/z (M+Na), Observed; 337.2161 m/z (M+H), 359.1982 m/z (M+Na)

IR 3276.36, 2935.77, 1688.72, 1514.68, 1448.52, 1240.40, 1200.72

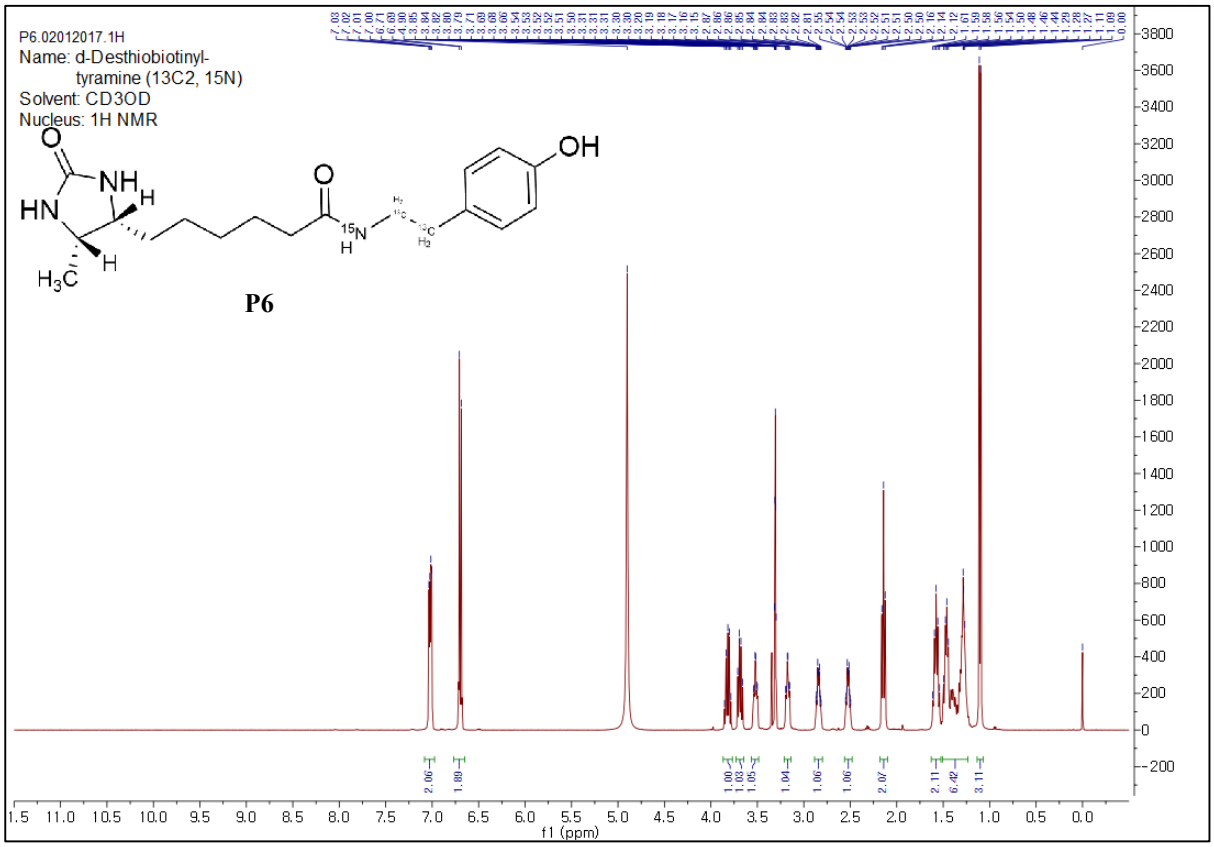

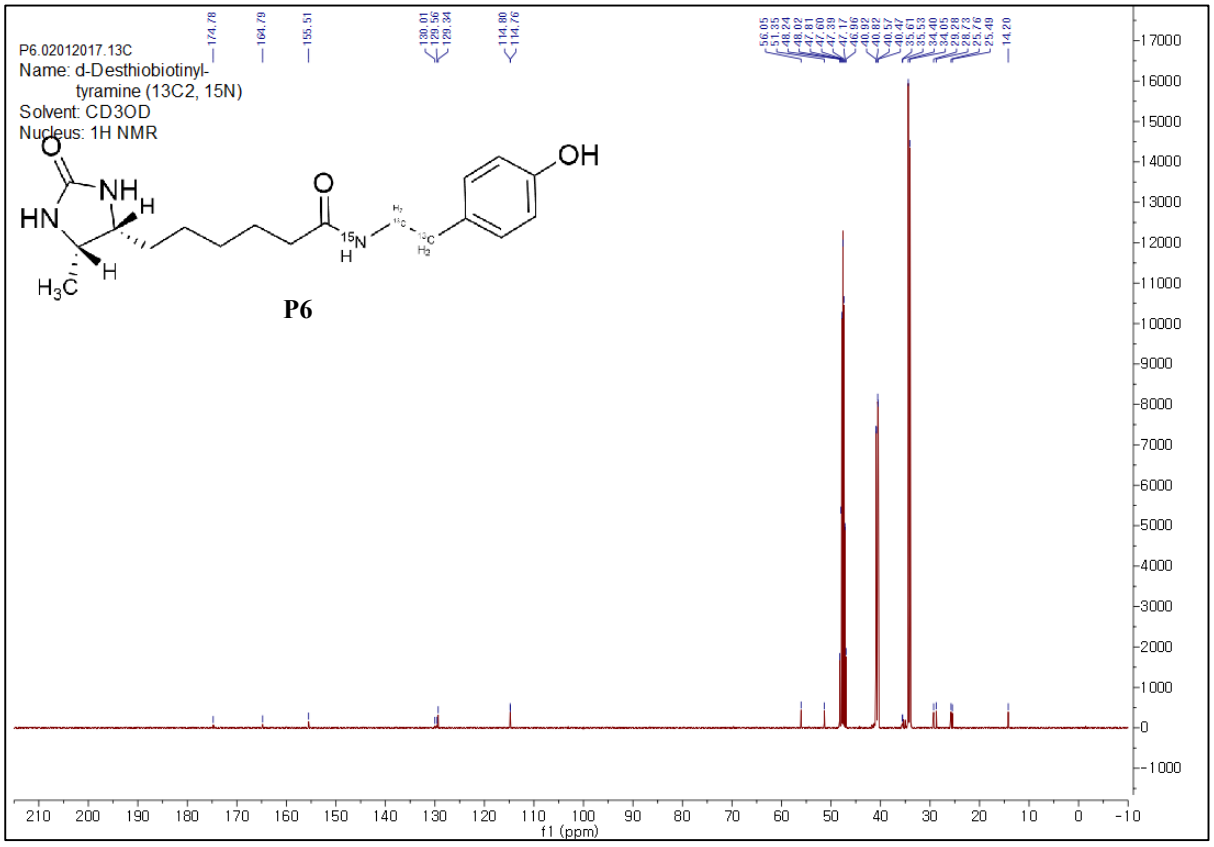

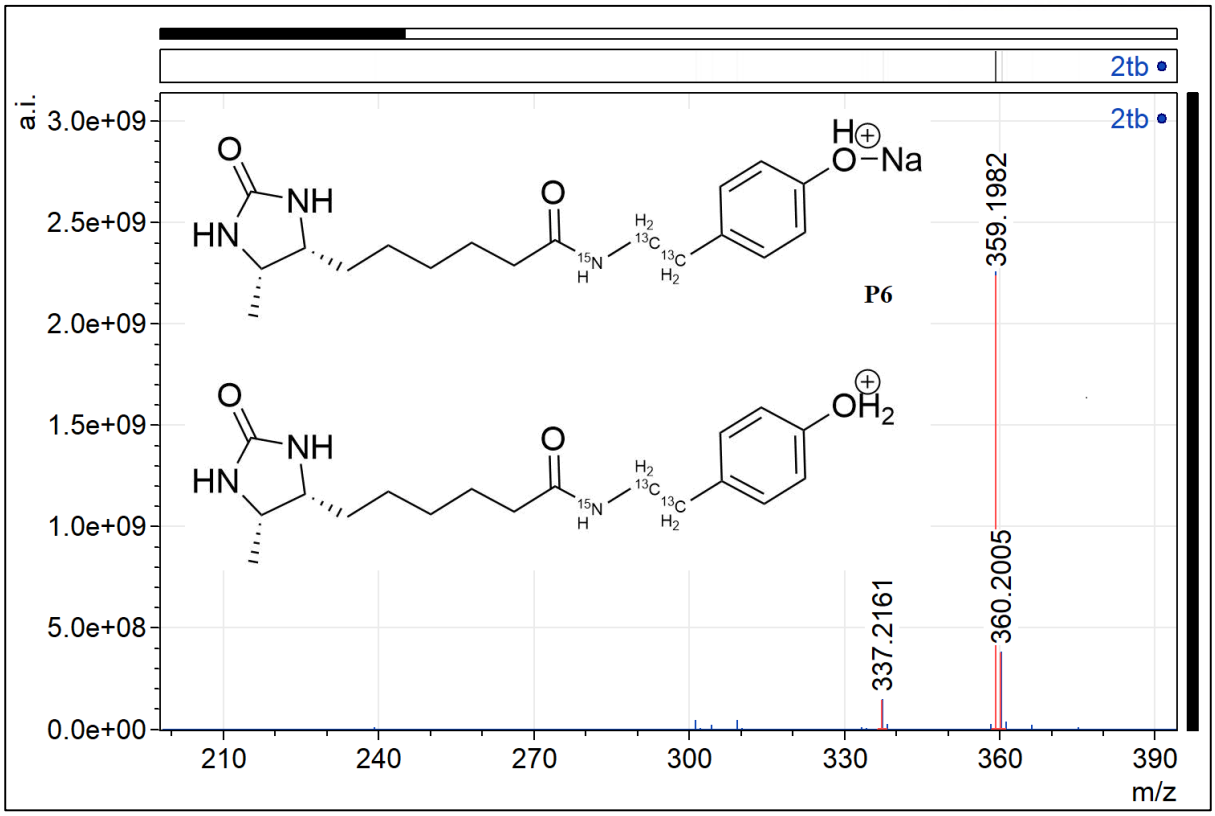

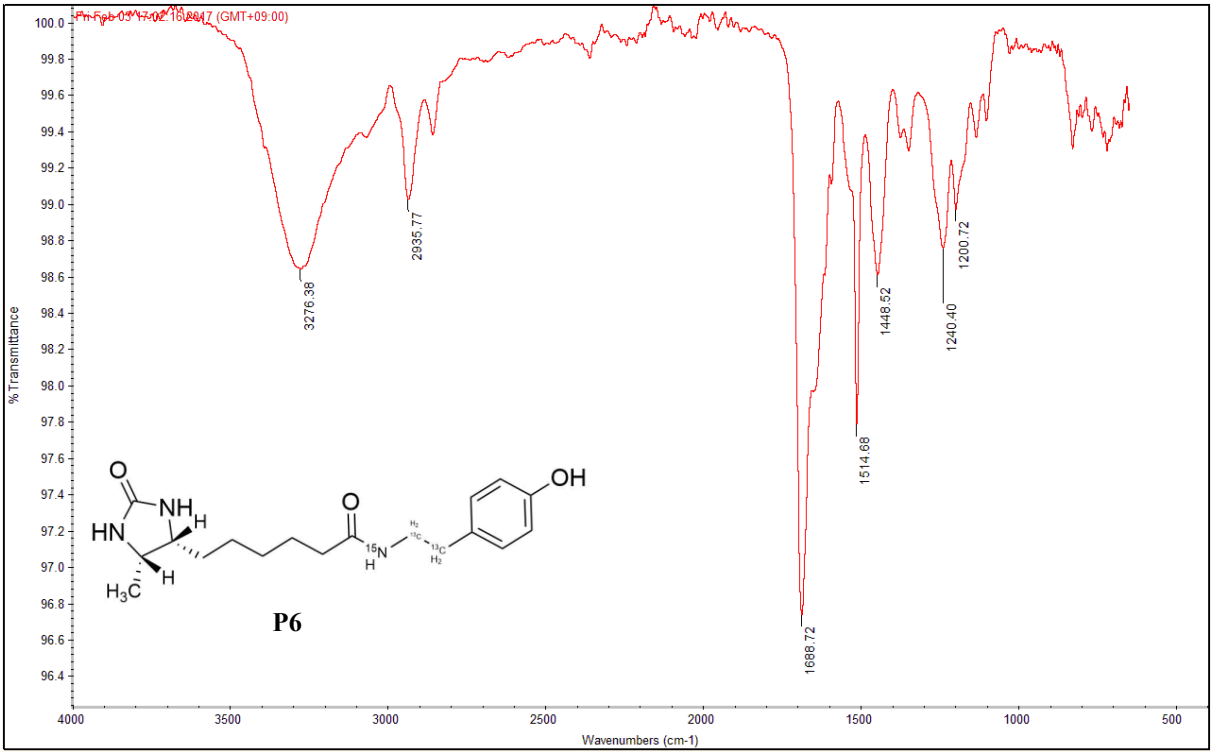

Synthesis of **d-Desthiobiotinyl-NHS ester** (**P7**).

The protocol was referred to the synthesis of d-biotinyl-NHS ester[3\20)]. d-Desthiobiotin (1.3 g, 6.07 mmol) was dissolved in DMF (20 mL) and N,N'-dicyclohexylcarbodiimide (DCC, 1.37 g, 6.67 mmol), N-hydroxysuccinimide (NHS; 0.91 g, 7.89 mmol) and triethylamine (1.3 mL, 9.10 mmol) were added. The mixture was stirred at room temperature for 24 h. The reaction product was filtered and concentrated. The obtained solid was extracted by ethyl acetate from ammonium chloride solution. The collected organic layer was evaporated and product was obtained as a white powder. Product was used in next step without further purification. (1.6 g, 5.14 mmol, 85 %)

TLC R_f = 0.1 (4:1, ethyl acetate/MeOH)

^{1}H NMR (400 MHz, $CDCl_3$) δ 5.27 (s, CO**NH**, 1H), 4.86 (s, CO**NH**, 1H), 3.86 (p, J = 6.6 Hz, **CH**CH_3, 1H), 3.71 (td, J = 8.1, 3.9 Hz, **CH**CH_2, 1H), 2.85 (s, 2NCO**CH_2**, 4H), 2.63 (t, J = 7.2 Hz, **CH_2**COO, 2H), 1.78 (p, J = 7.3 Hz, CH**CH_2**, 1H), 1.58-1.27 (m, 6H), 1.13 (d, J = 6.5 Hz, CH**CH_3**, 3H).

^{13}C NMR (101 MHz, $CDCl_3$) δ 127.87, 169.26, 168.60, 163.60, 55.93, 51.40, 29.50, 28.63, 25.89, 25.62, 24.32, 15.77.

HRMS (ESI) Calcd for $C_{14}H_{21}N_3O_5Na^+$; 334.1373 m/z (M+Na) Observed; 334.1370 m/z (M+Na).

IR 1735.32, 1699.90, 1206.26, 1068.07

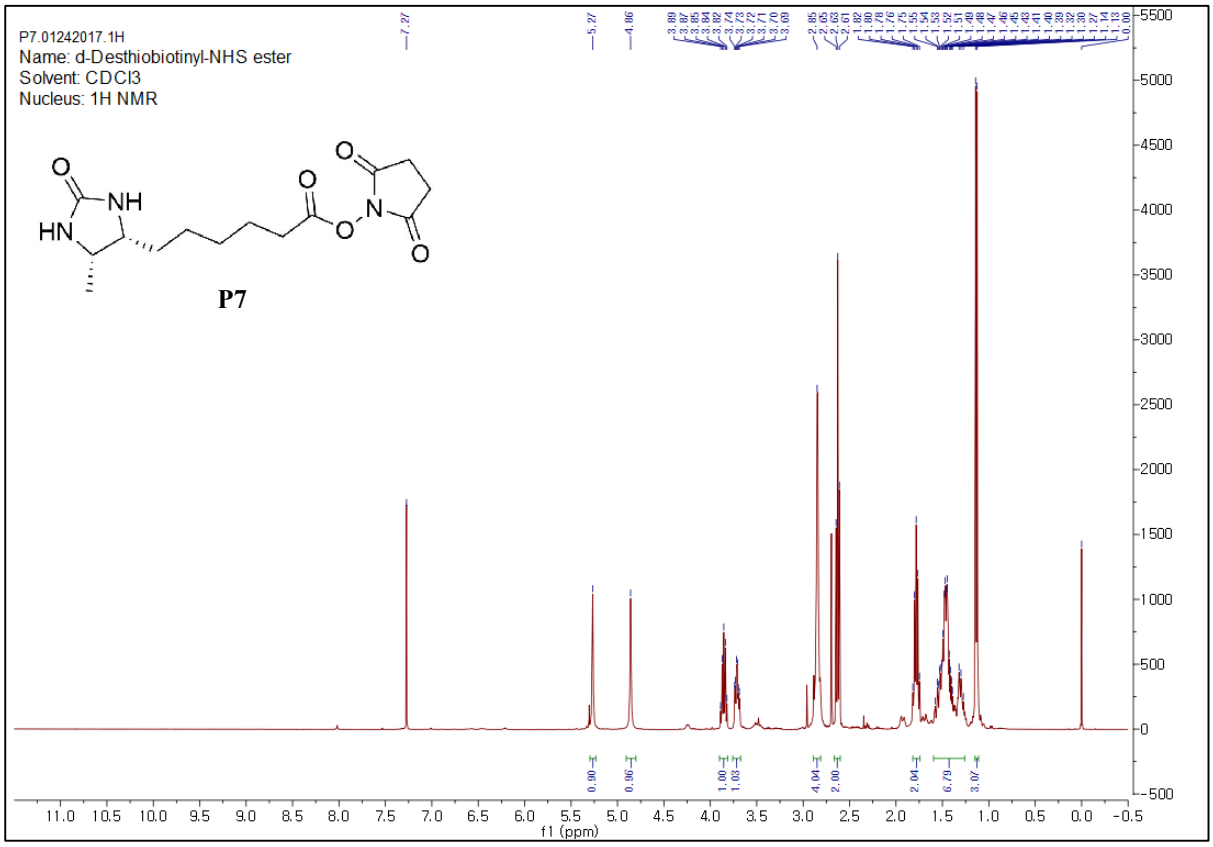

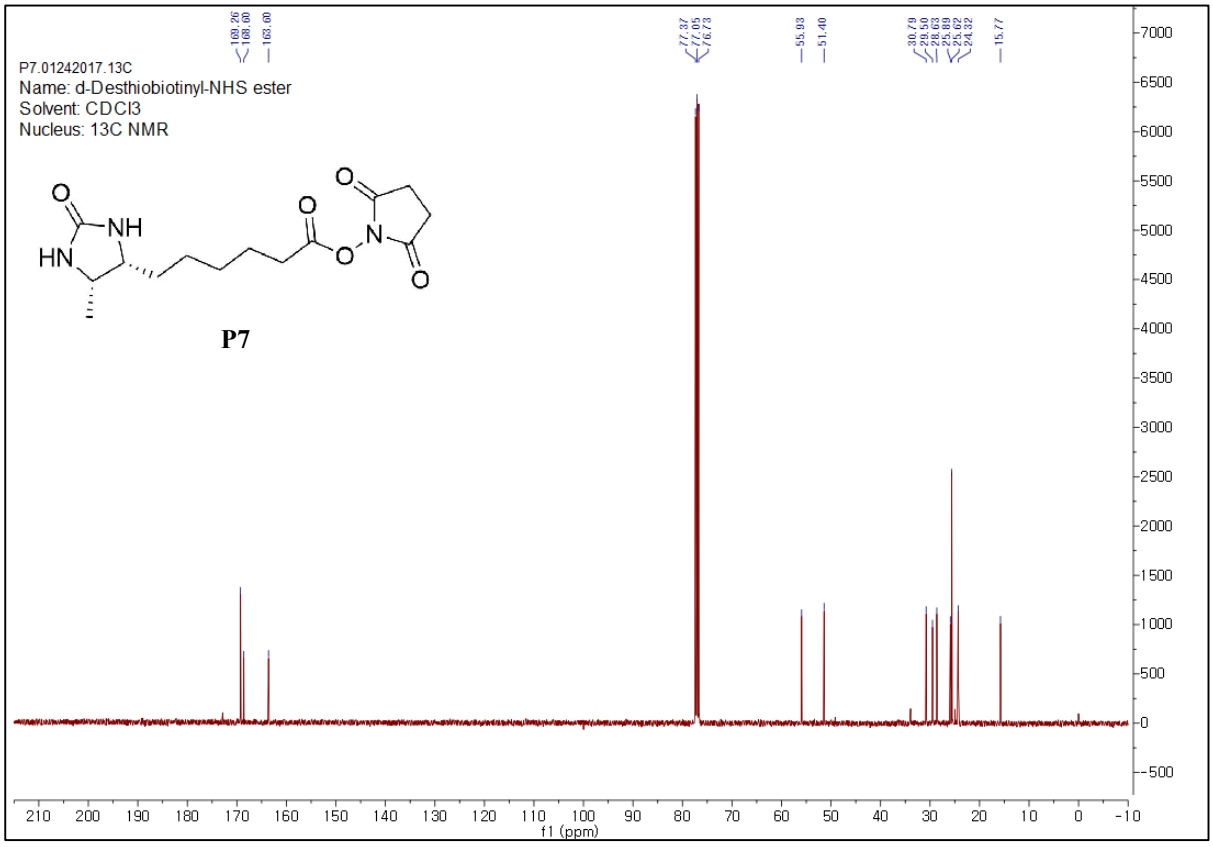

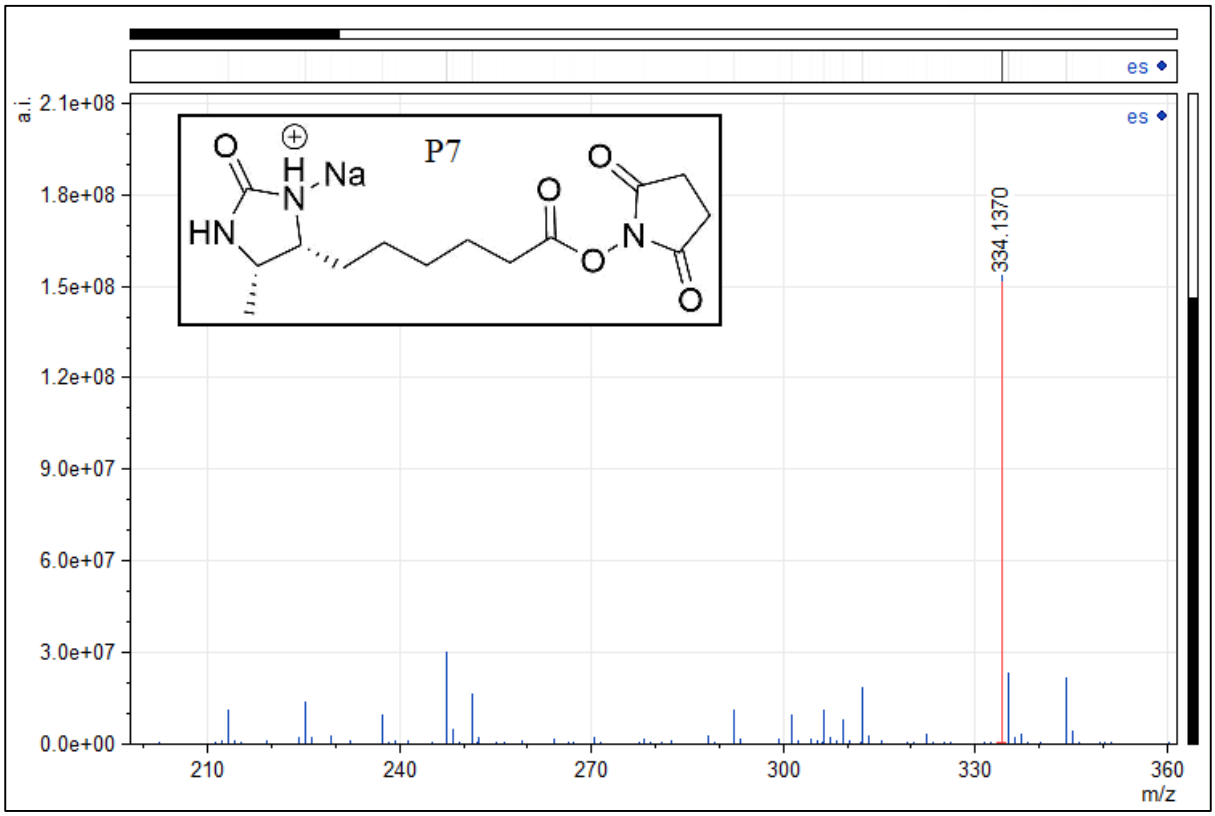

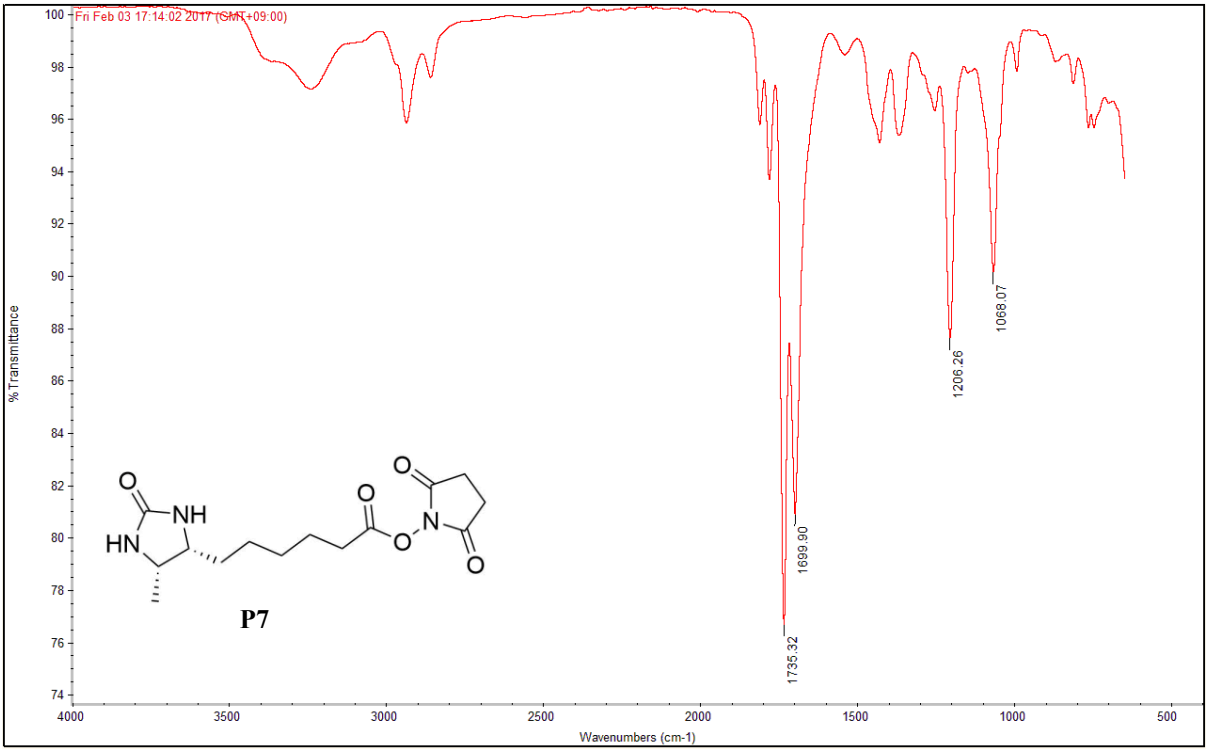

3.6 Reference

1. Rhee, H. W.; Zou, P.; Udeshi, N. D.; Martell, J. D.; Mootha, V. K.; Carr, S. A.; and Ting, A. Y. Proteomic Mapping of Mitochondria in Living Cells via Spatially Restricted Enzymatic Tagging *Science* **2013**, *339*, 1328−1331.
2. Roux, K. J.; Kim, D. I.; Raida, M.; and Burke, B. A promiscuous biotin ligase fusion protein identifies proximal and interacting proteins in mammalian cells, *J. Cell Biol.* **2012**, *196*(6), 801-810
3. Morriswood, B.; Havlicek, K.; Demmel, L.; Yavuz, S.; Sealey-Cardona, M.; Vidilaseris, K.; Anrather, D.; Kostan, J.; Djinovic´-Carugo, K.; Roux, K. J.; and Warren, G. Novel bilobe components in Trypanosoma brucei identified using proximity-dependent biotinylation. *Eukaryotic Cell* **2013**, *12*(2), 356-367
4. Choi-Rhee, E.; Schulman, H.; and Cronan, J. E. Promiscuous protein biotinylation by Escherichia coli biotin protein ligase. *Protein Sci.* **2004**, *13*(11), 3043-3050
5. Kotani, N.; Gu, J.; Isaji, T.; Udaka, K.; Taniguchi, N.; and Honke, K. Biochemical visualization of cell surface molecular clustering in living cells. *Proc. Natl. Acad. Sci. U.S.A.* **2008**, *105*(21), 7405
6. Martell, J. D.; Deerinck, T. J.; Sancak, Y.; Poulos, T. L.; Mootha, V. K.; Sosinsky, G. E.; Ellisman, M. H.; and Ting, A. Y. Engineered ascorbate peroxidase as a genetically encoded reporter for electron microscopy. *Nature Biotechnology* **2012**, *30*(11), 1143–1148
7. Wishart, J. F.; and Madhava Rao, B. S. in *Recent Trends in Radiation Chemistry* (World Scientific, Singapore) **2010**, pp. 577–596.
8. Mortensen, A.; and Skibsted, L. H. Importance of carotenoid structure in radical-scavenging reactions. *J. Agric. Food Chem.* **1997**, *45*, 2970-2977
9. Mayer, G.; and Bendayan, M. Biotinyl-tyramide: A novel approach for electron microscopic immunocytochemistry. *J. Histochem. Cytochem.* **1997**, *45*, 1449-1454
10. Minamihata, K.; Goto, M.; and Kamiya, N. Protein heteroconjugation by the peroxidase-catalyzed tyrosine coupling reaction. *Bioconjug. Chem.* **2011**, *22*, 2332
11. Rogers, M. S.; Hurtado-Guerrero, R.; Firbank, S. J.; Halcrow, M. A.; Dooley, D. M.; Phillips, S. E. V.; Knowles, P. F.; and McPherson, M. J. Cross-link formation of the cysteine 228-tyrosine 272 catalytic cofactor of galactose oxidase does not require dioxygen. *Biochemistry* **2008**, *47*, 10428–10439
12. Bhaskar, B.; Immoos, C. E.; Shimizu, H.; Sulc, F.; Farmer, P. J.; and Poulos, T. L. A novel heme and peroxide-dependent tryptophan-tyrosine cross-link in a mutant of cytochrome c peroxidase. *J. Mol. Biol.* **2003**, *328*, 157-166

13. Amini, F.; Kodadek, T.; and Brown, K. C. Protein affinity labeling mediated by genetically encoded peptide tags. *Angew. Chem. Int. Ed. Engl.* **2002**, *41*, 356-359
14. Ghesquiere, B.; Jonckheere, V.; Colaert, N.; Van Durme, J.; Timmerman, E.; Goethals, M.; Schymkowitz, J.; Rousseau, F.; Vandekerckhove, J.; and Gevaert, K. Redox Proteomics of Protein-bound Methionine Oxidation. *Mol. Cell. Proteomics* **2011**, *10*, M110.006866.
15. Nam, J. S.; Kang, M. G.; Kang, J.; Park, S. Y.; Lee, S. J.; Kim, H. T.; Seo, J. K.; Kwon, O. H.; Lim, M. H.; Rhee, H. W.; and Kwon, T. H. Endoplasmic Reticulum-Localized Iridium(III) Complexes as Efficient Photodynamic Therapy Agents via Protein Modifications. *J. Am. Chem. Soc.* **2016**, *138*, 10968−10977
16. Melville, D. B.; Dittmer, K.; Brown, G. B.; and Vigneaud, D. U. V. Desthiobiotin *Science* **1943**, *98*, 497– 499
17. Lee, S.-Y.; Kang, M.-G.; Shin, S.; Kwak, C.; Kwon, T.; Seo, J. K.; Kim, J. S.; and Rhee, H.-W. Architecture Mapping of the Inner Mitochondrial Membrane Proteome by Chemical Tools in Live Cells *J. Am. Chem. Soc.* **2017**, *139*, 3651−3662
18. Ntai, I.; Phelan, V. V.; and Bachmann, B. O. Phosphonopeptide K-26 biosynthetic intermediates in *Astrosporangium hypotensionis*. *Chem. Commun.* **2006**, 4518–4520
19. Panufnik, E.; and Kañska, M. Enzymatic synthesis of isotopomers of tyramine labeled with deuterium and tritium. *J Label Compd Radiopharm* **2007**, *50*, 85–89
20. Wang, T. P.; Chiou, Y. J.; Chen, Y.; Wang, E. C.; Hwang, L. C.; Chen, B. H.; Chen, Y. H.; and Ko, C. H. Versatile Phosphoramidation Reactions for Nucleic Acid Conjugations with Peptides, Proteins, Chromophores, and Biotin Derivatives. *Bioconjugate Chemistry* **2010**, *21*(9), 1642–1655
21. Park, S. B.; Barnes-Seeman, D.; Koehler, A. N.; and Schreiber, S. L. Small Molecule Printing. *United States Patent Application Publication* **2003**, US2003/0215876 A1

Acknowledgement

First of all, I would appreciate my advisor, professor Jung-Min Kee. I could get lots of advice, guidance and comments and it would be impossible for my growth and improvement without his help. My major was biology when undergraduate school and it took a time to be familiar with chemistry research in graduate school. Professor Kee always taught me and I could settle in chemical biology and be interested in my research field.

Also I wanted to give a thank for my lab members. When I was a lab manager in my lab, they followed and helped me a lot in spite of the lack of my ability. Especially, Yi-gun Choi was my research team partner and currently our project was accomplished under his efforts.

At last, it was a big honor for professor Hyun-Woo Rhee and Young S. Park to evaluate my research output.